Molecular mechanism of action and pharmacogenomics of curcumin, curcumin synthetic derivatives and combinations with curcumin in cancer therapy

Dissertation
zur Erlangung des Grades

“Doktor der Naturwissenschaften”

im Promotionsfach Pharmazie

am Fachbereich Chemie, Pharmazie und Geowissenschaften der Johannes Gutenberg-Universität in Mainz

vorgelegt von Edna Ooko
geboren am [redacted]

Mainz, März 2017

Betreuer:

Prof. Dr. [redacted]

Gutachter der Arbeit:

Prof. Dr. [redacted]

Prof. Dr. [redacted]

Datum der mündlichen Prüfung:

20.03.2017

Prüfungskommission:

Prof. Dr. [redacted]

Prof. Dr. [redacted]

Prof. Dr. [redacted]

Dr. [redacted] (Protokoll)

D77 (Dissertation Universität Mainz)

Publications as first author

- Ooko E, Alsalim T, Saeed B, Saeed ME, Kadioglu O, Abbo HS, Titinchi SJ, Efferth T. Modulation of P-glycoprotein activity by novel synthetic curcumin derivatives in sensitive and multidrug-resistant T-cell acute lymphoblastic leukemia cell lines. Toxicol Appl Pharmacol. 2016 Aug
- Ooko E, Saeed ME, Kadioglu O, Sarvi S, Colak M, Elmasaoudi K, Janah R, Greten HJ, Efferth T. Artemisinin derivatives induce iron-dependent cell death (ferroptosis) in tumor cells. Phytomedicine. 2015 Oct

Publications as co-author

- Efferth T, Banerjee M, Paul NW, Abdelfatah S, Arend J, Elhassan G, Hamdoun S, Hamm R, Hong C, Kadioglu O, Naß J, Ochwangi D, Ooko E, Ozenver N, Saeed ME, Schneider M, Seo EJ, Wu CF, Yan G, Zeino M, Zhao Q, Abu-Darwish MS, Andersch K, Alexie G, Bessarab D, Bhakta-Guha D, Bolzani V, Dapat E, Donenko FV, Efferth M, Greten HJ, Gunatilaka L, Hussein AA, Karadeniz A, Khalid HE, Kuete V, Lee IS, Liu L, Midiwo J, Mora R, Nakagawa H, Ngassapa O, Noysang C, Omosa LK, Roland FH, Shahat AA, Saab A, Saeed EM, Shan L, Titinchi SJ. Biopiracy of natural products and good bioprospecting practice. Phytomedicine. 2016 Feb

Posters

- Ooko E, Titinchi SJ, Efferth T. Curcumin and its synthetic derivatives as lead anticancer agents. 9th SFB35 Transmembrane Transporters in Health and Disease. Medical University of Vienna, Vienna Austria 31st August – 2nd Sept 2016.

- Ooko E, Titinchi SJ, Efferth T.Cytotoxic activity and inhibition of P-glycoprotein by 19 synthetic derivatives of Curcumin towards human CCRF-CEM and multidrug resistant

- CEM/ADR 5000 leukemia cells. 14th International congress for Ethnopharmacology. Puerto Varas, Chile September 2014

- Ooko E, Titinchi SJ, Efferth T.Synthetic derivatives of curcumin as lead agents for anticancer against leukemia 128. Versammlung der Gesellshaft Deutsche Naturforsher and Ärzte (GDNÄ). September 2014, Johannes Gutenberg University, Mainz, Germany

Oral Presentations

- Ooko E, Efferth T. Molecular docking a powerful tool in predictive and confirmatory work in Pharmaceutical Biology Research: A case study of curcumin and its synthetic derivative against P-glycoprotein in leukemic cells. 2015 Regional conference of the International Network of women Engineers and Scientists (INWES). 21st – 23rd October 2015. Speke Resort and Conference Center Kampala Uganda

Erklärung

Hiermit erkläre ich an Eides statt, dass ich diese Arbeit selbständig verfasst und keine anderen als die angegebenen Quellen und Hilfsmittel verwendet habe.

Mainz, Keine Unterschift zwecks Datenschutz

_____ _____

Ort, Datum Edna Ooko

Acknowledgement

Transformative achievements come from concerted and at times unrecognized contributions of many. A PhD is not an individual experience; rather a journey which includes several persons whom I would like to thank sincerely.

First I would like to really thank [redacted] my supervisor and advisor. I am honestly glad that I met and worked with and for you. It has been an exceptional experience for me. Thank you for offering me a place in your lab and allowing me to share in your passion for pharmaceutical biology; thank you also for your concern for me as a foreigner in Germany our scientific group has also served as a home away from home for me. Your advice will go a long way into making me a scientist you will be proud of and I am looking forward to what the future holds. I am also grateful to the DAAD (German Academic Exchange Program) for offering me a scholarship to pursue my studies here in Germany. Without them the possibility of undertaking this journey would never have seen the light of day.

I also want to appreciate my fellow PhD colleagues for their scientific support always helping me out in varied experiments and also teaching me how to interpret and analyze the results. Their experience has gone a long way in making my research experience enjoyable. I also want to recognize the team spirit and our travels to varied restaurants added an element of adventure and enjoyment to my life. I also would like to recognize the work of our group secretary [redacted] your assistance in my research work and daily life was invaluable pushed me a long way. I would also not go without mentioning [redacted] and [redacted] your friendship has seen me through it all, the happy moments, the sad moments and the moments of anxiety and uncertainty thank you so much.

Special note of thanks to my family they have been warm, un-boundlessly loving and a psychological, physical, spiritual and financial safety net, always loving and encouraging.

Abstract

Curcumin has been shown to be active against various cancers and it has also been seen to exhibit good synergism with other nutraceutical for example resveratrol, piperine and genistein. In this study we have investigated nineteen new synthetic derivatives of curcumin for their anticancer activity and further assessed the effect on cancer cells of a combination of curcumin and ascorbic acid (AA). The first part of this work focused on overcoming multidrug resistance and the nineteen synthetic derivatives of curcumin were tested on acute lymphoblastic CCRF-CEM leukemia cells and the P-gp overexpressing subline CEM/ADR5000. The cytotoxicity of the new synthetic derivatives was established using the resazurin assay. Ability to inhibit P-gp function was also assessed by the doxorubicin uptake assay and *in silico* studies of the same have been carried out using molecular docking tools and QSAR studies. The compounds displayed varied levels of cytotoxicity with some of them exhibiting lower IC_{50} values in comparison to the parent compound curcumin. The new synthetic derivatives also showed ability to inhibit P-gp function of extrusion of doxorubicin from the cells and some of them inhibited P-gp better than the control drug verapamil. These derivatives can be used to design novel and better P-gp inhibitors.

The second part of our study focused on the cytotoxic effect of a combination of curcumin with AA on varied cancer cell lines. Here we carried out the chemoprofiling of three different members of the *curcuma* species and observed that curcumin was present in all *curcuma* species while AA was only available in *C. longa*. The combination of curcumin and AA was tested for cytotoxicity on human cancer cell lines including CCRF-CEM and CEM/ADR5000 leukemia, HCT116p53$^{+/+}$ and HCT116p53$^{-/-}$ colon cancer, and U87MG and U87MG.ΔEGRF glioblastoma. The drug combination exhibited additive cytotoxicity in leukemia and colon cancer cell lines while in the glioblastoma cell lines additive to supra additive cytotoxicity was recorded. Further we assessed the pharmacogenomics of curcumin and AA by microarray-

based mRNA expression, COMPARE analysis and hierarchical cluster analysis. Gene profiles were obtained and they were used to predict sensitivity and resistance of the tumor cells to curcumin and AA. From these gene profiles we also established the gene functions that our compounds affected by assessing up and down regulation patterns as exhibited by the color coded heat map analysis. Both curcumin and AA affected varied groups of genes and varied functions in the cell lines. The pharmacogenomics results further supports the cytotoxicity results of additive effects.

Zusammenfassung

Curcumin besitzt nicht nur eine Wirksamkeit gegen verschiedene Krebsarten, sondern es wurden auch Synergien in Verbindung mit anderen Nutraceuticals wie Reservatol, Piperin und Genistein nachgewiesen. In der vorliegenden Arbeit untersuchte ich 19 neue synthetische Curcumin-Derivate auf ihre Wirksamkeit gegen Krebs. Außerdem bewertete ich den Effekt einer Kombination von Curcumin und Askorbinsäure (AA) auf Krebszellen. Der erste Teil der Arbeit konzentriert sich auf die Überwindung von Multidrug-Resistenzen. Aus diesem Grund wurden die 19 synthetischen Curcumin-Derivate an einer Zelllinie der akuten lymphoplastischen Leukämie (CCRF-CEM) und ihrer P-Glykoprotein-überexprimierenden Sublinie (CEM/ADR 500) getestet. Die Zytotoxizität der Derivate wurde mit einem Resazurin-Assay bestimmt. Die Fähigkeit zur Hemmung der P-Glykoprotein-Wirkung wurde mit einem Doxorubicin-Aufnhame-Test gemessen sowie mittels *in silico* Studien, bei denen molekulare Docking-Methoden und Berechnungen zu quantitative Struktur-Wirkungsbeziehungen (QSAR) verwendet wurden. Die Substanzen zeigten unterschiedliche Grade der Zytotoxizität, wobei einige im Vergleich zur Ursprungssubstanz sogar niedrigere IC_{50} Werte besaßen. Die neuen synthetischen Derivate besaßen außerdem die Fähigkeit die P-Glykoprotein-Wirkung zur Verdrängung von Doxorubicin aus den Zellen zu hemmen, einige sogar in höherem Maße als die Kontrolldroge Verapamil.

Der zweite Teil der Arbeit konzentrierte sich auf den zytotoxischen Effekt von Curcumin mit AA auf verschiedenen Krebsarten. Es wurden Chemoprofile der sekundären Pflanzenstoffe von drei verschiedenen Mitgliedern der *Curcuma*-Familie erstellt, wobei in allen drei Arten Curcumin gefunden wurde, jedoch nur in einer Art, *C. longa,* AA nachgewiesen wurde. Die Kombination von Curcumin mit AA wurde an verschiedenen menschlichen Krebszelllinien, unter anderem CCRF-CEM und CEM/ADR 5000 Leukämie-Zellen, HTC116p53$^{+/+}$ und HTC116p53$^{-/-}$ Darmkrebs-Zellen, sowie U87MG und U87MG.ΔEGRF Glioblastom-Zellen, getestet. Eine Kombination der Substanzen ergab einen additiven Effekt auf Leukämie- und Darmkrebs-Zellen, wohingegen die Glioblastom-Zelllinien additive bis supra additive Effekte zeigten. Desweiteren beschäftigte ich mich mit den pharmakogenomischen Eigenschaften von Curcumin und AA über Microarray-basierte mRNA Expressionsprofile,

COMPARE-Analyse und hierarchische Cluster-Analyse. Genprofile wurden erstellt und zur Vorhersage der Empfindlichkeit bzw. Resistenz der Tumorzellen gegenüber Curcumin und AA benutzt. Diese Genprofile zeigten hoch- und nieder-exprimierte Gene in den verschiedenen Zelllinien. Es wurde ebenfalls eine *color-coded heatmap analysis* für die betroffenen Gene erstellt. Beide, Curcumin und AA beeinflussten vielfältige Gengruppen und unterschiedliche Funktionen innerhalb der Zelllinien. Die pharmakogenomischen Ergebnisse unterstützen die Ergebnisse zu dem additiven zytotoxischen Effekt der beiden Substanzen.

Table of contents

List of Abbreviations

Abbreviation	Connotation
ABC	ATP binding cassette
ABCB1	ATP-binding cassette sub-family B member 1/Pglycoprotein/MDR1
Abl	Abelson tyrosine protein kinase
ADP	Adenosine diphosphate
Akt	Murine thymoma viral oncogene homolog
AML	Acute myeloid leukemia
ALL	Acute lymphocytic leukemia
APS	Ammonium persulfate
ARF	ADP Ribosylation Factors
ATCC	American Type Culture Collection
ATP	Adenosine triphosphate
Bax	Bcl-2-associated X protein
Bcl-2	B-cell CLL/lymphoma 2
BCR	Breakpoint cluster region
BD	Becton Dickinson
BET	Bromodomain and extraterminal domain
BH3	Bcl-2 homology 3
bHLH-Lz	Basic helix-loop-helix leucine zipper
BSA	Bovine serum albumin
C lobe	Carboxy-terminal lobe
CAK	CDK-activating kinase
CD	Cluster of differentiation
CDC25	Cell division cycle 25
CDK	Cyclin dependent kinases
cDNA	Complementary DNA
cRNA	Complementary RNA
CI	Combination index
CTD	Carboxy-termianl domain
CTLA4	Cytotoxic T-lymphocyte-associated protein 4
DAG	Diacylglycerol
DKFZ	German Cancer Research Center
DMEM	Dulbecco’s modified eagle medium
DMSO	Dimethyl sulfoxide
DNA	Deoxyribonucleic acid
DPBS	Dulbecco’s phoshpate-buffered saline
E2F	E2 promoter binding factor
E-box	Enhancer box
EDTA	Ethylene diamine tetraacetic acid
EGFR	Epidermal growth factor receptor

ELISA	Enzyme linked immunosorbent assay
ERK	Extracellular signal-regulated kinases
FACS	Fluorescence-activated cell sorting
FBS	Fetal bovine serum
FDA	US Food and Drug Administration
FITC	Fluorescein isothiocyanate
GBM	Glioblastoma multiforme
GSK-3	Glycogen synthase kinase-3
HER1	Human epidermal growth factor receptor type 1/EGFR/ErbB1
HER2/neu	Human epidermal growth factor receptor type 2
HGF	Hepatocyte growth factor
HIV	Human Immunodeficiency Virus
HRP	Horseradish peroxidase
IC50	Half maximal inhibitory concentration
IPA	Ingenuity Pathway Analysis
JAK	Janus-activated kinase
JNK	Jun N-terminal Kinase
LUMO	Lowest unoccupied molecular orbital
MAD	Median absolute deviation
MAD1	Mitotic arrest deficient 1
MAPK	Mitogen-activated protein kinase
MAX	Myc-associated factor X
MDM2	Mouse double minute 2 homolog
MDR	Multidrug resistance
MDR1	Multidrug resistance protein 1/ABCB1/P-glycoprotein
MEK	Mitogen-activated protein kinase kinase
MGMT	O6-methylguanine-DNA-methyltransferase
mRNA	Messenger ribonucleic acid
MS4A3	Membrane-spanning 4-domains, subfamily A, member 3
mTOR	Mammalian target of rapamycin
MYB	v-myb Avian myeloblastosis viral oncogene homolog
MYC	c-myc Avian myelocytomatosis viral oncogene homolog
Nec-1	Necrostatin-1
NF-kB	Nuclear factor of kappa light polypeptide gene enhancer in B-cells
NK	Natural killer
NSCLC	Non-small-cell lung cancer
P53	Tumor protein 53/TP53
PARP	Poly (ADP-ribose) polymerase
PCNA	Proliferating cell nuclear antigen
PCR	Polymerase chain reaction
PDB	Protein data bank
P-gp	P-glycoprotein
PI	Propidium iodide

PI3K	Phosphatidylinositol 3-kinase
PKC	Protein kinase C
PLC	Phospholipase C
PS	Phosphatidylserine
PTEN	Phosphatase and tensin homolog
PVDF	Polyvinyl difluoride
RAC1	Ras-related C3 botulinum toxin substrate 1
Raf	Rapidly accelerated fibrosarcoma proto-oncogene
Ras	Rat sarcoma viral oncogene homolog
RIP	Receptor interacting protein
RNA	Ribonucleic acid
ROS	Reactive oxygen species
RPMI 1640	Roswell Park Memorial Institute 1640
RT-PCR	Reverse transcription PCR
S-180	Sarcoma 180
SAPK	Stress-activated protein kinases
SDS-PAGE	Sodium dodecyl sulfate-polyacrilamide gel electrophoresis
SEM	Standard error of mean
SNP	Single nucleotide polymorphism
Src	Sarcoma proto-oncogene tyrosine-protein kinase
STAT	Signal transducer and activator of transcription
STR	Short tandem repeat
TAD	Transcriptional activation domain
TBST	Tris-buffered saline-Tween20
TCM	Traditional Chinese Medicine
TEMED	Tetramethylenediamine
TGF	Transforming growing factor
TK	Tyrosine kinase
TKIs	Tyrosine kinase inhibitors
Tris	Tris (hydroxymethyl) aminomethane
ULBP	UL-16 binding proteins
VEGF	Vascular endothelial growth factor
VMD	Visual Molecular Dynamics
WHO	World Health Organization

1. Introduction

1.1 General facts about Cancer

Ferlay *et al* estimated that there are 14.1 million new cases and 8.2 million deaths in 2012 caused by cancer worldwide. WHO estimates for 2011 state that cancer now causes more death than all coronary heart disease and stroke [1]. **Table 1** below shows the estimated number of cases and deaths (in thousands) for all cancers combined (excluding non-melanoma skin cancers) and for 27 specific cancers in men, women and both sexes, together with the corresponding ASRs and the cumulative risk; while **figure 1** shows the global incidence burden in 2012 in more developed and less developed regions. Leukemia as a cancer has about 47,500 new cases with more deaths in men than women at 32,000 deaths in men in Europe [2].

By definition cancer is a group of diseases involving abnormal cell growth with the potential to invade or spread to other parts of the body. There are four types of cancers 1) Carcinoma – these arise from the epithelial sheet that covers the surfaces for example skin, colon etc. and approximately 90% of all human cancers are carcinomas. 2) Sarcoma – these include cancers of the connective tissues such as the muscle, bone, cartilage and fibrous tissue and approximately 2% of all cancer are sarcomas. 3) Leukemia – these originate from blood forming cells. 4) Lymphoma – these originate from cell of the immune system, 8% of all cancers are leukemia and lymphoma [3]. Leukemia develops from hematopoietic stem cells that escape the normal control mechanisms thereby interrupting their capacity to differentiate in mature blood cells. As a result of uncontrolled proliferation of hematological progenitor cells, excessive number of malignant cells accumulates in the bone marrow where they replace normal marrow tissue and affect physiological production of blood cells [4, 5]. Hanahan Douglas and Weinberg Robert in their review state that cancer cells are distinct from normal cells in six different ways and these are biological capabilities acquired during the multistep development of human tumors, cancer cells can: a) sustain proliferative signaling, b) evade growth suppressors, c) resist cell death by evading apoptosis, d) enable replicative immortality,

e) induce angiogenesis and f) activate invasion and metastasis [6]. Furthermore they show emergence of two other traits which are a) the Warburg effect where the tumor can form macromolecules needed for building new cells by shifting energy metabolism to aerobic glycolysis and b) the tumor evades the immune system by attenuating components of the immune system [6-8] approximately 2% of all cancer are sarcomas.

Table 1. Estimated new cancer cases (thousands), ASRs (per 100,000) and cumulative risks to age 75 (percentage) by sex and cancer site worldwide, 2012

	Both sexes				**Male**				**Female**			
Cancer site	**case**	**%**	**ASR (World)**	**Cum.risk (0-74)**	**cases**	**%**	**ASR (World)**	**Cum.risk (0-74)**	**cases**	**%**	**ASR (World)**	**Cum.risk (0-74)**
Lip, oral cavity	300	2,1	4,0	0,5	119	2,7	5,5	0,6	101	1,5	2,5	0,3
Nasopharynx	87	0,6	1,2	0,1	61	0,8	1,7	0,2	26	0,4	0,7	0,1
Other pharynx	142	1,0	1,9	0,2	115	1,5	3,2	0,4	27	0,4	0,7	0,1
Oesophagus	456	3,2	5,9	0,7	323	4,3	9,0	1,1	133	2,0	3,1	0,4
Stomach	951	6,8	12,1	1,4	631	8,5	17,4	2,0	320	4,8	7,5	0,8
Colorectum	1360	9,7	17,2	2,0	746	10,0	20,6	2,4	614	9,2	14,3	1,6
Liver	782	5,6	10,1	1,1	554	7,5	15,3	1,7	228	3,4	5,4	0,6
Gallbladder	178	1,3	2,2	0,2	77	1,0	2,1	0,2	101	1,5	2,3	0,3
Pancreas	338	2,4	4,2	0,5	178	2,4	4,9	0,6	160	2,4	3,6	0,4
Larynx	157	1,1	2,1	0,3	138	1,9	3,9	0,5	19	0,3	0,5	0,1
Lung	1825	12,9	23,1	2,7	1242	16,7	34,2	3,9	583	8,7	13,6	1,6
Melanoma of skin	232	1,6	3,0	0,3	121	1,6	3,3	0,4	111	1,7	2,8	0,3
Kaposi sarcoma	44	0,3	0,6	0,1	29	0,4	0,8	0,1	15	0,2	0,4	0,0
Breast	1677	11,9	43,3	4,6					1677	25,2	43,3	4,6
Cervix uteri	528	3,7	14,0	1,4					528	7,9	14,0	1,4
Corpus uteri	320	2,3	8,3	1,0					320	4,8	8,3	1,0
Ovary	239	1,7	6,1	0,7					239	3,6	6,1	0,7
Prostrate	1112	7,9	31,1	3,8	1112	15,0	31,1	3,8				
Testis	55	0,4	1,5	0,1	55	0,7	1,5	0,1				
Kidney	338	2,4	4,4	0,5	214	2,9	6,0	0,7	124	1,9	3,1	0,3
Bladder	429	3,1	5,3	0,6	330	4,4	9,0	1,0	99	1,5	2,2	0,2

Brain, nervous system	257	1,8	3,4	0,3	140	1,9	3,9	0,4	117	1,8	3,0	0,3
Thyroid	298	2,1	4,0	0,4	68	0,9	1,9	0,2	230	3,5	6,1	0,6
Hodgkin lymphoma	66	0,5	0,9	0,1	39	0,5	1,1	0,1	27	0,4	0,7	0,1
Non-Hodgkin lymphoma	386	2,7	5,1	0,5	218	2,9	6,0	0,6	168	2,5	4,1	0,4
Multiple myeloma	114	0,8	1,5	0,2	62	0,8	1,7	0,2	52	0,8	1,2	0,2
Leukaemia	352	2,5	4,7	0,4	201	2,7	5,6	0,5	151	2,3	3,9	0,4
All cancers except non-melanoma skin cancer	14090	100	182,3	18,5	7427	100	205	21	6663	100	165,3	16,4

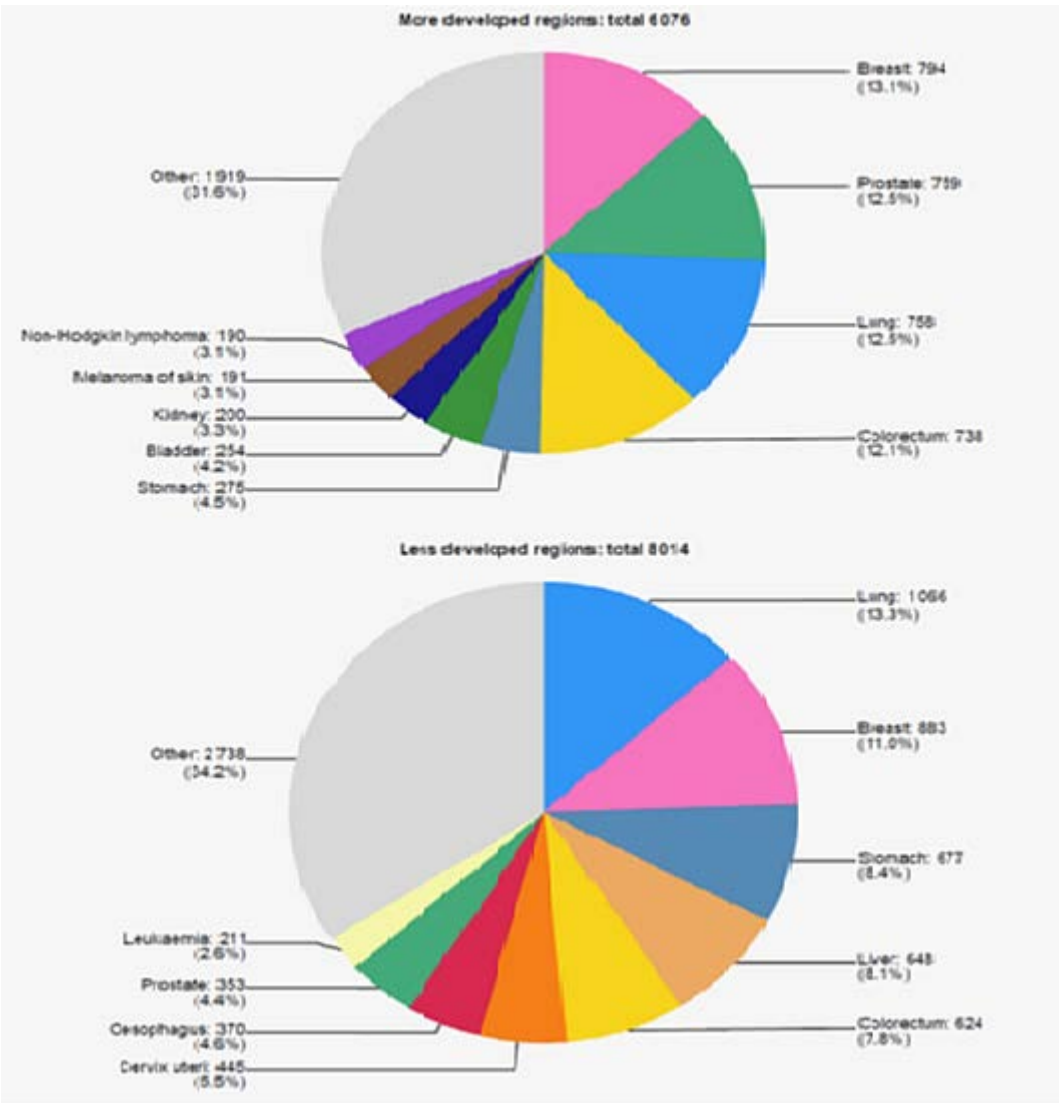

Figure 1. Estimated global numbers of new cases (thousands) with proportions for (a) more developed and (b) less developed regions, both sexes combined, 2012. The area of the pie is proportional to the number of new cases.

1.2 Cancer Treatment

Currently the main methods established to treat cancer are: surgery, radiation and chemotherapy[9] and these methods are frequently used in combination. Surgery aims at removing the whole tumor [10], radiotherapy causes cell death by inducing DNA damage [11] and chemotherapy is the use of drugs to treat the tumor [12].

Chemotherapy

Chemotherapy is a general strategy to fight different types of diseases. In the treatment of cancer it is a strategy to fight cancer with one or more cytotoxic drugs. Chemotherapy has been used since the 1940's as an established treatment option for cancer [13]. Very early steps in the development of chemotherapy for cancer were made in 1908 by investigations of arsenicals. Further advancements were witnessed in 1946 when sulfur mustards were shown to have therapeutic effect this was reported after the first patients were successfully treated around 1943 [14-16]. This was the post-world war 2 era and the publications showed that the sulfur mustard caused a reduction in the lymphoma patients. Since then major attempts to synthesize and test varied chemicals as inhibitors to cancer growth. Much success has been seen and there has been the introduction of substances such as chlorambucil, cyclophosphamide, methotrexate, purine analogues, *Vinca* alkaloids and anthracycline [12, 13]. Cancer chemotherapy has evolved much and the drugs produced are essential in the fight against cancer but the cytotoxic substances produced exhibit adverse effects on normal highly proliferating cells leading to severe side effects. The side effects include myelosuppression, immunosuppression, nausea, vomiting, fever diarrhea, hair loss, bleeding problems and organ damage e.g. (lung, liver, kidney and heart) [17].

In overcoming the above stated side effects much of the research shifted strategy to a new concept of targeted therapy. Instead of therapy that affects all rapidly proliferating cells which interferes with DNA or microtubule function, the focus was on cancer specific molecular

abnormalities. These abnormalities could then be targeted by monoclonal antibodies or small molecules [18]. This search for effective and less toxic molecules for chemotherapy is still ongoing and natural products are proving to be a rich source for identification of new compounds. Today the screening of natural products represents one of the many approaches used to discover new products.

1.3 Natural products in cancer chemotherapy

For many years natural products have played a very important role in health care and prevention of diseases [19]. The earlier civilizations of Chinese Indian and North Africans used natural sources for curing various diseases. A 4000 years old Sumerian clay tablet with records of remedies for various illnesses is the earliest known written document [20]. In the nineteenth century scientists began to isolate active components from varied medicinal plants. Friedrich setürner isolated morphine from *Papaver somniferum* in 1806 and since then natural products have been extensively screened for their medicinal purposes. Between 1981 – 2006 almost a hundred anticancer agents have been developed of which twenty five are natural product derivatives, eighteen are natural product mimics, eleven candidates are derived from a natural product pharmacophore and nine are pure natural products. Thus natural sources make a very significant contribution to the health care system [21]. Several important drugs such as Taxol, camptothecin, morphine and quinine have been isolated from plant sources. The first two are widely used as anticancer drugs, while the remaining are analgesic and antimalarial agents, respectively.

1.3.1 Plants and their products used as anticancer agents

One of the early compounds isolated as an anticancer agent was podophyllotoxin, a compound obtained from *Podophyllum peltatum* in 1944. In 1974 it was shown that it acts as an anticancer agent by binding irreversibly to tubulin. Etoposide and teniposide, the modified analogs of

podophyllotoxin, however, cause cell death by inhibition of topoisomerase II, thus preventing the cleavage of the enzyme- DNA complex and arresting the cell growth. Both these analogs are used in the treatment of various cancers [22-24].

The Madagascar periwinkle, *Catharanthus roseus* a member of the Apocynaceae family, is a rich source of indole alkaloids which include the anticancer alkaloids vincristine and vinblastine. Both vinblastine and vincristine are now known to prevent cell division by inhibiting mitosis in the cell cycle. They irreversibly bind to tubulin, thereby blocking cell multiplication and eventually causing cell death [25].

In 1963 the Pacific yew tree, *Taxus brevifolia* was discovered to possess anticancer properties and paclitaxel was its active component. Paclitaxel irreversibly binds to β-tubulin, thus promoting microtubule stabilization. This tubulin- microtubule equilibrium is essential for cell multiplication, and its stabilization causes programmed cell death [26-28].

Camptothecin from the deciduous tree *Camptotheca acuminata,* is also an anticancer agent. It causes cell death by DNA damage. However, camptothecin itself is too insoluble to be used as a drug but its several water-soluble analogs, namely, topotecan and irinotecan have been developed as effective drugs [29, 30].

1.3.2 Turmeric

Turmeric is derived from the plant *Curcuma longa* a perennial herb belonging to the ginger family, is cultivated extensively in south and southeast tropical Asia. The rhizome of the plant is the most useful part of the plant for culinary and medicinal purposes. Turmeric is a gold-colored spice commonly used in the Indian subcontinent for health care, food preservation and as a yellow dye for textiles. Turmeric has been used in Indian and Chinese medicines to treat colic, toothaches, menstrual difficulties and chest pains. In addition it was used in solving stomach and liver problems, healing wounds and lightening of scars and as a cosmetic. In 1280 Marco Polo mentioned turmeric in his writings and in the 13th century turmeric was introduced

to Europe by Arab traders. Turmeric contains many different phytochemicals with curcumin being the most active component and it is mainly responsible for the yellow color of turmeric and its therapeutics effects. Curcumin makes up 2 – 5 % of turmeric [31].

1.3.2.1 Structure and chemistry of Curcumin

Curcumin was first isolated in 1842 by Vogel and its structure ($C_{21}H_{20}O_6$) was first described in 1910 by Lampe and Milobedeska and shown to be diferuloylmethane. The curcumin ((1*E*, 6*E*)-1, 7-Bis (4-hydroxy-3-methoxyphenyl)-1, 6-heptadiene-3, 5-dione) is a bioactive diphenylheptanoid and contains a variety of functional groups. The structure of curcumin consists of two methoxy phenolic groups linked by a seven carbon linker consisting of α, β-unsaturated β-diketone moiety **Figure 2**. The α, β-unsaturated β-diketone group exhibits keto-enol tautomerism due to strong intramolecular hydrogen bonding in the 1, 3-diketone functionality [32]. Thus, the naturally occurring curcumin exists as an equilibrium mixture of two tautomeric forms in solution. The enol form is the most dominant structure of curcumin in solution as it is stabilized by intramolecular H-bonding. The aromatic moiety is involve in π-π interaction, whereas, phenolic moiety and keto-enol group participate in hydrogen bonding interactions. Due to flexibility provided by seven carbon linker, the molecule can easily adopt a conformation suitable for overall hydrophobic interaction [33].

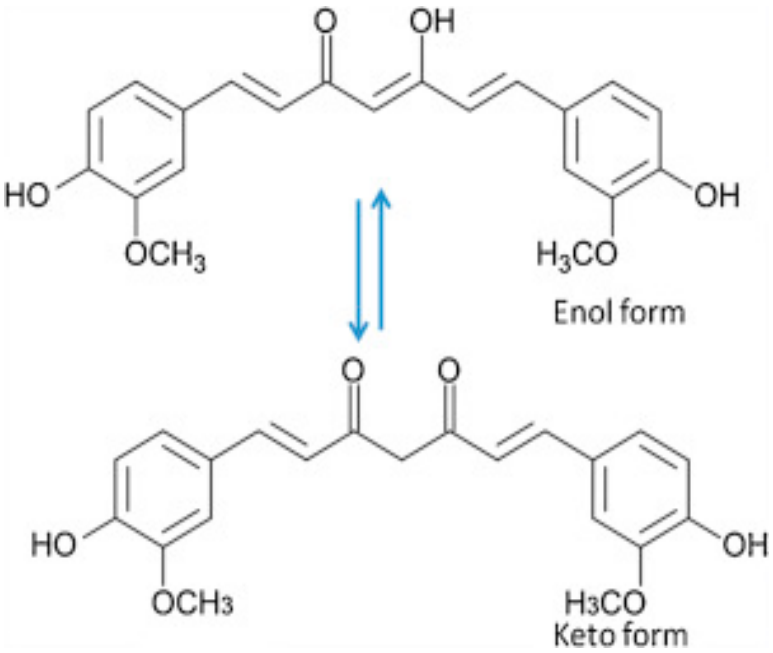

Figure 2. Structure of curcumin. Keto form is the predominant specie in water.

1.3.2.2 Curcumin uses and molecular targets

Curcumin from turmeric has been used as antiseptic, analgesic, anti-inflammatory, antioxidant, antimalarial, insect-repellant, and wound healer [34-37]. Curcumin has considerable potential against a wide variety of both malignant and non-malignant diseases. Curcumin exhibits activity against numerous inflammatory diseases, including pancreatitis [38, 39], arthritis [40, 41], inflammatory bowel disease [42], gastritis [43], allergy [44, 45], and fever [46, 47], possibly through the downregulation of inflammatory markers. It is also active against autoimmune diseases, including scleroderma [48], psoriasis [49], multiple sclerosis [50], and diabetes [51-53]. Curcumin also exhibits a great potential against various types of cancers. Its mechanism of action involves, firstly, the suppression of tumor cell proliferation by down-regulation of anti-apoptotic gene products, activation of caspases and induction of tumor suppressor genes [54-56]. Secondly, curcumin suppresses tumor invasion by down-regulation of matrix metalloproteinases and cell surface adhesion molecules [57-59]. Thirdly, curcumin

inhibits angiogenic cytokines leading to suppression of angiogenesis [60-62] and lastly the anti-inflammatory and cytotoxic effects of curcumin contribute to its antitumor activity [63-65].

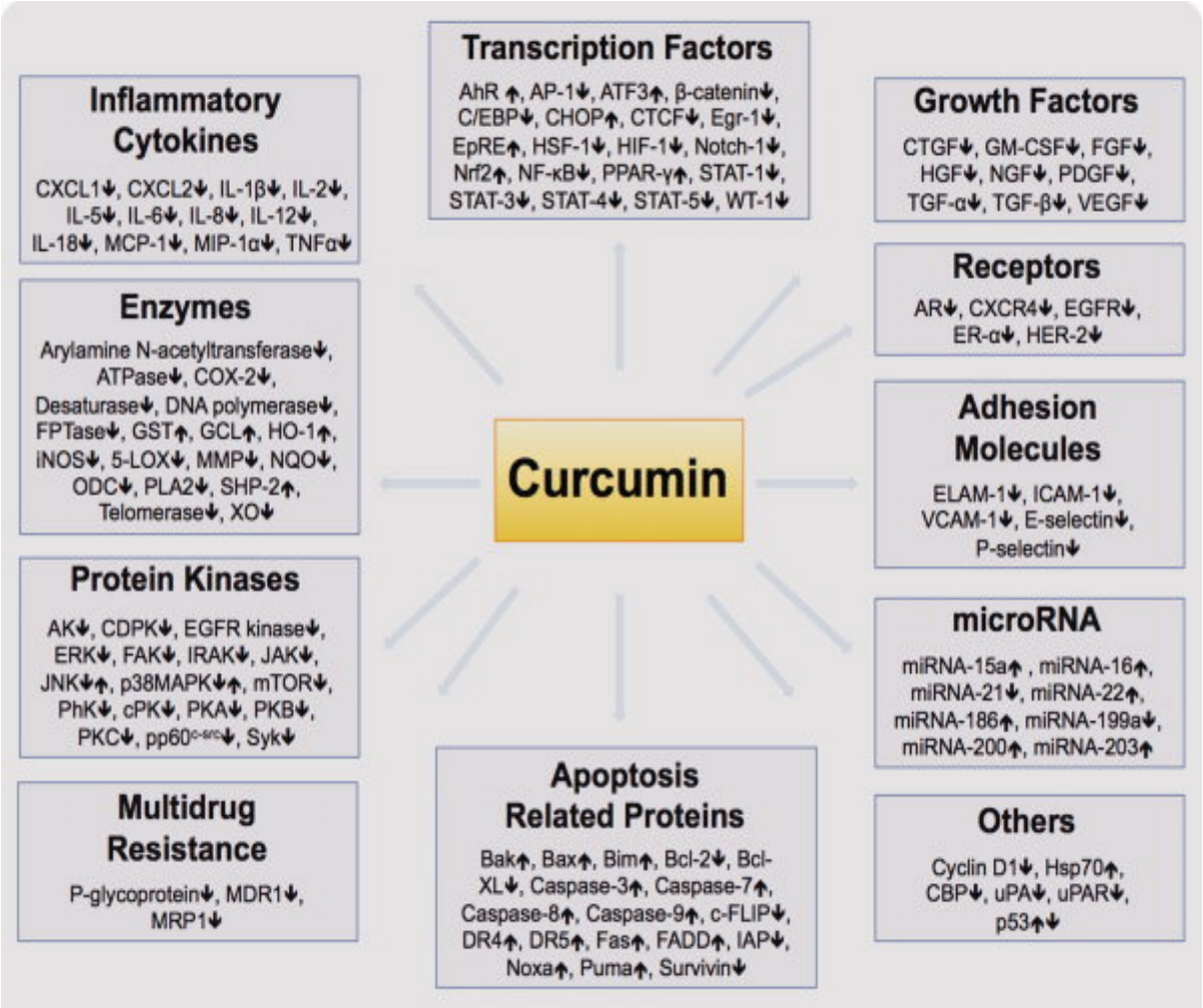

Figure 3. Molecular targets of curcumin

Molecular targets of curcumin (5-LOX, 5-lipoxygenase, AhR, aryl hydrocarbon receptor, AK, autophosphorylation-activated protein kinase, AP-1, activator protein-1, AR, androgen receptor, ATF3, activating transcription factor 3, Bcl-2, B-cell lymphoma protein 2, c-FLIP, Cellular FLICE inhibitory protein, C/EBP, CCAAT/enhancer-binding protein, CBP, P300/CREB-binding protein, CDPK, Ca^{2+}-dependent protein kinase, CHOP, C/EBP homologous protein, cPK, protamine kinase, CTCF, transcriptional repressor CTCF, CTGF, connective tissue growth factor, CXCL, chemokine (C-X-C motif) ligand, CXCR 4, chemokine (C-X-C motif) receptor 4, DR, death receptor, EGF, epidermal growth factor, EGFR, epidermal growth factor receptor, Egr-1, early growth response -1, ELAM-1, endothelial leukocyte adhesion molecule-1, EpRE, electrophile response element, ER-α, estrogen receptor-α, ERK, extracellular signal regulated kinase, FADD, Fas-associated death domain, FAK, focal adhesion kinase, FGF, fibroblast growth factor, FPTase, farnesyl protein transferase, GCL, glutamyl cysteine ligase, GM-CSF, granulocyte macrophage colony stimulating factor, GST, gluthathione-*S*-transferase, HER-2, human epidermal growth factor receptor-2, HGF, hepatocyte growth factor, HIF-1, hypoxia inducible factor-1, HO-1, hemeoxygenase-1, HSF-1, heat shock factor-1, HSP 70, heat-shock protein 70, IAP, inhibitor of apoptosis protein, ICAM-1, intracellular cell adhesion molecule-1, IL, interleukin, iNOS, inducible nitric oxide synthase, IRAK, IL-1 receptor-associated kinase, JAK, janus kinase, JNK, c-jun N-terminal kinase, MAPK, mitogen activated protein kinase, MCP-1, monocyte chemoattractant protein-1, MIP-1, macrophage inflammatory protein-1, MIP-1α, macrophage inflammatory protein-1α, MMP, matrix metalloproteinase, MRP, multidrug resistance protein, mTOR, mammalian target of rapamycin, NF-κB, nuclear factor-kappa B, NGF, nerve growth factor, NQO, NAD(P)H:quinone oxidoreductase, Nrf2, nuclear factor erythroid 2-related factor 2, ODC, ornithine decarboxylase, PDGF, platelet derived growth factor, PhK, phosphorylase kinase, PKA, protein kinase A, PKB, protein kinase B, PKC, protein kinase C, PLA2, phospholipase A2, PPAR-γ, peroxisome proliferator-activated receptor-γ, SHP, Src homology 2 domain-containing tyrosine phosphatase, Syk, spleen tyrosine kinase, TF, tissue factor, TGF-α, transforming growth factor-α, TNF, tumor necrosis factor, uPA, urokinase-type plasminogen activator, VCAM-1, vascular cell adhesion molecule-1, VEGF, vascular endothelial growth factor, WT-1, Wilms' tumor gene 1, XO, xanthine oxidase).(Retrieved from (Sjishir Shishodia. BioFactors 2012) with permission from IUBMB Copyright 2012).

1.3.2.3 Pharmacokinetics and Pharmacodynamics of curcumin

Curcumin also has proven safety, with a dose of 8 g per day being well tolerated in a phase II trial for advanced pancreatic cancer [66]. These favorable pharmacological properties are offset by difficulty with the administration of curcumin. This is because curcumin has low water solubility (0.00134 mg/mL) at 25 °C and is unstable at neutral and basic pH due to dissociation of the phenolic proton leading to degradation [67]. Curcumin degradation is blocked by antioxidants at pH 7.4 [68], but the molecule is relatively unstable in the small intestine. Poor absorption coupled with extensive metabolism of curcumin molecules that are absorbed markedly limits the oral bioavailability [69-71]. For example, when curcumin was administered orally to Sprague–Dawley rats at a dose of 1 g/kg, negligible amounts were found in rat plasma and 75 % was excreted in feces [72]. Curcumin given orally at 2 g/kg in rats gives a maximum serum concentration of 1.35 ± 0.23 μg/mL in 0.83 h with an elimination half-life of 1.70 ± 0.58 h, but in humans, an oral dose of 2 g results in very low or undetectable amounts of curcumin in serum, with a maximum concentration of 0.006 ± 0.005 μg/mL after 1 h [73]. Thus, therapeutic levels of curcumin are not attainable following oral administration [74], and the intravenous route is no more effective. Curcumin undergoes extensive metabolism in the liver and intestine. In human hepatocyte suspensions, 35 % of the initial curcumin remains after 2 h of incubation, and the level in rat hepatocyte suspensions was close to the detection limit after the same incubation time [75]. Metabolism in hepatocytes yields major metabolites of hexahydrocurcumin and hexahydrocurcuminol, but curcumin glucuronide and curcumin sulfate are the predominant metabolites found in rat plasma after oral or intravenous administration [75]. An in vitro study of metabolism of curcumin in subcellular fractions of rat and human intestines showed the presence of hexahydrocurcumin and curcumin sulfate in cytosolic fractions of both species and curcumin glucuronide in microsomal fractions. The presence of curcumin glucuronide and curcumin glucuronide/sulfate conjugates in rat plasma after oral

administration of curcumin suggests that glucuronidation of curcumin occurs primarily in the intestinal mucosa, with subsequent conjugation with sulfate in the liver [76].

1.3.3 Ascorbic acid (AA)

Ascorbic acid is a ketolactone and an important dietary micronutrient. AA is found in most plants and is synthesized from glucose. It is a water-soluble antioxidant and enzyme cofactor. Unlike most mammals, humans do not have the ability to endogenously synthesize this nutrient and, therefore, have to obtain AA through diet. There are two chemical forms of AA: the reduced form (ascorbic acid; AA) and the oxidized form (dehydroascorbic acid; DHA) [77]. AA appears as an essential micronutrient involved in many biochemical and biological functions. It is well known for its potent antioxidant properties, as it is able to scavenge free radicals and reactive oxygen species (ROS). Thus, it has been associated with decreased oxidative stress *in vivo* [78, 79]. High doses of AA can reduce inflammatory biomarkers such as C-reactive protein (CRP), tumor necrosis factor (TNF-α), interferon-γ (IFN-γ), and the interleukins IL-1, IL-2, IL-6, IL-8 [80, 81]. AA is a cofactor *in vivo* for enzymes involved in the biosynthesis of collagen, carnitine, neurotransmitters and neuropeptide hormones as well as enzymes involved in regulation of epigenetic or transcription factors [82, 83]. Furthermore, AA is a cofactor in the synthesis of the neurotransmitters norepinephrine, dopamine, and serotonin and neuropeptide hormones such as oxytocin [84, 85]. Extensive studies have been carried out on AA in the treatment of cancer and vast literature exists on AA and cancer. In 1949, AA was first proposed to be used for cancer therapy [86, 87]. The first comprehensive review on AA and cancer was published in 1979 and an updated review came 25 years later [88, 89]. AA may act as a prodrug causing the formation of AA radical and hydrogen peroxide in the extracellular space [90]. In a clinical trial, AA exerted antitumor activity in patients with advanced cancer as a stand-alone therapy as well as in combination with other anticancer agents [91]. The conjugation of AAwith extracts of medical herbs stimulated apoptosis and disrupted the cell cycle in different cancer cell lines. Furthermore, AA was pro-oxidant generating hydrogen

peroxide-dependent cytotoxicity towards various cancer cells without adversely affecting normal cells. AA together with sodium nitrite induced genotoxicity due to oxidative DNA damage. High concentrations of AA killed tumor cells *in vitro* with high efficiency and inhibited angiogenesis in mice bearing sarcoma [92-96].

For our study we used AA in combination with curcumin to assess the anticancer activity of this combination of two natural products. Due to the diversity of natural products, their anticancer mechanisms are numerous and distinctive in different components. The rationale for combination therapy is to use drugs that act by different mechanisms, thereby broadening target spectrum and increasing therapeutic effectiveness while decreasing the likelihood of drug resistance [97]. When treated with one drug alone, a cancer cell that develops a mutation that confers resistance to the drug will acquire proliferative advantage, which finally leads to the tumor relapses. By that time switching to a second drug is likely to no avail since a cell resistant to both drugs may have already emerged. But during combination therapy (using both drugs simultaneously), cells that are singly resistant to either drug will be eliminated by the other drug immediately, which therefore reduces the chance of a doubly mutated cell emerging and improves the cure rates [98]. In cancer therapy, the application of combination therapy was inspired in the 1960s when doctors successfully combined the antifolate methotrexate, tubulin inhibitor vincristine, the purine nucleotide synthesis inhibitor 6-mercaptoturine and the steroidal agent prednisone to treat pediatric leukemia [97].

1.4 Multidrug Resistance

Multidrug resistance is a phenomenon characterized by tumors exhibited simultaneous resistance to a number of structurally and functionally unrelated chemotherapeutic agents. A number of mechanisms have been described to explain MDR, they can be classified into cellular and non-cellular mechanisms [99, 100]. Non-cellular drug resistance can arise as a consequence of in vivo tumor growth. Here we observe in solid tumors higher vascular

permeability and absence of a functional lymphatic system. Thus poor tumor vascularization results in reduced drug access to regions within solid tumors and thus tumors are shielded from cytotoxicity[101]. Cellular based resistance can be caused by altered activity of specific enzyme systems e.g. glutathione S-transferase, GST and topoisomerase which can decrease the cytotoxic activity of drugs in a manner independent of intracellular concentrations. Further changes in the balance of proteins that control apoptosis can also reduce chemo sensitivity [102-104]. Other cellular based resistance are caused by transport based classical MDR mechanisms, here the focus is on the ATP-binding cassette (ABC) family of membrane transport ATPase. The ABC transporters involved in MDR are P-glycoprotein (P-gp) and multidrug resistance associated protein (MRP), which can be overexpressed in malignant cells and serve to pump anticancer drugs out of the cell, resulting in lack of intracellular levels of the drug necessary for effective therapy[105]. Much of the work carried out for this thesis focused on P-gp so in the subsequent sections P-gp will be discussed in detail.

1.4.1 P-gp History Structure and Function

P-gp is a member of the ATP-dependent membrane transport proteins. It is a plasma membrane protein and was first characterized in multidrug resistant Chinese hamster ovary cells [106, 107]. P-gp has been shown to pump substrates out of tumor cells through an ATP-dependent mechanism in a unidirectional manner resulting in reduced intracellular drug concentration thus decreased cytotoxicity of a broad spectrum of antitumor drugs. It is present in human, mouse and hamster cells [108]. In humans, P-glycoprotein is encoded by a small gene family consisting of two adjacent genes *MDR1 (ABCB1)* and *MDR2/3 (ABCB4)* encoding class I (involved in MDR) and class II (involved in phosphatidylcholine transport) isoforms, respectively. P-glycoprotein is found in most tissues but is highly and functionally expressed in specific tissues including the luminal membranes of various segments of the gastrointestinal tract (GIT), the blood-brain barrier (BBB), blood-testis barrier, blood-inner ear barrier, placenta, and in excretory cells such as hepatocytes in the liver, adrenal gland epithelia and

proximal tubule epithelia in the kidney. P-gp prevents the permeation and persistence of hydrophobic agents in the central nervous system, it also has an important role in tranepithelial transport of substrates into bile, urine and the gastrointestinal tract lumen. It confers a protective role to mediate xenobiotic efflux in tissues such as the brain, testis and placenta [109, 110].

Gene sequence analysis for mammalian P-gp has revealed the presence of two similar halves, each containing 6 putative transmembrane segments, and an ATP-binding consensus motif. The human protein is composed of 1280 amino acids with 12 transmembrane domains and 43% sequence homology between the two halves. The membrane topology of P-glycoprotein was first elucidated by molecular biology techniques such as Cys-mutagenesis and later by electron microscopy revealing (like other ABC transporters) that it is comprised of two homologous halves each consisting of six transmembrane (TM) segments and a cytosolic nucleotide-binding domain (NBD). The NBD contains highly conserved motifs: 1) Walker A and B motifs that are found in other ATP-binding proteins and 2) Walker C (ABC signature), which is exclusive to the ABC superfamily. Mutagenesis analysis has shown that the drug binding cavity is composed of TM segments of both halves, especially TMs 4, 5 and 6 in the N-terminal half and TMs 9, 10, 11 and 12 in the C-terminal half. High resolution crystal structures of bacterial ABC transporters (MsbA and Sav1866) remained the source of structural knowledge of P-glycoprotein especially in regards to the arrangement of the highly conserved NBDs. However, in terms of TMDs, these structures were largely controversial especially after the withdrawal of MsbA structures in 2006 due to a data processing error. It was only until 2009, when a relatively high resolution structure of mouse P-glycoprotein has been published by Aller *et al.* confirming and shedding light on the most important features of the protein. The captured conformation by Aller *et al.* is inward-facing and nucleotide-free spanning ~136 Å perpendicular and ~70 Å planar to the transmembrane bilayer forming an internal cavity within

the bilayer of ~ 6000 Å3 capable of accommodating at least two compounds simultaneously with two portals allowing access of hydrophobic ligands from the membrane [111, 112].

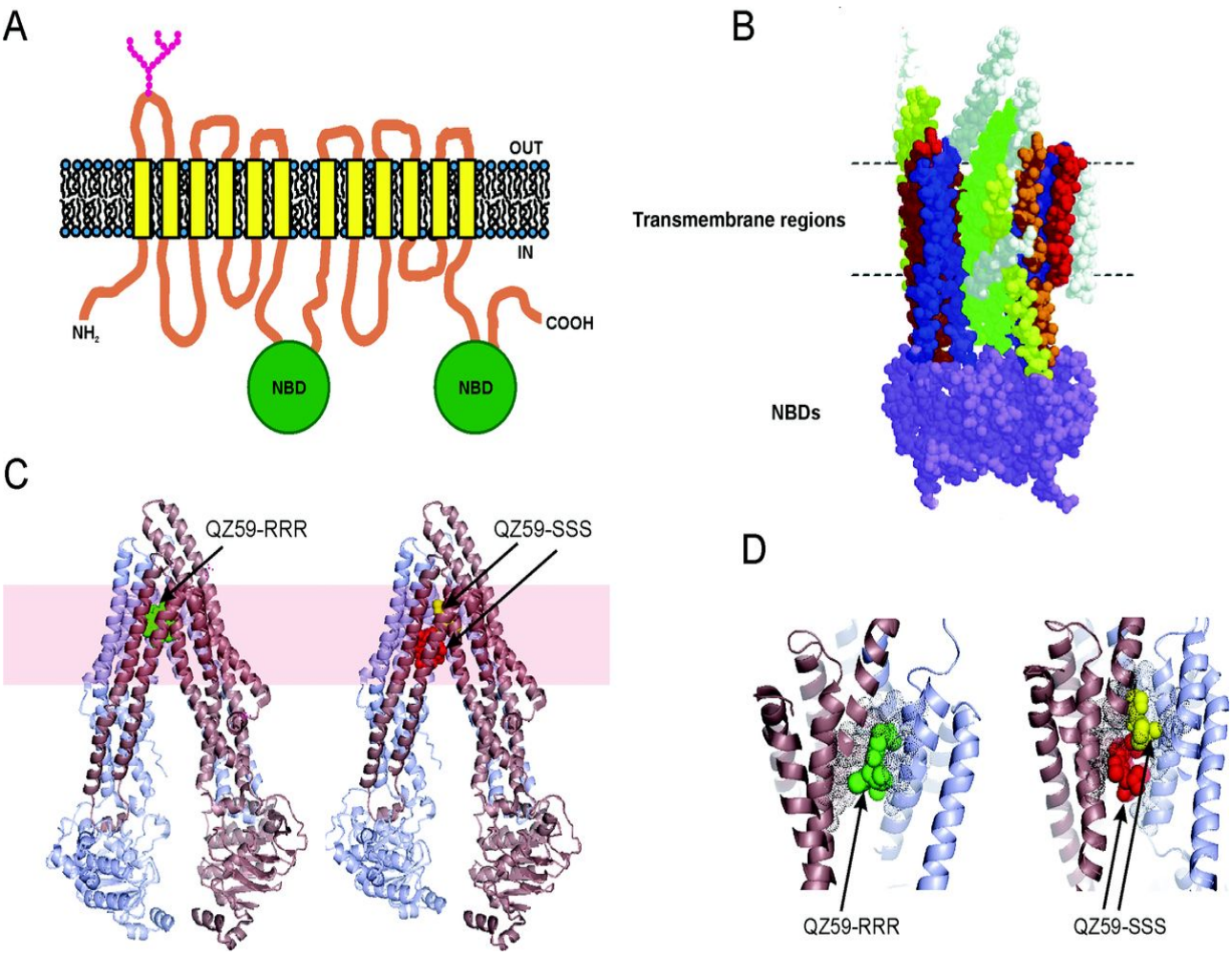

Figure 4. Topology and structure of Pgp(**A**) Topological model of Pgp, showing the two homologous halves, each with six TMHs and one NBD. (**B**) Medium-resolution cryo-EM structure of hamster Pgp bound to the non-hydrolysable nucleotide analogue AMP-PNP (adenosine 5′-[β,γ-imido]triphosphate). (**C**) High-resolution X-ray structures of mouse Pgp bound to a single molecule of the cyclic peptide substrate QZ59-RRR (left-hand panel, peptide in green; generated from PDB code 3G60) and two molecules of its stereoisomer QZ59-SSS (right-hand panel, peptides in red and yellow; generated from PDB code 3G61). The approximate location of the membrane is indicated by the coloured bar. (**D**) Close-up views of the peptides inside the substrate-binding pocket; QZ59-RRR interacting with the middle site (left), and two molecules of QZ59-SSS occupying the upper and lower sites (right). (Retrieved from (Frances J. Sharom. Essays Biochem. 2011) with permission from Portland press; Copyright 2011).

Several hypothesis have been put forward explaining the transport function of P-gp. To begin model of Higgins and Gottesman postulates that it encounters xenobiotics in the inner leaflet of the plasma membrane and flips the agents to the outer leaflet, where they diffuse into the extracellular region [113]. Other postulations are that P-gp increases intracellular pH depolarizing plasma membrane electrical potential of the cell by acting as a proton pump or a chloride channel, thus reducing intracellular accumulation of weak bases or reducing pH-dependent binding of agents to their intracellular targets. Also another idea is the hydrophobic vacuum cleaner model proposed by Gottesman and Pastan that the P-gp interacts directly with substrates in the plasma membrane and pumps them out of the cell [114].

The drug transport by P-glycoprotein involves entry of the substrate to the drug-binding pocket, conformational change and then release of drug [115]. According to the alternating access and switch models, substrates enter the drug-binding cavity through the transmembrane domains (TMDs). When this happens, an ATP-driven closure of the NBD dimer occurs in a tweezers-like motion. This leads to a decrease in the distance between the intracellular segments of TMDs thereby shifting from the inward-facing to the outward-facing conformation with a concomitant switch from high to low drug-binding affinity thereby extruding drugs and solutes to the extracellular space [115, 116].

Alternating sites:

In the alternating sites mechanism, only one catalytic site can be in a transitional state at any instant and the two sites alternate in catalysis indicating asymmetry between the NBDs at some point during the catalytic cycle. According to this model, the catalytic cycle proceeds as follows: 1) initial loose binding of ATP at both NBDs leads to the formation of a closed dimer. 2) One ATP molecule is tightly bound and committed to hydrolysis. 3) This ATP enters the transition state and the release of hydrolysis products (Pi and ADP) leads to dimer opening allowing another ATP binding to occur. In the next catalytic cycle, hydrolysis occurs at the opposite site, hence the name: alternating sites [115].

Switch model:

According to this model, the NBDs in the resting state are nucleotide-free forming an open dimer configuration. Then, binding of two ATPs leads to a closed dimer configuration. The two ATP molecules are hydrolyzed sequentially with the hydrolysis products remaining bound to the protein. This in turn leads to a sequential release of Pi and then ADP restores the protein to its basal configuration. Unlike the alternating sites model, hydrolysis of two ATP molecules is required to fulfil one catalytic cycle [116].

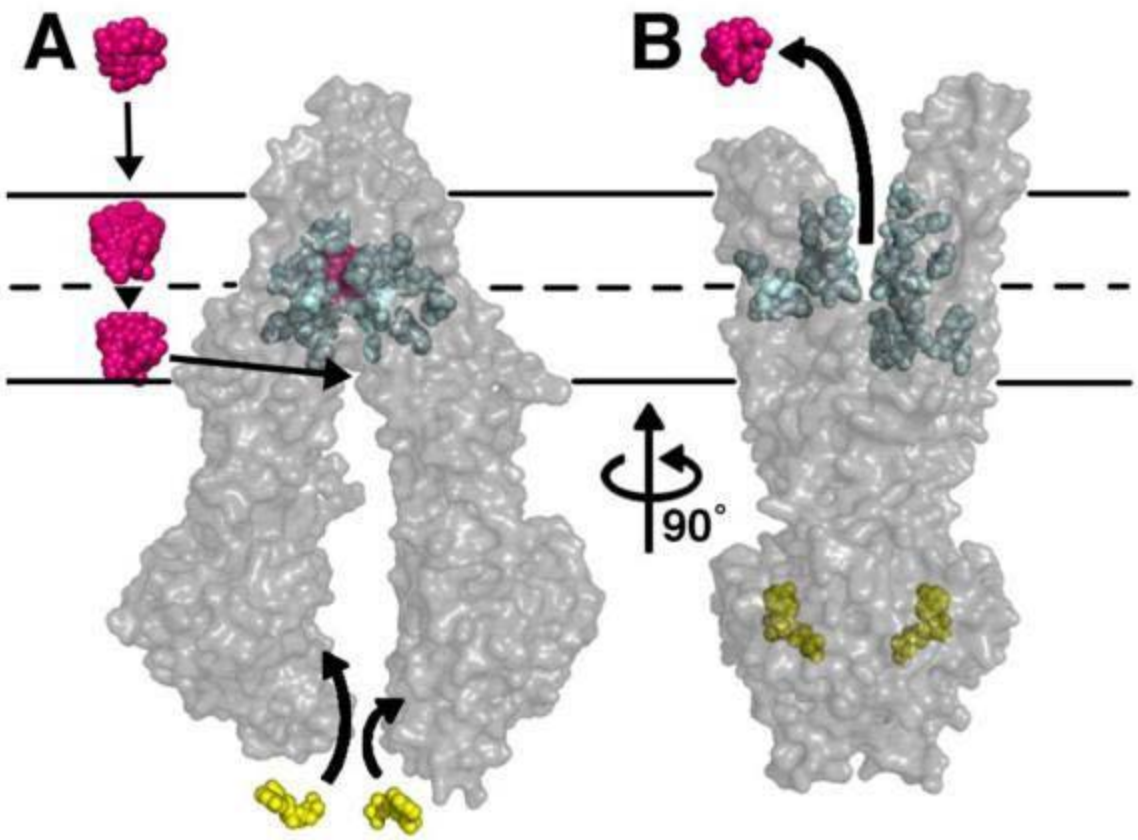

Figure 5. General scheme of P-glycoprotein efflux cycle. The substrate (magenta) partitions into the lipid bilayer from the outer leaflet to the inner leaflet. Then it gets trapped by the internal drug-binding cavity interacting with amino acids (cyan). ATP (yellow) binds to the NBDs leading to a conformational change extruding the ligand to the extracellular space. (Retrieved from (S. G. Aller *et, al*. Science 2009) with permission from AAAS; Copyright 2009).

Despite the identification of numerous P-glycoprotein inhibitors, the exact mechanism of this inhibitory process remains to be fully elaborated. Some inhibitors have been described to act through competitive interactions with the substrate over a mutual binding site [117], while

others may allosterically interact by binding to different sites than those occupied by substrates and thereby preventing the translocation and dissociation of the substrate [118]. Some agents interact with the nucleotide binding domain (NBD) causing an inhibition of the ATPase activity. One model explaining P-glycoprotein inhibition is that the transporter may handle substrates and modulators in exactly the same way, however, the flip-flop rate across the membrane bilayers is the decisive step, where it is very fast in case of modulators. Therefore, P-glycoprotein cannot keep pace with the fast flip-flop rate of the modulators and is kept busy from transporting the slower substrates [88]. A further "indirect" mechanism of inhibition is the alteration of membrane fluidity. Some agents such as anesthetics (e.g. diethyl ether) and mild neutral detergents were reported to modulate multidrug resistance and cause concomitant increase of membrane fluidity, which may have a direct consequence on the "flippase" function of P-glycoprotein or cause an indirect effect via increasing the passive movement of the substrate within the membrane through alteration of the transmembrane microenvironment [119, 120]. Hence, compounds increasing the membrane fluidity lead in turn to increased flip-flop rates of substrates, which P-glycoprotein is not able to keep up with. Our approach in this part study was to use nineteen new synthetic derivatives of curcumin and assess their ability to inhibit the function of P-gp which was the extrusion of doxorubicin from the multidrug resistant cell line CEM/ADR5000. From previous studies curcumin has been shown to be able to inhibit P-gp function and we were ready to assess the ability of the new synthetic derivatives of curcumin.

2. Aim of the thesis

Despite significant advances in treatment modalities over the last decade, neither the incidence of the disease not the mortality due to cancer has altered in the last thirty years. Available anti-cancer drugs exhibit limited efficacy due to rapid development of multidrug resistance, buildup of severe side effects and also cost related implications as medication for cancer is expensive. Thus identification of pharmacological agents that do not have these disadvantages is required. Curcumin, is one such agent that has been extensively studied over the last three to four decades for its potential anti-inflammatory and anti-cancer effects. However curcumin activity is limited by its weak bioavailability due to poor absorption and rapid metabolism as well as its low water solubility. Several strategies are being tested to overcome these limitations and the research conducted and presented in this thesis hopes to contribute and become one of the strategies. This thesis aims at the following:

1. **To evaluate from a pool of nineteen synthetic derivatives of curcumin a curcumin-derived molecule with better bioavailability and improved selectivity in vitro against sensitive and multidrug resistant T-cell acute leukemia cell lines.**

   19 synthetic derivatives of curcumin were screened for their cytotoxicity against sensitive and multidrug resistant P-glycoprotein overexpressing leukemia cells to gain insight on their cytotoxic ability; further their ability to inhibit P-glycoprotein was tested both in assay and in silico using molecular docking and a quantitative structure activity relationship model was used to predict a good correlation between the biological activity and the predicted activity from molecular docking.

2. **To analyze and exhibit that curcumin is a better anticancer agent when in combination with ascorbic acid *in vitro* against sensitive and multidrug resistant T-cell acute leukemia cell lines among other cancer cell lines; further to explain the interaction between the two compounds using pharmacogenomics analysis**

3. Results

3.1 Curcumin and it synthetic derivatives overcoming MDR

Despite its huge anticancer potential the use of curcumin is limited by its weak bioavailability and its low water solubility. Several strategies are being tested to overcome these limitations and many structurally modified curcumin derivatives have been chemically synthesized and evaluated in the pursuit of creating a 'perfect curcumin'. As part of our study we assess nineteen new synthetic derivatives of curcumin and the role they play in overcoming multidrug resistance by examining their ability to inhibit P-gp activity. We also carry out some *in silico* studies to establish their binding ability to P-gp and the quantitative structure activity relationships.

3.1.1 Chemical structures of curcumin synthetic derivatives used in this study.

Curcumin synthetic derivatives were prepared by our collaborators from the University of Western Cape in South Africa. Two series of curcumin derivatives *viz.* the chloro series (series A) and the asymmetric series (series B) were synthesized by reaction of acetyl acetone or 3-chloroacetylacetone with boric oxide. The intermediate boron complex was reacted with an appropriate benzaldehyde leading to curcumin derivatives. The yield of the series B compounds was poor due to a simultaneous reaction of acetylacetone and two different aldehydes. The percentage yields of the syntheses and the purity of each compound synthesized in the 1A and 1B series are displayed in **Table 2** while the novel compounds *viz.*, the 1A and 1B series structures are illustrated in **Fig.6** and **Fig.7** below

Table 2: Percentage yield and percentage purity of Series 1A and 1B synthetic derivatives of curcumin.

Drug	**Yield (%)**	**Purity (%) (GC)**
1A2	56%	>99%
1A3	33%	>99%
1A4	25%	>99%
1A5	40%	>99%
1A6	31%	>99%
1A7	28%	>99%
1A8	25%	>99%
1A9	47%	>99%
1A10	39%	>99%
1A11	40%	>99%
1B1	18%	>99%
1B2	15%	>99%
1B3	17%	>99%
1B4	18%	>99%
1B5	19%	>99%
1B6	18%	>99%
1B7	18%	>99%
1B8	17%	>99%

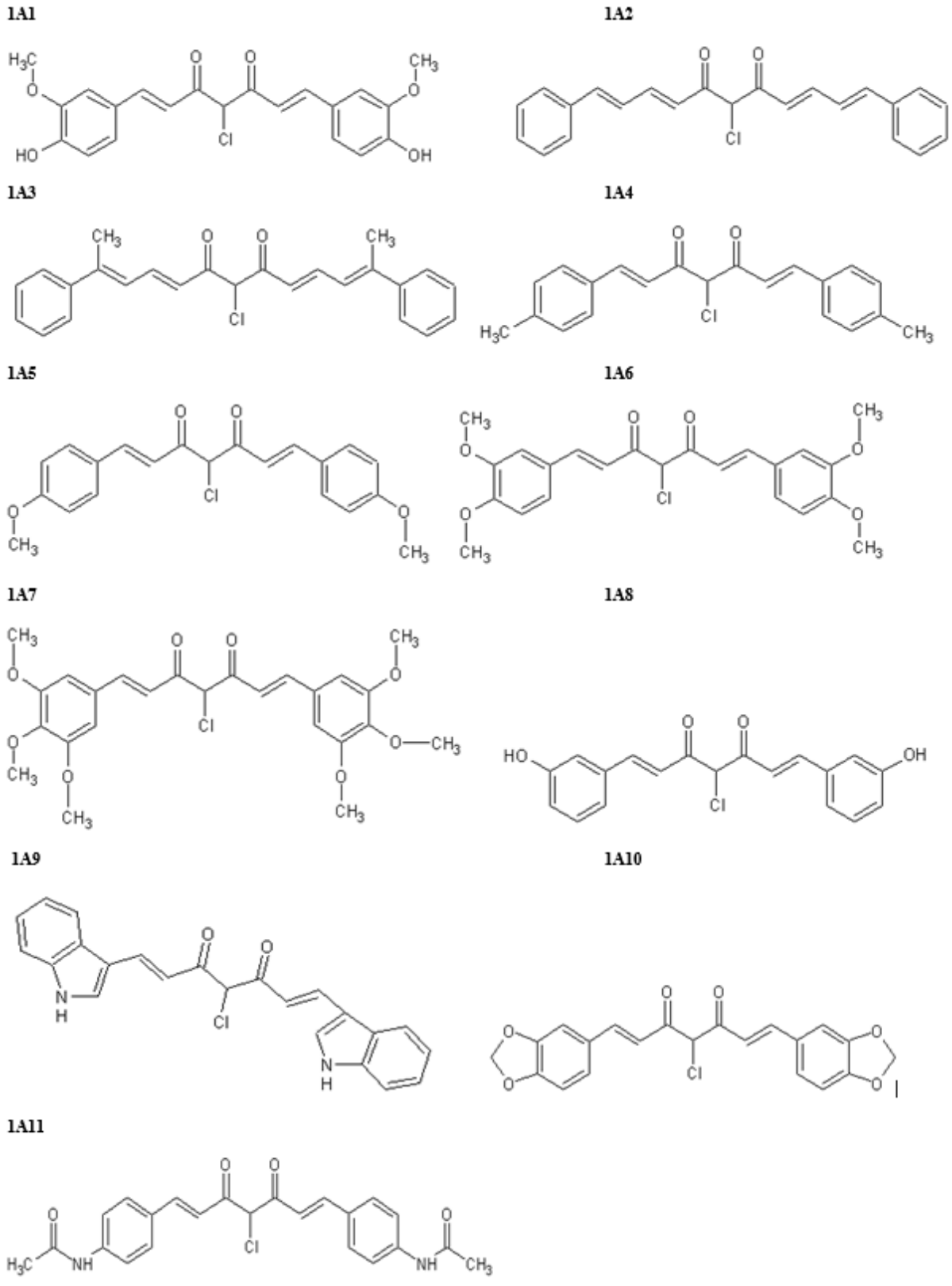

Fig. 6: Structures of synthetic derivatives curcumin A-series.

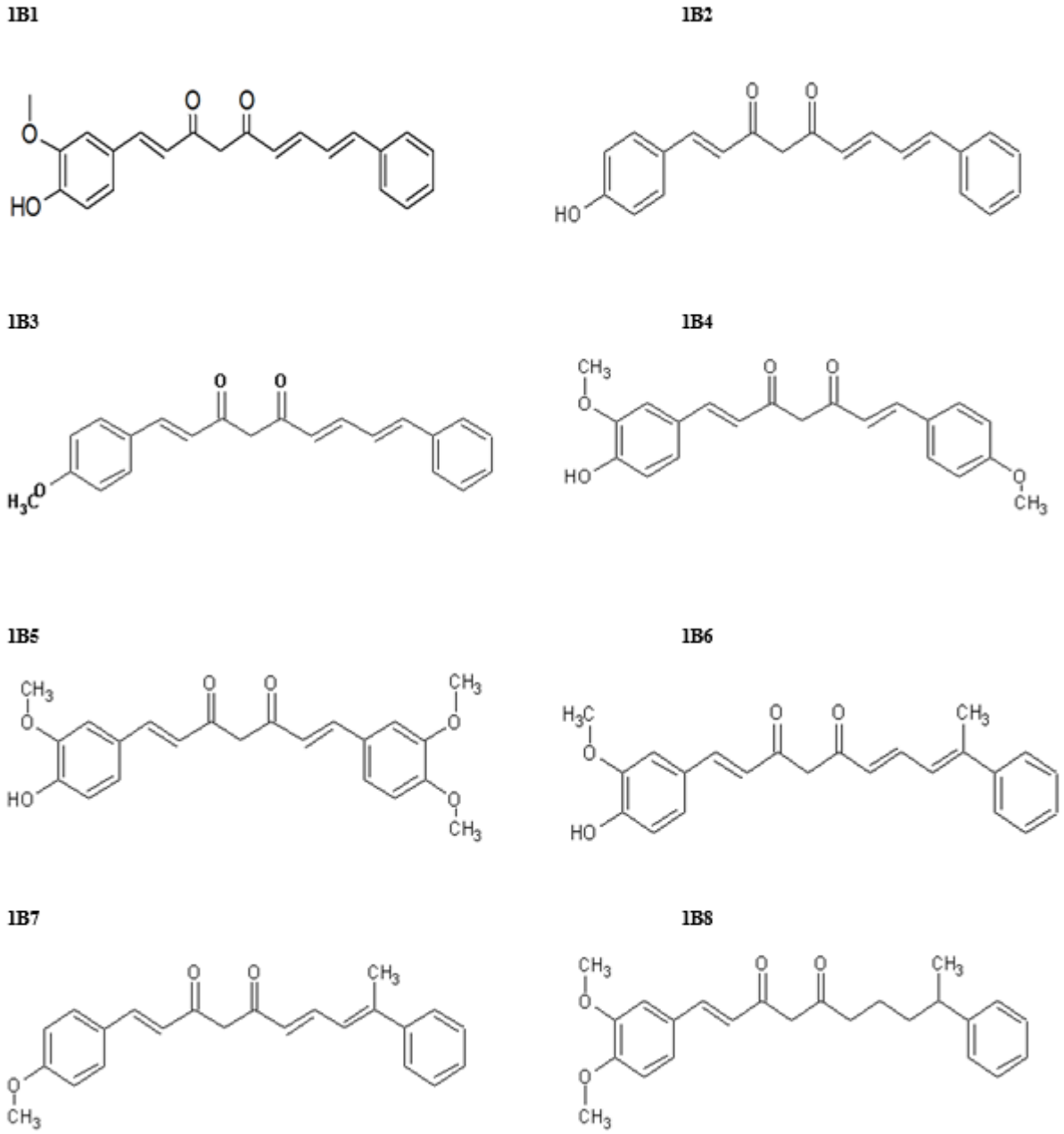

Fig. 7: Structures of synthetic derivatives of curcumin B-series.

3.1.2 Cytotoxicity of curcumin and it synthetic derivatives in sensitive and MDR leukemia cells

Resazurin assays was carried out in sensitive CCRF–CEM and multidrug-resistant CEM/ADR5000 cells using the 19 synthetic curcumin derivatives. Doxorubicin and curcumin were used as positive controls and the corresponding IC_{50} values are shown in **Table 3**. The degrees of resistance were obtained by dividing the IC_{50} values of resistant CEM/ADR5000 cells by the IC_{50} values of sensitive CCRF–CEM cells of each compound. A degree of resistance of > 1.2 indicated that the compound kills parental cells more effectively than MDR

cells and this was termed cross-resistance, while a degree of resistance < 0.9 indicated that the drug killed MDR cells more efficiently. This kind of hypersensitivity has been termed collateral sensitivity [121]. The degrees of resistance of the 19 curcumin derivatives varied from 0.72 to 3.44. Curcumin itself and 10 derivatives revealed degrees of resistance above 1.2, while three had values of below 0.9. Six derivatives had values of between 0.9 and 1.2. This indicates that CEM/ADR5000 cells exhibited cross-resistance to 10 compounds, collateral sensitivity to 3 compounds and regular sensitivity to the other 6 compounds. The collateral sensitive drugs were 1A8, 1A6, and 1B8.

Table 3: IC_{50} of curcumin and derivatives towards sensitive CCRF-CEM and multidrug-resistant CEM/ADR5000 cells. Degrees of resistance were calculated by the IC_{50} CEM/ADR5000/IC_{50} CCRF-CEM ratio. Shown are mean values ± SD of four independent experiments with each six parallel measurements.

Drug	**CCRF-CEM (µM)**	**CEM/ADR5000 (µM)**	**Degree of resistance**
1A8	0.8 ± 0.05	0.7 ± 0.03	0.875
1A11	1.2 ± 0.008	2 ± 0.03	1.67
1A2	1.4 ± 0.02	1.3 ± 0.12	0.93
1A7	1.6 ± 0.03	3.5 ± 0.05	2.19
1B2	1.6 ± 0.12	5.5 ± 0.14	3.44
1A6	1.8 ± 0.01	1.4 ± 0.04	0.78
1A3	4.6 ± 0.05	4.8 ±0.01	1.04
1A9	5.1 ± 0.59	5.0 ± 0.25	0.98
1A5	5.1 ± 0.09	5.4± 0.26	1.06
Curcumin	5.2 ± 0.05	6.3 ± 0.33	1.21
1A4	6.1 ± 0.38	5.8 ± 0.13	0.95
1B4	6.3 ± 0.02	7.6 ± 0.22	1.21
1B6	6.4 ± 0.06	8.4 ± 0.47	1.31
1A1	6.6 ± 0.05	6.8 ± 0.6	1.03
1B3	6.7 ± 0.04	9.0 ± 0.45	1.34

1B1	7.8 ± 0.02	13.2 ± 0.61	1.69
1A10	9.7 ± 0.02	12.4 ± 0.52	1.28
1B5	6.2 ± 0.002	11.2 ± 0.58	1.13
1B8	10.5 ± 0.35	7.6 ± 0.008	0.72
1B7	15 ± 0.88	20.2 ± 0.25	1.35
Doxorubicin	0.0044 ± 0.0003	2.44 ± 0.12	553.29

3.1.3 Molecular Docking

To investigate the possible binding modes of the 19 derivatives, molecular docking at two predefined sites of P-gp was performed. These sites included the transmembrane(TM) domain, whose amino acids have been subcategorized into three drug binding sites the H-(Hoechst 33342) site, the R-(rhodamine 123) site and the M-(modulator) site [122]. The other site was the ATP-binding domain [123]. Compound 1A9 exhibited the lowest predicted binding energies for both the TM-binding domains and the nucleotide binding domain of − 9 and − 9.78 kcal/mol, respectively. In the TM-binding domain, other derivatives that exhibited predicted low binding energies were compounds 1A3 and 1B5 with − 8.77 and − 8.28 kcal/mol, respectively. In the nucleotide binding domain, 1A10 and 1B2 yielded binding energies of − 9.33 and − 9.28 respectively. Overall, the predicted binding energies in the nucleotide binding domain were lower than those of the TM-binding domain. In the TM-domain, most of the amino acids in close contact with the placed ligands were those that are part of the M-site. **Fig. 8** and **Fig. 9** show the amino acids involved in binding of the selected curcumin derivatives to P-gp in the TM and nucleotide binding domains. The compounds predominantly bound to the amino acids Gly73, Thr76, Gln326, Gln330, Val 331, Thr333 and Ile340 which have been shown to be amino residues present in the M-site of the TM domain. They also interacted with the amino acids Ser474, Val476, Gln441, Gln438, Ser909, Gln912 and Val 908, which are predominant in Nucleotide binding domain 1 and which is believed to contribute only slightly to ATP hydrolysis [124].

1A9

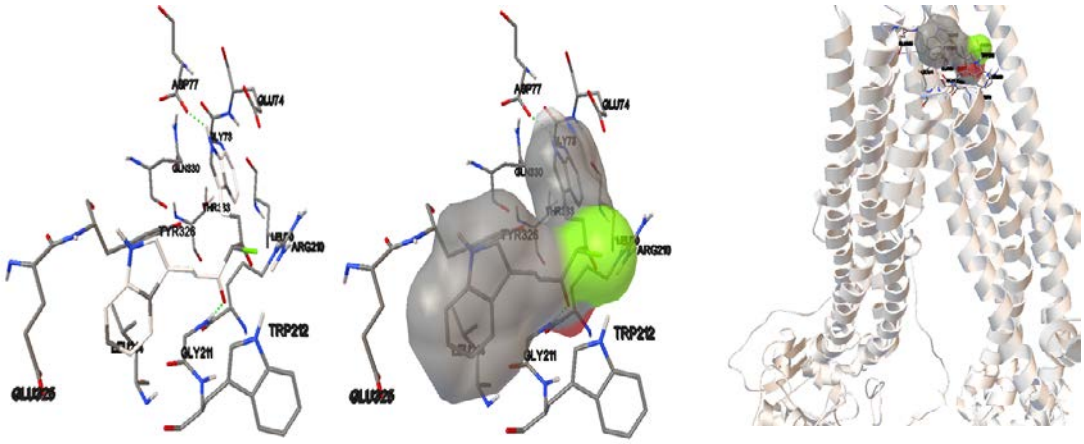

1A3

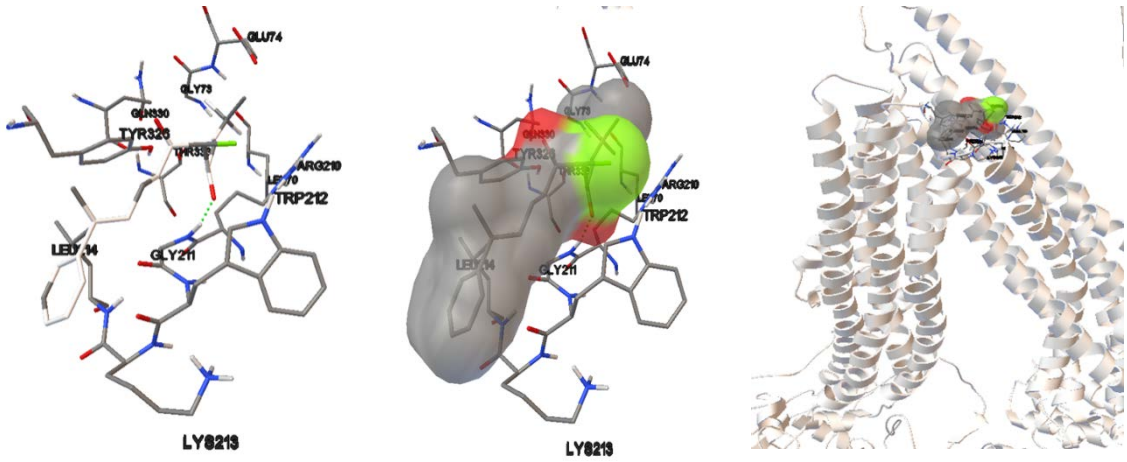

1B5

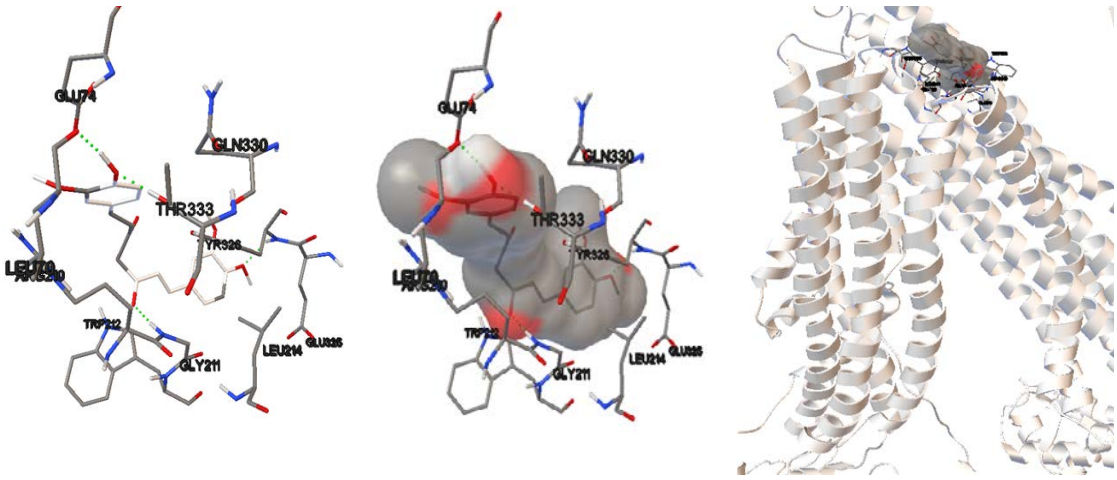

Figure 8: Molecular docking of 1A9, 1A3 and 1B5 with the lowest binding energies among the panel of 19 derivatives in the transmembrane domain of P-gp.

1A9

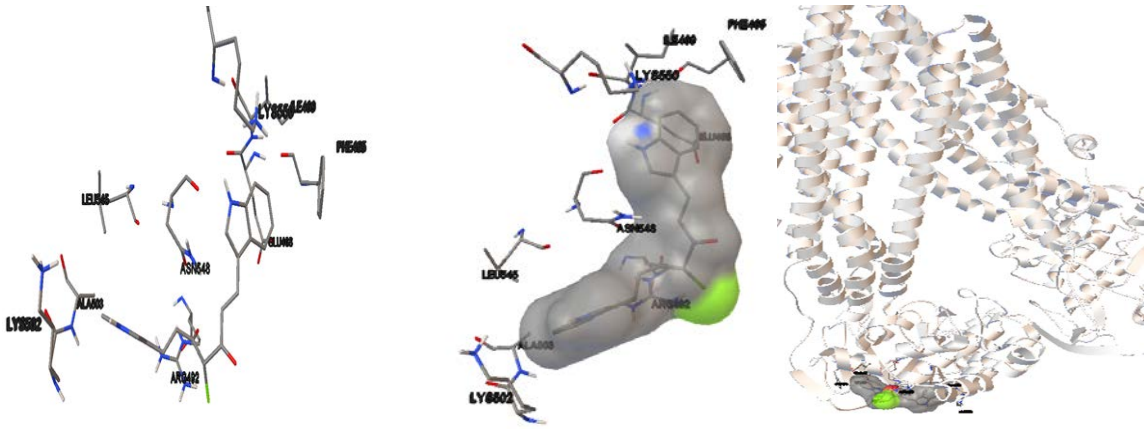

1A10

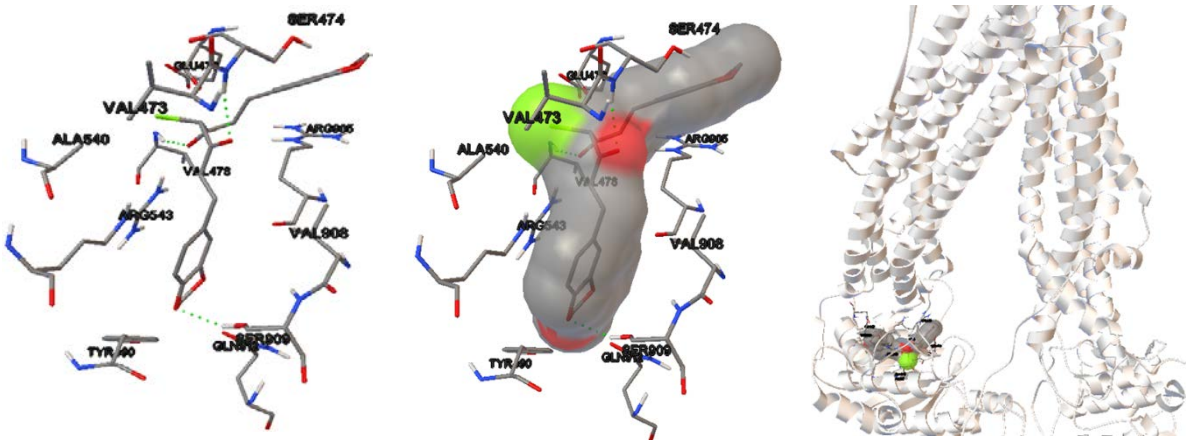

1B2

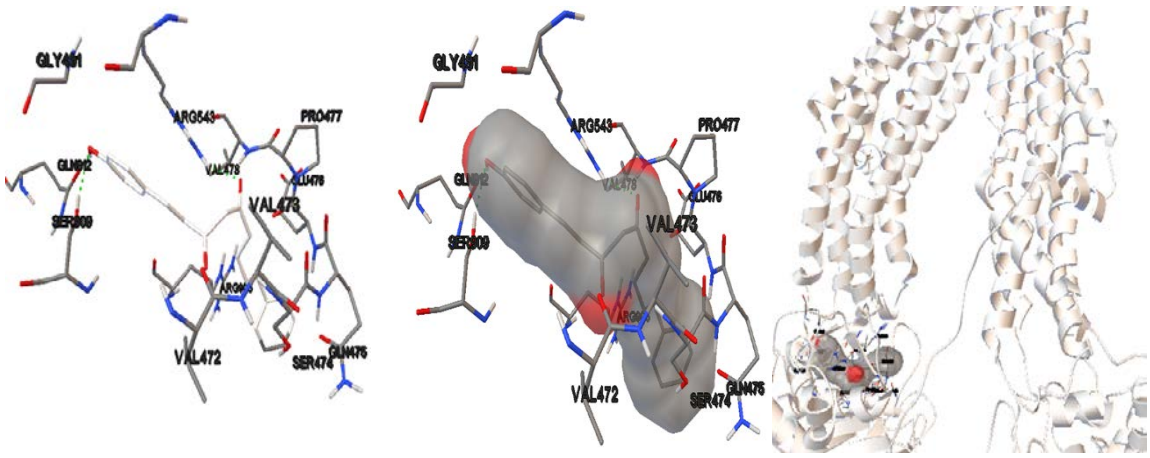

Figure 9: Molecular docking of 1A9, 1A10 and 1B2 with the lowest binding energies among the panel of 19 derivatives in the nucleotide binding domain of P-gp.

3.1.4 Quantitative structure activity relationship

As a precondition to performing QSAR analyses, the binding energies to P-gp of 48 curcumin derivatives taken from the PubChem database were calculated by molecular docking **Table 4**. The interactions obtained ranged from − 10.37 kcal/mol to − 1.57 kcal/mol in the TM-binding domain and from − 10.11 kcal/mol to − 4.91 kcal/mol in the ATP-binding domain. The inhibition constants obtained ranged between 0.04 μM to 132.5 μM. The amino acids involved in binding with the ligands, and the amino acids involved in hydrogen binding were also determined **Table 5**.

Table 4: Binding energies and inhibition constants obtained from defined docking of curcumin derivatives on P-glycoprotein for both transmembrane and nucleotide binding sites of P-gp. The values represent means ± standard deviation of three independent runs.

		Transmembrane binding domain		Nucleotide binding domain	
		Binding Energies (kcal/mol)	pKi (μM)	Binding Energies (kcal/mol)	pKi (μM)
Training set	N-(3-nitrophenylpyrazole)curcumin	-10.37 ± 0.32	0.03 ± 0.02	-10.11 ± 0.05	0.04 <0.01
Test set	1A9	-9.78 ± 0.17	0.07 ± 0.02	-9 ± 0.1	0.24 ± 0.04
Test set	1A10	-9.33 ± 0.31	0.16 ± 0.07	-7.87 ± 0.16	2.27 ± 0.62
Test set	1B2	-9.28 ± 0.11	0.16 ± 0.03	-8 ± 0.04	1.46 ± 0.1
Test set	1B1	-9.27 ± 0.29	0.17 ± 0.09	-7.7 ± 0.47	1.39 ± 0.2
Test set	1A1	-9.22 ± 0.14	0.18 ± 0.04	-7.3 ± 0.47	2.85 ± 0.27
Test set	1A2	-9.17 ± 0.49	0.23 ± 0.14	-7.8 ± 0.05	1.92 ± 0.14
Test set	1B3	-9.11 ± 0.28	0.23 ± 0.1	-7.6 ± 0.06	2.89 ± 0.27
Test set	1A8	-9 ± 0.16	0.26 ± 0.07	-8.1 ± 0.02	1.32 ± 0.88
Test set	1A3	-8.9 ± 0.4	0.34 ± 0.22	-8.77 ± 0.06	0.38 ± 0.04
Test set	1A4	-8.8 ± 0.36	0.39 ± 0.21	-6.91 ± 0.24	2.71 ± 0.28
Training set	N-(4-methoxyphenylpyrazole)curcumin	-8.78 ± 0.40	0.43 ± 0.30	-8.74 ± 0.27	0.42 ± 0.21
Training set	Bisdemethoxycurcumin isoxazole	-8.76 ± 0.07	0.38 ± 0.05	-8.99 ± 0.20	0.20 ± 0.09
Test set	1B7	-8.74 ± 0.13	0.4 ± 0.08	-7.64 ± 0.13	2.88 ± 0.22
Training set	Di-O-(2-Thienoyl)curcumin	-8.71 ± 0.36	0.46 ± 0.24	-8.96 ± 0.24	0.29 ± 0.12
Test set	1A5	-8.55 ± 0.12	0.55 ± 0.1	-6.5 ± 0.43	13.13 ± 3.03
Test set	1A6	-8.55 ± 0.12	0.55 ± 0.1	-6.2 ± 0.02	29.17 ± 0.88
Test set	1B6	-8.47 ± 0.43	0.72 ± 0.43	-6.9 ± 0.51	5.71 ± 1.48
Training set	N-phenylpyrazole curcumin	-8.44 ± 0.10	0.65 ± 0.11	-9.36 ± 0.45	0.16 ± 0.10
training set	N-(4-flurophenylpyrazole)curcumin	-8.38 ± 0.13	0.73 ± 0.17	-9.63 ± 0.58	0.11 ± 0.10
Test set	1B4	-8.38 ± 0.03	0.78 ± 0.37	-7.58 ± 0.07	2.78 ± 0.3
Training set	4-benzylidene curcumin	-8.33 ± 0.19	0.81 ± 0.23	-8.59 ± 0.65	0.69 ± 0.54
Training set	Di-O-chloroacetylethylcurcumin	-8.26 ± 0.54	0.54 ± 0.11	-7.22 ± 0.29	4.10 ± 1.25
Training set	Curcumin-difluorinated	-8.20 ± 0.63	1.90 ± 0.12	-8.16 ± 0.12	1.15 ± 0.30

Test set	1B8	-8.2 ± 0.1	0.99 ± 0.17	-7.7 ± 0.49	1.59 ± 0.08
Training set	4-(4-hydroxybenzylidene)curcumin	-8.17 ± 0.19	0.96 ± 0.19	-8.33 ± 0.71	1.12 ± 0.91
Training set	4-(4-hydroxy-3-methoxybenzylidene)curcumin	-8.10 ± 0.35	1.30 ± 0.76	-8.85 ± 0.65	0.48 ± 0.45
Test set	1B5	-8.06 ± 0.27	1.13 ± 0.75	-8.28 ± 0.26	0.84 ± 0.29
Training set	Curcumin pyrazole	-8.01 ± 0.12	1.36 ± 0.26	-9.04 ± 0.13	0.24 ± 0.06
Training set	Curcumin tri adamantylaniniethylcarbonate	-7.91 ± 0.20	1.65 ± 0.60	-8.66 ± 0.71	0.67 ± 0.61
Training set	CN2622435	-7.89 ± 0.14	1.66 ± 0.37	-8.65 ± 0.10	0.46 ± 0.08
Training set	Curcumin bis-acetate	-7.86 ± 0.35	1.91 ± 0.95	-8.18 ± 0.37	1.14 ± 0.58
Training set	HO-3867	-7.82 ± 0.29	1.40 ± 0.09	-7.92 ± 0.48	1.08 ± 0.37
Training set	ACI05TIL	-7.74 ± 0.23	2.23 ± 0.80	-8.53 ± 0.20	0.56 ± 0.21
Training set	Tetrahydrocurcumin isoxazole	-7.71 ± 0.16	2.32 ± 0.68	-8.83 ± 0.42	0.40 ± 0.29
Training set	Allyl-curcumin	-7.70 ± 0.28	1.72 ± 0.04	-7.40 ± 0.38	2.73 ± 0.74
Training set	Monodemethoxycurcumin	-7.52 ± 0.23	2.48 ± 0.26	-8.16 ± 0.15	1.06 ± 0.26
Training set	Ethyl curcumin	-7.51 ± 0.14	3.18 ± 0.71	-8.35 ± 0.15	0.77 ± 0.19
Training set	Bisdemethoxycurcumin	-7.51 ± 0.12	3.15 ± 0.58	-8.65 ± 0.16	0.46 ± 0.12
Test set	1A11	-7.50 ± 0.26	3.38 ± 1.28	-7.24 ± 0.26	0.41 ± 0.06
Training set	Demethlcurcumin	-7.48 ± 0.12	3.34 ± 0.62	-8.88 ± 0.07	0.31 ± 0.04
Training set	Curcumin-d6	-7.45 ± 0.25	2.75 ± 0.27	-8.43 ± 0.29	0.71 ± 0.29
Training set	GNF-pf-2695	-7.42 ± 0.23	3.00 ± 0.57	-7.19 ± 0.07	5.44 ± 0.67
Training set	(13C)-curcumin	-7.39 ± 0.20	4.62 ± 0.52	-8.09 ± 0.28	1.27 ± 0.62
Training set	Curcumin-a-d-glucuronide	-7.38 ± 0.22	4.08 ± 0.15	-8.24 ± 0.20	0.94 ± 0.34
Training set	Curcumin	-7.31 ± 0.16	4.06 ± 1.16	-8.52 ± 0.16	0.58 ± 0.15
Training set	Di-O-(2-hydroxyethyl)curcumin	-7.20 ± 0.05	5.30 ± 0.39	-6.92 ± 0.56	14.67 ± 1.82
Training set	Mono-O-(2-hydroxyethyl)curcumin	-7.13 ± 0.37	6.69 ± 0.36	-7.35 ± 0.44	2.67 ± 0.35
Training set	Lestestuianin B	-7.06 ± 0.30	4.97 ± 0.55	-8.46 ± 0.64	0.82 ± 0.55
Training set	CN535140	-7.06 ± 0.30	5.13 ± 0.94	-8.20 ± 0.19	1.00 ± 0.28
Training set	Didemethlcurcumin	-7.05 ± 0.13	6.89 ± 1.50	-9.11 ± 0.12	0.21 ± 0.05
Training set	CID 10595440	-7.00 ± 0.12	8.16 ± 0.13	-8.06 ± 0.18	1.28 ± 0.36
Training set	(18FP)-curcumin	-6.99 ± 0.06	7.50 ± 0.74	-7.58 ± 0.46	1.83 ± 0.89
Training set	Monovalinlylcurcumin	-6.97 ± 0.68	5.00 ± 1.13	-8.29 ± 0.37	0.94 ± 0.47
Training set	CID 10666836	-6.96 ± 0.14	7.06 ± 1.03	-8.02 ± 0.08	1.34 ± 0.19
Test set	1A7	-6.79 ± 0.01	0.03 ± 0.03	-7 ± 0.34	5.59± 0.28
Training set	Momoglycinoyl curcumin	-6.75 ± 0.28	12.17 ±0.62	-8.62 ± 0.92	0.83 ± 0.66
Training set	Curcumin monoglucoside	-6.62 ± 0.51	0.02 < 0.01	-7.45 ± 0.41	2.59 ± 0.87
Training set	Tetrahydro curcumin-d6	-6.61 ± 0.39	20.76 ±0.02	-8.19 ± 0.51	1.20 ± 0.75
Training set	Di-O-chloropropionylethylcurcumin	-6.31 ± 0.15	25.87 ±0.86	-6.82 ± 0.51	5.61 ± 1.50
Training set	Hexahydrocurcumin	-6.03 ± 0.28	0.04 ± 0.02	-7.28 ± 0.41	6.90 ± 0.25
Training set	Curcumin tri trithiadiazolaminoethylcarbonate	-5.79 ± 0.20	0.06 ± 0.02	-6.18 ± 0.92	0.08 ± 0.01
Training set	Curcumin diglucoside	-5.46 ± 0.31	0.11 ± 0.05	-6.26 ± 0.93	0.06 ± 0.01
Training set	Curcumin-a-d-glucuronide triacetate methyl ester	-5.33 ± 0.33	0.13 ± 0.07	-6.19 ± 0.59	0.05 ±0.01
Training set	Curcumin 4-O-beta-d-gentiobiosyl 4-O beta-d-glucoside	-3.38 ± 0.34	4.65 ± 0.51	-4.33 ± 0.70	0.94 ± 0.67
Training set	Tetrahydrocurcumin	2.16 ± 0.76	13.37 ±0.50	-7.67 ± 0.38	3.48 ± 0.41
Training set	Curcumin 4,4-O-beta-D-digentiobioside	-1.57 ± 0.49	0.08 ± 0.07	-4.91 ± 0.81	0.40 ± 0.37

Table 5: Amino acids of P-gp involved in binding of curcumin derivatives and amino acids involved in hydrogen binding in both the nucleotide and transmembrane binding sites of P-glycoprotein.

	Nucleotide binding domain		Transmembrane binding domain	
	No. of amino acids	Amino acids in H bonds	No. of amino acids	Amino acids in H bonds
N-(3-nitrophenylpyrazole)curcumin	12	3(Arg666, Arg669, Ser667)	9	1(Lys234)
1A9	9		12	2(Asp77, Gly211)
1A10	11	3(Ser474, Val476, Ser909)	11	4(Thr333, Gly211, Tyr326, Asp77)
1B2	12	2(Ser909, Arg543)	11	3(Glu74, Thr333, Gly211)
1B1	15	2(Ser 909, gln912)	11	2(Gly73, Thr333)
1A1	11	2(Gln441, arg547)	11	3(Trp212, Gly211, Tyr326)
1A2	13	1(Arg543)	11	1(Gly211)
1B3	15	1(Arg547)	11	2(Tyr326, Gly211)
1A8	12	2(Gln 438, Val 908)	11	3(Thr333, Leu70, Gly211)
1A3	12	2(Gln438, Val908)	11	1(Gly211)
1A4	13	1(Ser474)	11	3(Trp212, Gly211, Tyr326)
N-(4-flurophenylpyrazole)curcumin	12	2(Ser675, Arg664)	12	
N-phenylpyrazole curcumin	12	2(Ser675, Arg664)	11	2(Lys234, Gln347)
1B7	14	3(Val 474, Glu476, Arg543)	9	4(Glu74, Gly211, Tyr326, Thr333)
Didemethlcurcumin	10	4(Ala677, Ser675, Ser661, Lys665)	12	1(Phe303)
1A5	12	3(Ser474, Val 478, Ser909)	10	3(Thr333, Gly211, Tyr326)
1A6	14	3(Gln438, Gln475, Arg543)	10	1(Arg210)
1B6	14	1(Gln441)	11	2(Glu74, Glu325)
Curcumin pyrazole	15	2(Gln1118, Ser671)	10	2(Lys234, Gln347)
Bisdemethoxycurcumin isoxazole	11	2(Ser1204, Ser671)	11	1(Ser222)
1B4	12	3(Arg543, Arg547, Gly471)	10	2(Gly73, Thr333)
Di-O-(2-Thienoyl)curcumin	15	1(Arg670)	10	
Demethlcurcumin	10	5(Ser661, Thr563, Ile663, Lys665, Ala677)	9	1(Val338)
4-(4-hydroxy-3-methoxybenzylidene)curcumin	15	3(Ser660, Arg670, Gln629)	11	1(Lys234)
1B8	10	3(Ser 474, Glu476, Arg543)	10	2(Leu70, Thr333)
Tetrahydrocurcumin isoxazole	12	2(Gln1118, Gln678)	12	2(Lys234, Val338)
N-(4-methoxyphenylpyrazole)curcumin	10	2(Arg664, Ser675)	9	
1B5	11	2(Val 478, Arg547)	10	4(Gly211, Tyr326, Thr333, Leu70)
Curcumin tri adamantylaniniethylcarbonate	13	2(Leu258, Glu255)	15	
Bisdemethoxycurcumin	11	3(Ser660, Lys665, Ser1204)	10	2(Ala342, Ser222)
CN2622435	12	3(Lys665, Arg670, Ala677)	9	
Momoglycinoyl curcumin	13	4(Ala667, Arg669, Ile663, Asp562)	12	2(Gln347, Lys234)
4-benzylidene curcumin	13	3(Glu566, Arg673, Thr563)	8	
ACI05TIL	13	4(Ser1204, Ala1205, Ala1202, Ser667)	13	2(Ile306, Phe200)
Curcumin	14	3(Lys665, Leu1176, Ile663)	8	
Lestestuianin B	10	5(Ser660, Lys665, Ser671, Gln676, Glu1119)	12	2(Ile306, Phe200)
Curcumin-d6	13	3(Lys665, Der671, Glu634)	10	

Ethyl curcumin	16	3(Ser671, Ile663, Glu634)	10	
4-(4-hydroxybenzylidene)curcumin	15	3(Ala677, Arg666, Ser671)	12	1(Ala342)
1A11	11	1(Val607)	11	1(Gly211)
Monovalinlylcurcumin	14	5(Ser660, Lys665, Arg670, Asp562, Glu1119)	12	1(Lys234)
Curcumin-a-d-glucuronide	16	6(Lys665, Ser660, Arg670, Arg673, Ile663, Thr630)	12	
CN535140	17	5(Ser660, Lys665, Arg670, Asp562, Ser671)	12	1(Ile306)
Tetrahydro curcumin-d6	18	3(Arg669, Lys665, Gln676)	8	
Curcumin bis-acetate	8	3(Ser655, Arg659, Arg670)	12	
Curcumin-a-d-glucuroride-d3	12	4(Arg673, Arg669, Ser590, Glu1119)	8	1(Gln347)
Monodemethoxycurcumin	12	3(Ile663, Ser671, Glu64)	10	
(13C)-curcumin	10	4(Ser661, Ser660, Lys665, Ala677)	12	1(Lys234)
CID 10595440	10	3(Ser655, Ala631, Glu1119)	9	1(Ser222)
CID 10666836	11	3(Lys665, Ala677, Ser671)	10	1(Gln725)
HO-3867	8	1(Arg664)	8	
Tetrahydrocurcumin	16	3(Ser660, Lys665, Arg670)	8	
(18FP)-curcumin	11	3(Ala667, Lys665, Ser671)	10	
Curcumin monoglucoside	13	6(Thr563, Arg670, Ala677, Gln678, Asp679, Gly674)	13	
Allyl-curcumin	14	1(Ala677)	9	1(Lys234)
1A7	14	1(Arg543)	11	1(Gly211)
Mono-O-(2-hydroxyethyl)curcumin	12	6(Lys665, Arg670, Ala677, Asp679, Glu1119, Gln676)	12	1(Gln347)
Hexahydrocurcumin	12	5(Ser671, Arg670, Lys665, Ala677, Gln676)	9	
Di-O-chloroacetylethylcurcumin	15	1(Lys665)	14	1(Lys234)
GNF-pf-2695	9	1(Arg659)	10	
Di-O-(2-hydroxyethyl)curcumin	19	1(Arg669)	10	1(Lys234)
Di-O-chloropropionylethylcurcumin	14	2(Arg669, Ala677)	7	
Curcumin diglucoside	16	6(Thr684, Ala677, Ile663, Ser660, Ser661, Lys665)	12	1(Ala985)
Curcumin-a-d-glucuronide triacetate methyl ester	11	3(Lys515, Gln535, Arg680)	10	1(Lys234)
Curcumin tri trithiadiazolaminoethylcarbonate	13	3(Glu625, Asp689, Ile648)	13	
Curcumin 4,4-O-beta-D-digentiobioside	19	4(Ala640, Ser1235, Ile648, Glu636)	9	4(Tyr953, Asp188, Gln347, Tyr307)
Curcumin 4-O-beta-d-gentiobiosyl 4-O beta-d-glucoside	12	4(Gln535, Ser675, Gln625, Ala650)	13	

As a next step, QSAR analyses were performed. Seven descriptor variables were correlated with binding energies for all compounds in the training set of 48 compounds from the PubChem database and in the test set of our own 19 compounds. The predicted activity for the training set with the binding energy correlated well with the QSAR descriptors ($R = 0.7914$ and $p < 0.001$)

as shown in Fig. 10. Comparable results were found for the test set and this is clearly exhibited in **Fig. 11** ($R = 0.7942$, $p < 0.001$).

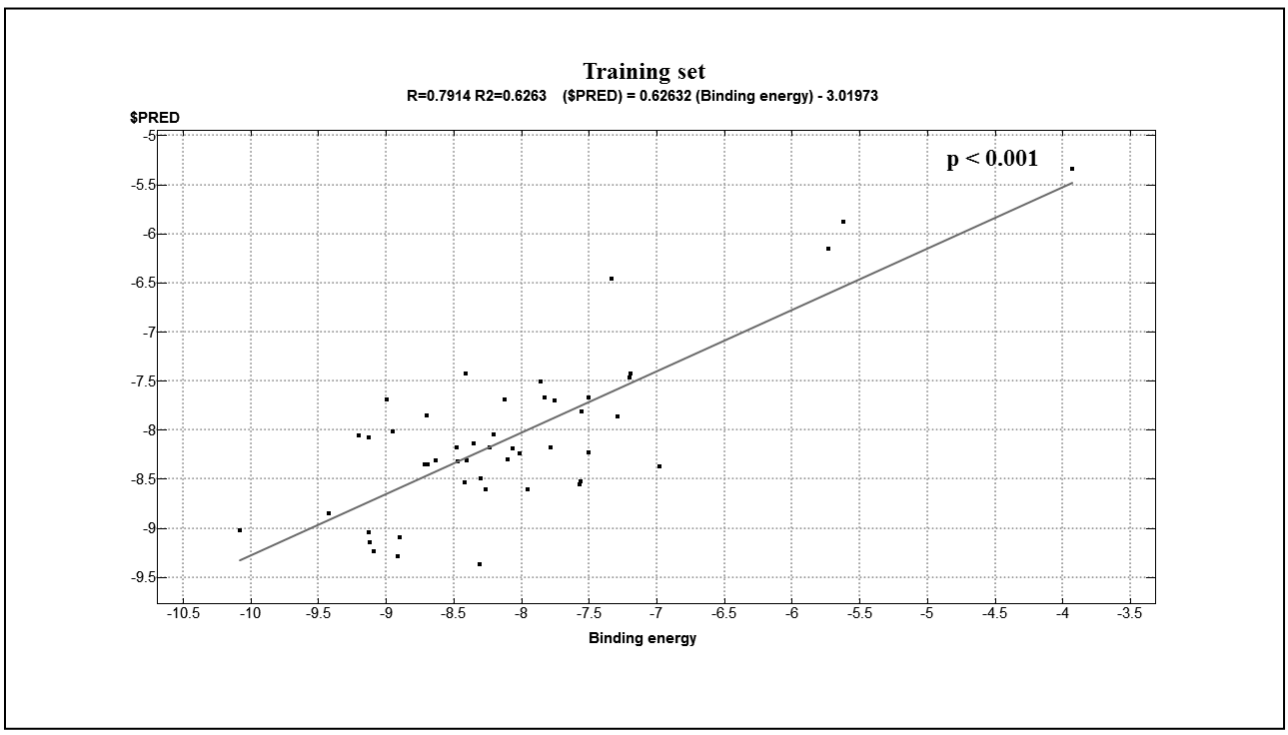

Figure 10: Correlation plot between predicted activity and the binding energy of the training set of 48 curcumin derivatives taken from the PubChem database (http://www.ncbi.nlm.nih.gov/pccompound/).

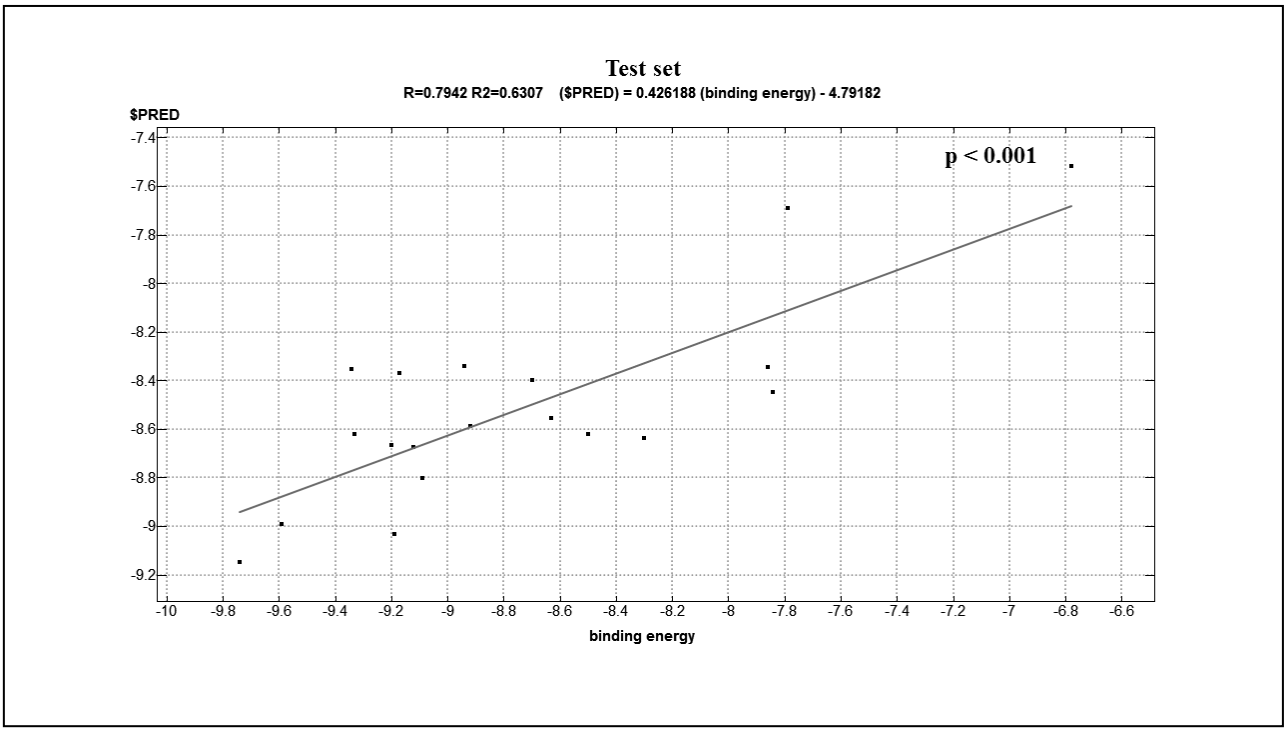

Figure 11: Correlation plot of predicted activity and binding energies of test set 19 curcumin derivatives synthesized in the present investigation.

3.1.5 Doxorubicin uptake assay analysis

The fluorescence measurement of doxorubicin by flow cytometry can be used to measure the inhibition of P-gp by specific inhibitors [125]. As shown in **Fig. 12**, CEM/ADR5000 cells took up doxorubicin considerably less than CCRF–CEM cells by a factor of 4. Verapamil was used as control compound since it is one of the best known P-gp inhibitors [126]. Verapamil partially increased doxorubicin uptake in CEM/ADR5000 cells. However, the level of CCRF–CEM cells was not reached. It is remarkable that 6 (1A2, 1A4, 1A6, 1A8, 1A9, 1B8) out of the 19 curcumin derivatives increased doxorubicin uptake in resistant cells to the same levels as in sensitive ones or even exceeded these levels.

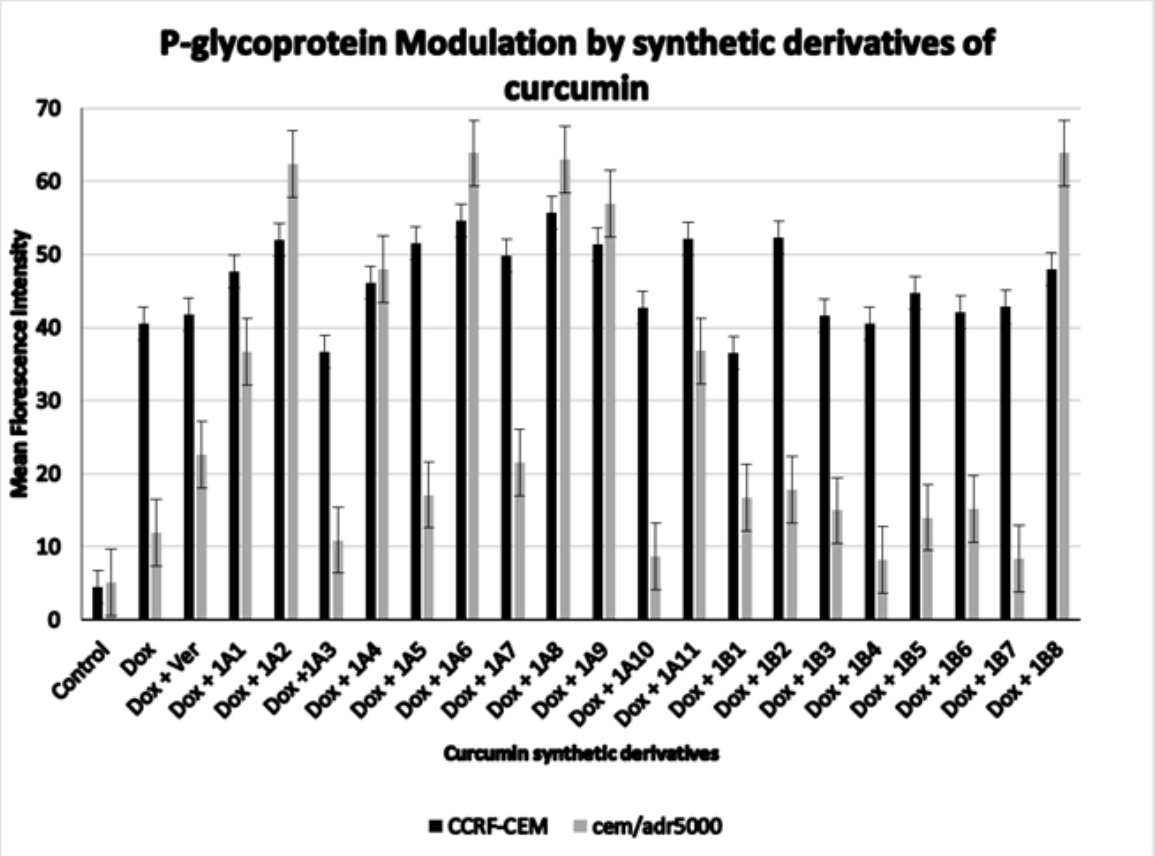

Figure 12: Effect of curcumin derivatives on doxorubicin accumulation in sensitive CCRF-CEM and multidrug-resistant CEM/ADR5000 cell lines. Doxorubicin fluorescence alone or in combination with the derivatives. Verapamil was used as a positive control for P-gp inhibition. Each bar represents a mean of three independent measurements with two replicates in one measurement.

3.1.6 Effect of curcumin and four synthetic derivatives on P-gp-ATPase activity

The effect of each compound on the respective activity (considered as 100%) was calculated as percentage increase/decrease. Cyclosporine A (CsA) was used as control inhibitor of P-gp-ATPase activity. The compounds did not induced basal P-gp-ATPase activity in a comparable manner to verapamil. In addition to basal P-gp-ATPase activity, we also investigated verapamil-stimulated P-gp-ATPase activity. Here also the compounds did not increases verapamil-stimulated P-gp-ATPase activity. Cyclosporine A caused a slight decrease of verapamil-stimulated P-gp-ATPase activity. These results are clearly exhibited in **Fig. 13**.

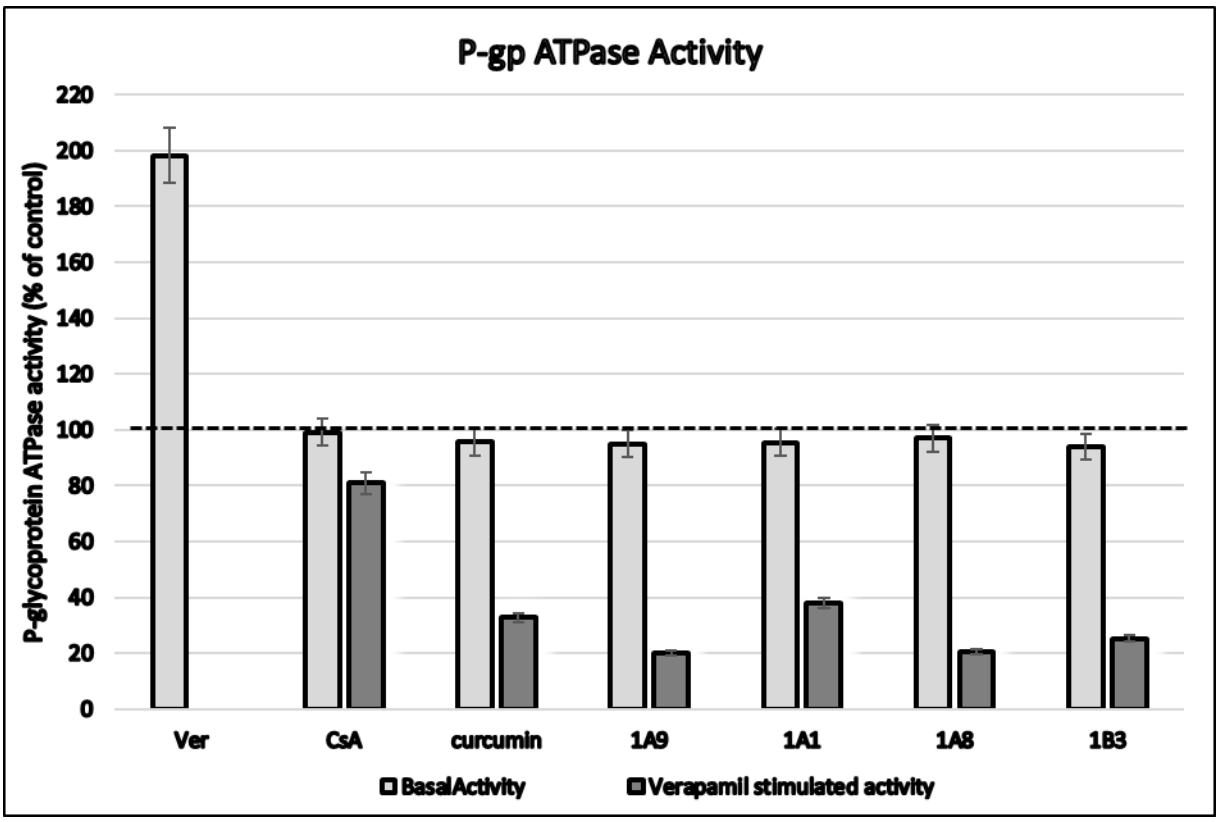

Figure 13: Effect of synthetic derivatives of curcumin on basal and verapamil stimulated P-glycoprotein ATPase activity. Each compound was tested at (50uM). Verapamil was used at a concentration of (20uM). The percentage of modulation of P-glycoprotein-ATPase activity is compared to P-glycoprotein-ATPase activity without test compound was calculated for each compound. The data from the basal and verapamil-stimulated activities were set at 100% in the respective calculation for each compound. Each bar represents a mean percentage of modulation ±SEM of two independent measurements.

3.1.7 Cytotoxicity of curcumin, 1A6 and 1A8 in combination with doxorubicin

Resazurin assay was carried out on P-gp overexpressing CEM/ADR500 cells using a combination of doxorubicin and curcumin or its synthetic derivatives 1A8 and 1A6. The combinations were made with doxorubicin at a constant concentration and the curcumin or its synthetic derivatives at varying concentrations and for the result we picked the highest concentration of curcumin that was combined with doxorubicin. Doxorubicin was tested alone on the cell line CEM/ADR5000 then further as a combination with the varied modulators. Dose response curves demonstrating the respective combinations are shown in the **Fig. 14**. A higher cytotoxicity upon co-treatment with the modulators can be clearly noticed by an overall shift of

the curve to the left. From our results the combination of doxorubicin and our modulators shows this shift to the left with fold change ranging from 5 to 10 for curcumin, 1A8 and 1A6 respectively.

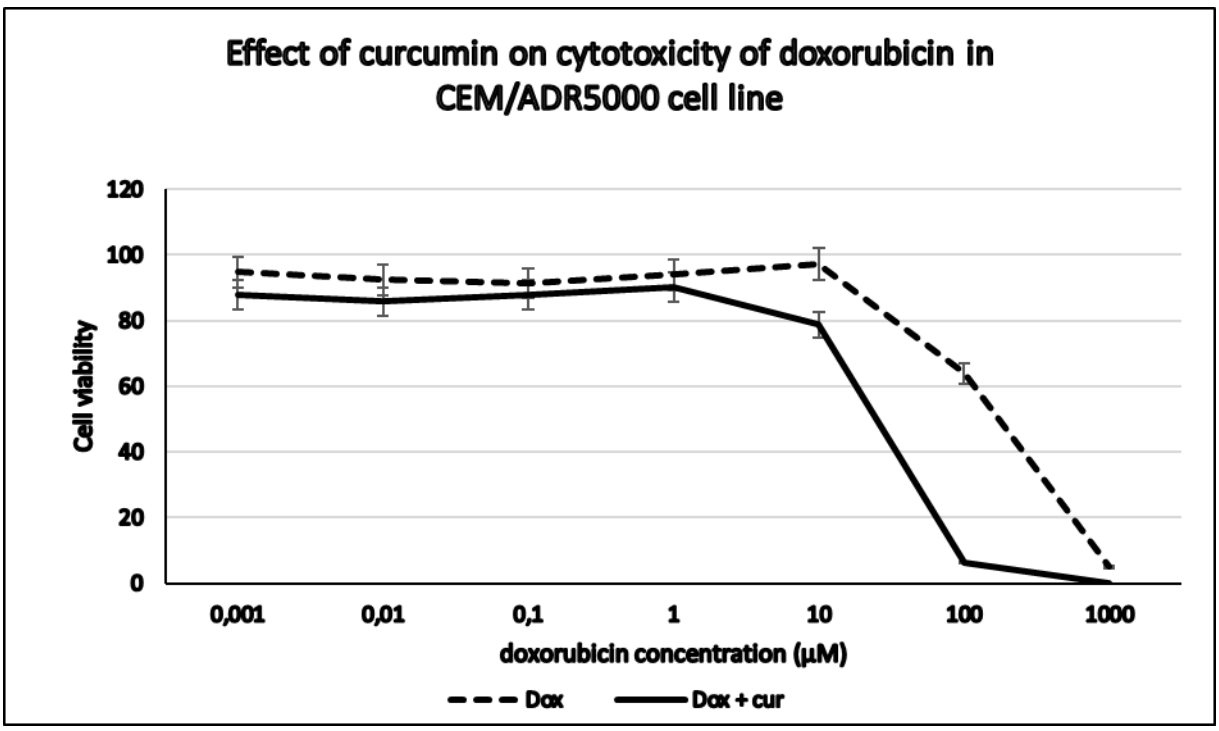

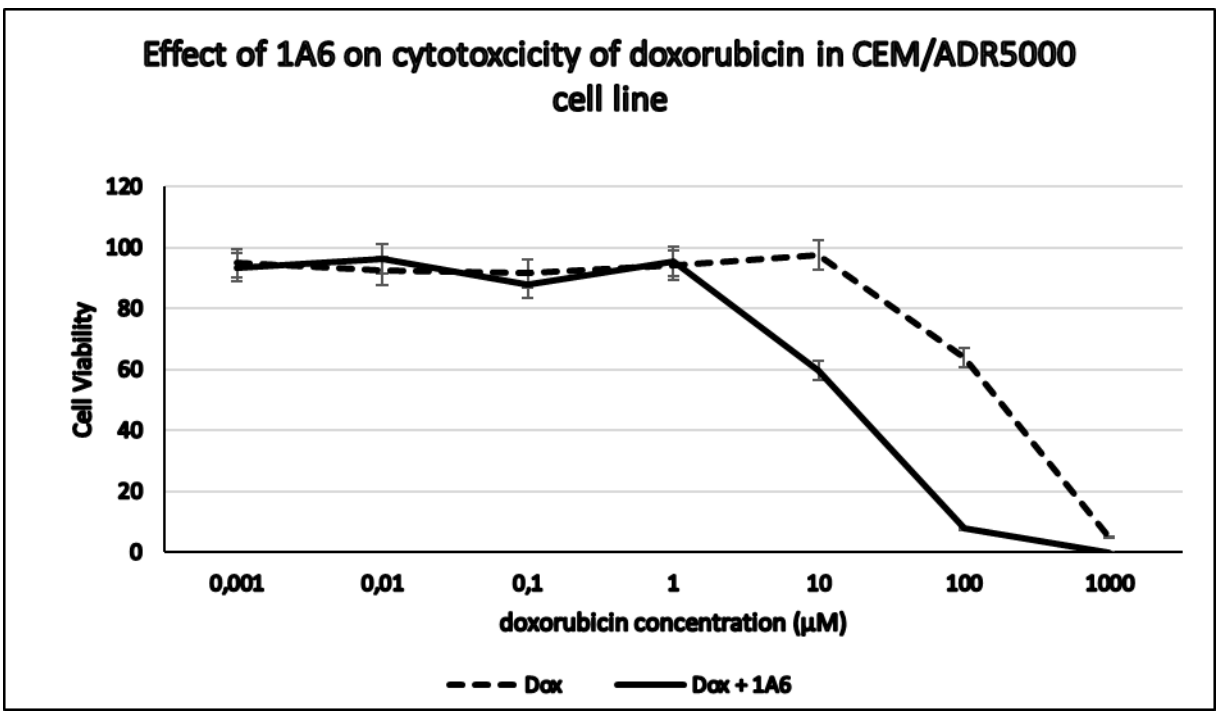

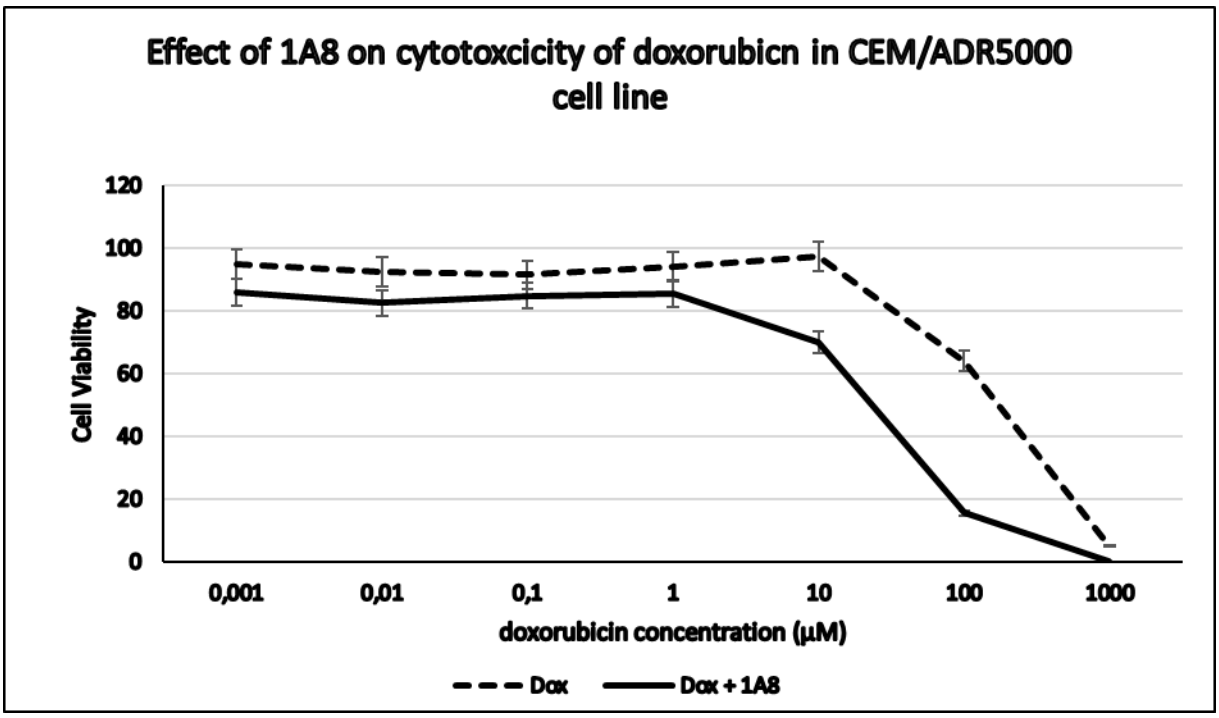

Figure 14: Effect of curcumin, 1A6 and 1A8 on the cytotoxicity of doxorubicin in P-glycoprotein overexpressing CEM/ADR5000 cells. Experiments have been repeated at least twice and for each concentration at least in triplicates. Each point represents mean ± SEM.

We also conducted the same assays in drug sensitive CCRF–CEM cells as negative controls for the expression of P-gp. The corresponding dose-response curves are shown in **Fig. 15**. The combination of doxorubicin and our modulators that is curcumin and its synthetic derivatives compared with doxorubicin alone in CCRF–CEM cells minor changes was exhibited with the fold changes ranging between 0.75 and 1.40. This strengthens the evidence that the reversal of multidrug resistance observed in CEM/ADR5000 cells is P-gp related.

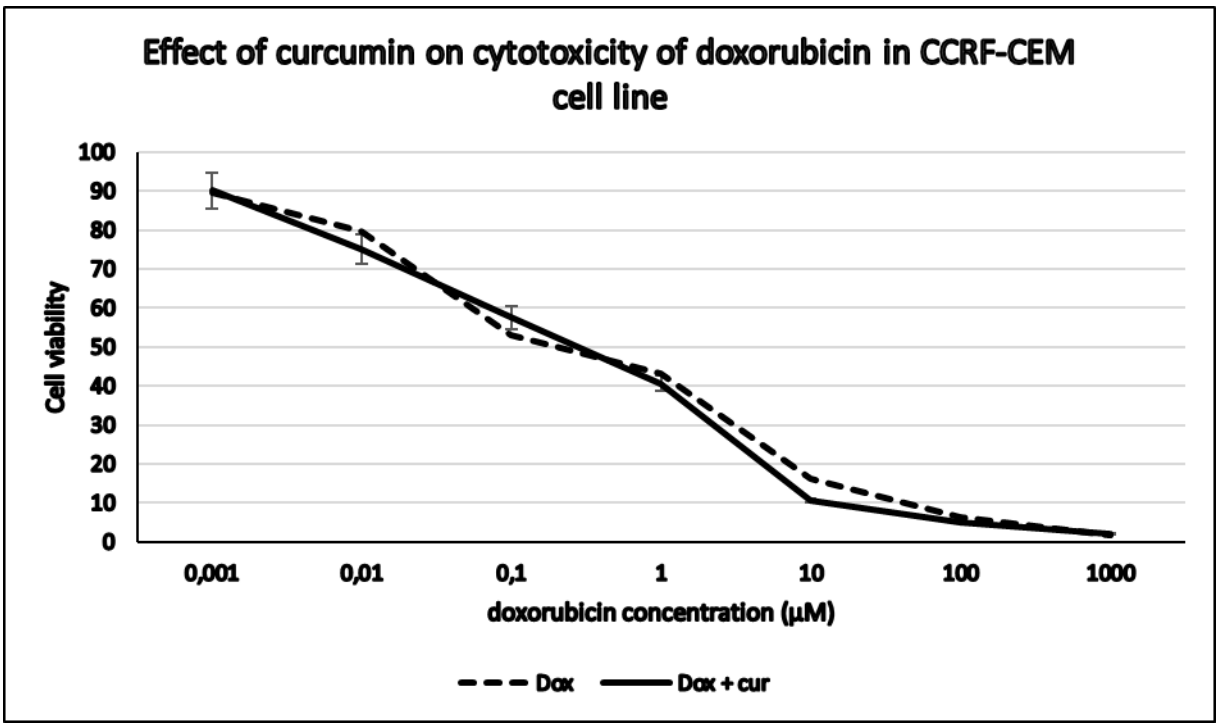
Effect of curcumin on cytotoxicity of doxorubicin in CCRF-CEM cell line
Cell viability
100
90
80
70
60
50
40
30
20
10
0
0,001
0,01
0,1
1
10
100
1000
doxorubicin concentration (µM)
Dox
Dox + cur

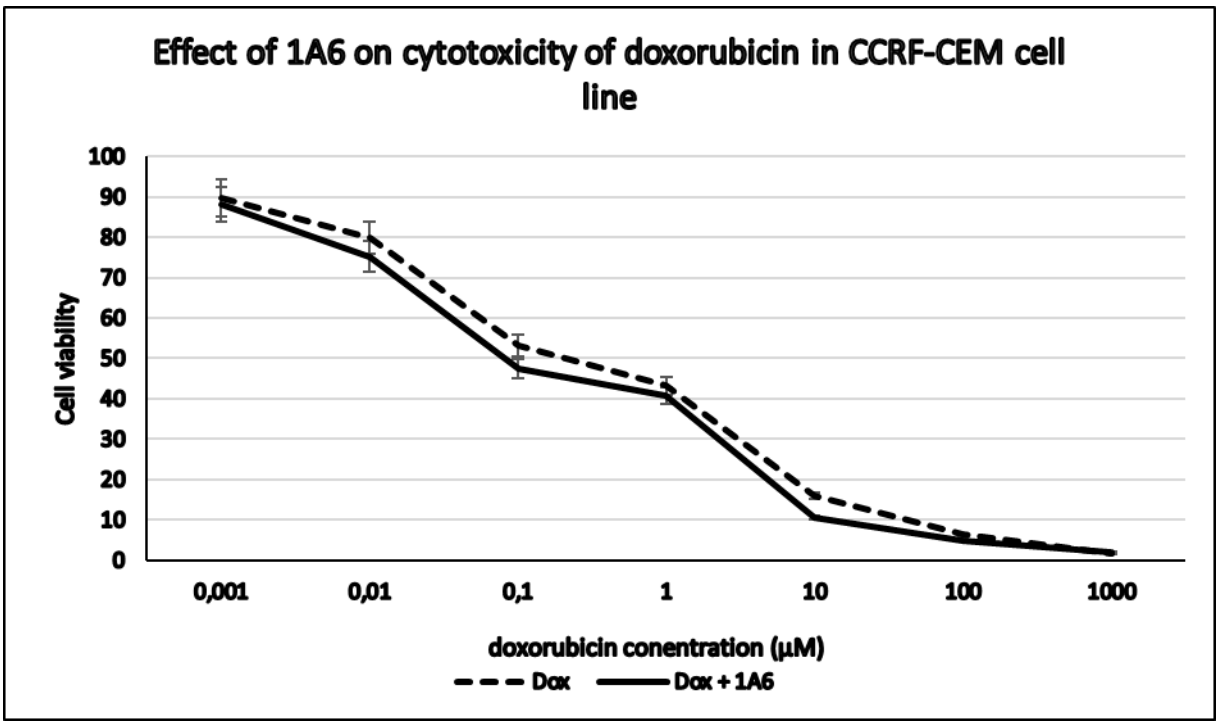
Effect of 1A6 on cytotoxicity of doxorubicin in CCRF-CEM cell line
Cell viability
100
90
80
70
60
50
40
30
20
10
0
0,001
0,01
0,1
1
10
100
1000
doxorubicin conentration (µM)
Dox
Dox + 1A6

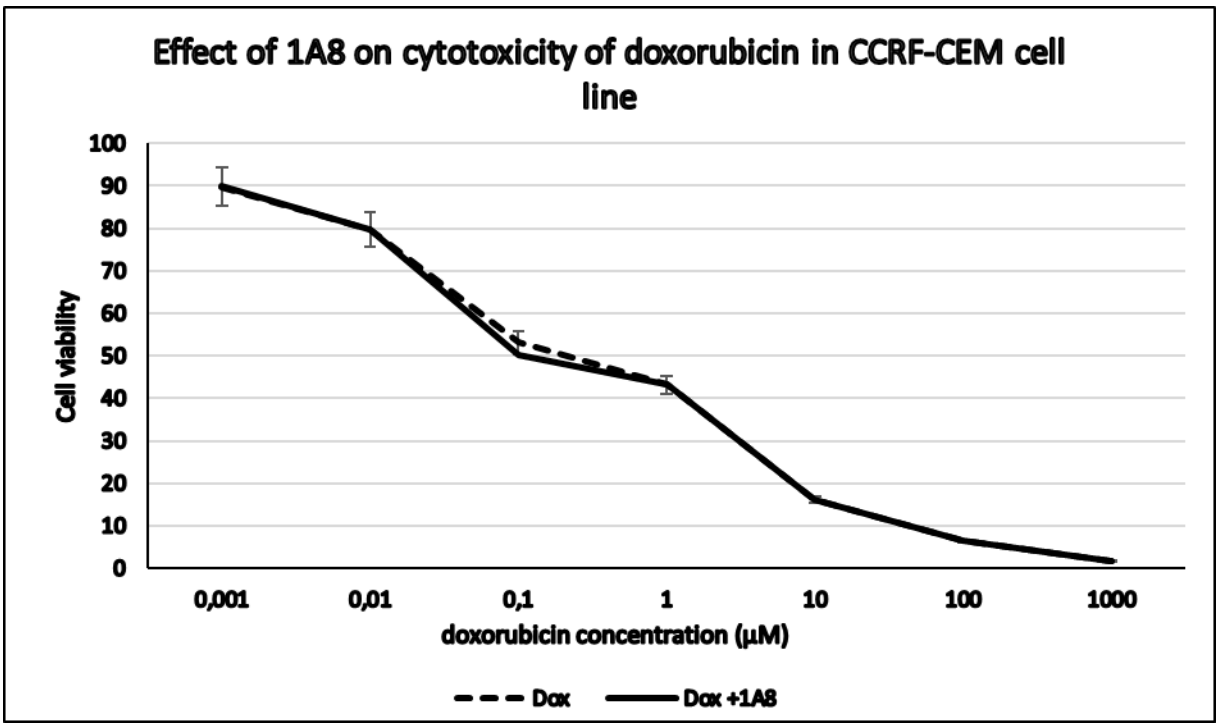

Figure 15: Effect of curcumin, 1A6 and 1A8 on the cytotoxicity of doxorubicin in drug sensitive CCRF-CEM cells. Experiments have been repeated at least twice and for each concentration at least in triplicates. Each point represents mean ± SEM

3.2 Curcumin in combination with AA

3.2.1 Chemoprofiling of different *Curcuma* species.

As a first step, we established chemoprofiles of three *Curcuma* species (*C. longa*, *C. zedoaria* and *C. xanthorrhiza*) based on the chemical compositions of these species deposited at Dr. Duke's Phytochemical and Ethnobotanical Databases (http://www.arsgrin.gov/cgi-bin/duke/farmacy2.pl). We subjected the chemical composition of these plants to hierarchical cluster analysis **Figure 16**. A total of 114 phytochemicals have been included in the analysis, which are listed in detail in **Table 6**. Three compounds were commonly found in all three *Curcuma* species (curcumin, D-camphor, and desmethoxycurcumin). Ten compounds were found in two of the three species, whereas all other compounds were found in only one *Curcuma* species. This specific distribution of phytochemicals enables specific clustering and separation of the *Curcuma* species.

Figure 16. Dendrogram obtained by hierarchical cluster analysis of phytochemical constituents of *Curcuma longa*, *C. zedoaria* and *C. xanthorrhiza*. The chemical compounds included in this cluster analysis are listed in detail in **Table 6**.

Table 6. Phytochemical constituents of three different *Curcuma* species. Data were taken from Dr. Duke's Phytochemical and Ethnobotanical Databases (http://www.arsgrin.gov/cgi-bin/duke/farmacy2.pl).

	C. longa	***C. zedoaria***	***C. xanthorrhiza***
1,4-CINEOLE	0	1	0
1,8-CINEOLE	1	1	0
2-BORNANOL	1	0	0
2-HYDROXY-METHYL-ANTHRAQUINONE	1	0	0
4-HYDROXY-CINNAMOYL-(FERULOYL)-METHANE	1	0	0
ALPHA-ATLANTONE	1	0	0
ALPHA-PHELLANDRENE	0	0	1
ALPHA-PINENE	1	1	0
ALPHA-TERPINEOL	1	0	0
AMYLOSE	0	1	0
ARABINOSE	1	0	0
AR-CURCUMENE	0	0	1
AR-TURMERONE	1	0	0
ASCORBIC-ACID	1	0	0
ATLANTONE	0	0	1
AZULENE	1	0	0
BETA-CAROTENE	1	0	0
BETA-CURCUMENE	0	0	1
BETA-PINENE	1	0	0
BETA-SESQUIPHELLANDRENE	1	0	0
BIS-(PARA-HYDROXY-CINNAMOYL)-METHANE	1	0	0
BISABOLENE	1	0	0

BIS-DESMETHOXYCURCUMIN	1	1	0
BORNEOL	1	0	1
CAFFEIC-ACID	1	0	0
CALCIUM	1	0	0
CALCIUM-OXALATE	0	0	1
CAPRYLIC-ACID	1	0	0
CARBOHYDRATES	1	0	0
CARYOPHYLLENE	1	0	0
CINEOLE	1	0	0
CINNAMIC-ACID	1	0	0
CUMINYL-ALCOHOL	1	0	0
CURCULONE	0	1	0
CURCUMADIOL	0	1	0
CURCUMANOLIDE-A	0	1	0
CURCUMANOLIDE-B	0	1	0
CURCUMENE	1	0	0
CURCUMENOL	1	1	0
CURCUMENONE	0	1	0
CURCUMIN	1	1	1
CURCUMOL	0	1	0
CURDIONE	1	1	0
CURLONE	1	0	0
CURZERENONE	1	1	0
CURZERENONE-C	1	0	0
CYCLO-ISOPRENEMYRCENE	1	0	0
D-ALPHA-PHELLANDRENE	1	0	0
D-ALPHA-PINENE	0	1	0
D-BORNEOL	0	1	0
D-CAMPHENE	1	1	0
D-CAMPHOR	1	1	1
DEHYDROCURDIONE	0	1	0
DEHYDROTURMERONE	1	0	0
DESMETHOXYCURCUMIN	1	1	1
DICINNAMOYLMETHANE	1	0	0
DIDESMETHOXYCURCUMIN	1	0	0
DIFERULOYL-METHANE	1	1	0
DIHYDROCURCUMIN	1	0	0
DI-P-COUMAROYL-METHANE	1	1	0
D-SABINENE	1	0	0
ENT-CURZERENONE	0	1	0
EPICURZERENONE	0	1	0
ETHYL-P-METHOXYCINNAMATE	0	1	0
EUGENOL	1	0	0
FERULOYL-P-COUMAROYL-METHANE	1	1	0
FURANODIENE	0	1	0
FURANODIENONE	0	1	0
GAMMA-ATLANTONE	1	0	0

GERMACRONE-4,5-EPOXIDE	0	1	0
GUAIACOL	1	0	0
ISOBORNEOL	1	0	0
ISOCURCUMENOL	0	1	0
ISOCURZERENONE	0	1	0
ISOFURANODIENONE	0	1	0
ISOFURANOGERMACRENE	0	1	1
L-ALPHA-CURCUMENE	1	0	0
L-BETA-CURCUMENE	1	0	0
L-CYCLOISOPRENEMYRCENE	0	0	1
LIMONENE	1	0	0
LINALOL	1	0	0
MONODESMETHOXYCURCUMIN	1	0	1
NIACIN	1	0	0
O-COUMARIC-ACID	1	0	0
P,P'-DIHYDROXYDICINNAMYOLMETHANE	0	1	0
P-COUMARIC-ACID	1	0	0
P-CYMENE	1	0	0
P-HYDROXYCINNAMOYLFERULOYLMETHANE	0	1	0
P-METHOXY-CINNAMIC-ACID	1	0	0
PROCURCUMENOL	0	1	0
PROTOCATECHUIC-ACID	1	0	0
P-TOLYMETHYCARBINOL	0	0	1
P-TOLYMETHYLCARBINOL	1	0	0
PYROCURCUMENONE	0	1	0
PYROCURZERENONE	0	1	0
RIBOFLAVIN	1	0	0
SESQUITERPENE-ALCOHOLS	0	1	0
SESQUITERPENES	0	1	0
SYRINGIC-ACID	1	0	0
TERPINENE	1	0	0
TERPINEOL	1	0	0
THIAMIN	1	0	0
TURMERONE	1	0	1
UKONAN-A	1	0	0
UKONAN-B	1	0	0
UKONAN-C	1	0	0
UKONAN-D	1	0	0
VANILLIC-ACID	1	0	0
XANTHORRHIZOL	0	0	1
ZEDERONE	0	1	0
ZEDOARONE	0	1	0
ZINGIBERENE	1	0	1
ZINGIBEROL	0	0	1

3.2.2 Tumor type-dependent activity of ascorbic acid.

We hypothesized that the cytotoxic effect of *C. longa* against cancer cells is not solely caused by its main compound, curcumin, but that other compounds may also contribute to this activity of the plant. To prove this hypothesis, we mined the NCI database for compounds found in *C. longa* and six compounds were identified **Figure 17a**, *i.e.* AA, limonene, guaiacol, p-cymene, azulene, and curcumin. Although AA was not the most toxic compound among the six tested, we decided to continue our investigations with AA, because of its far distribution not only in *C. longa* but also in many other plants as well and it's enormous relevance for human health in general. Further investigations were then carried out using AA in the NCI panel of cell lines. Leukemia and melanoma cell lines were most sensitive, while brain and lung cancer cell lines were the most resistant ones **Figure 17b**. Established anticancer drugs frequently show high sensitivity towards leukemia, but resistance towards melanoma. Hence, it is interesting that AA was active against melanoma cell lines.

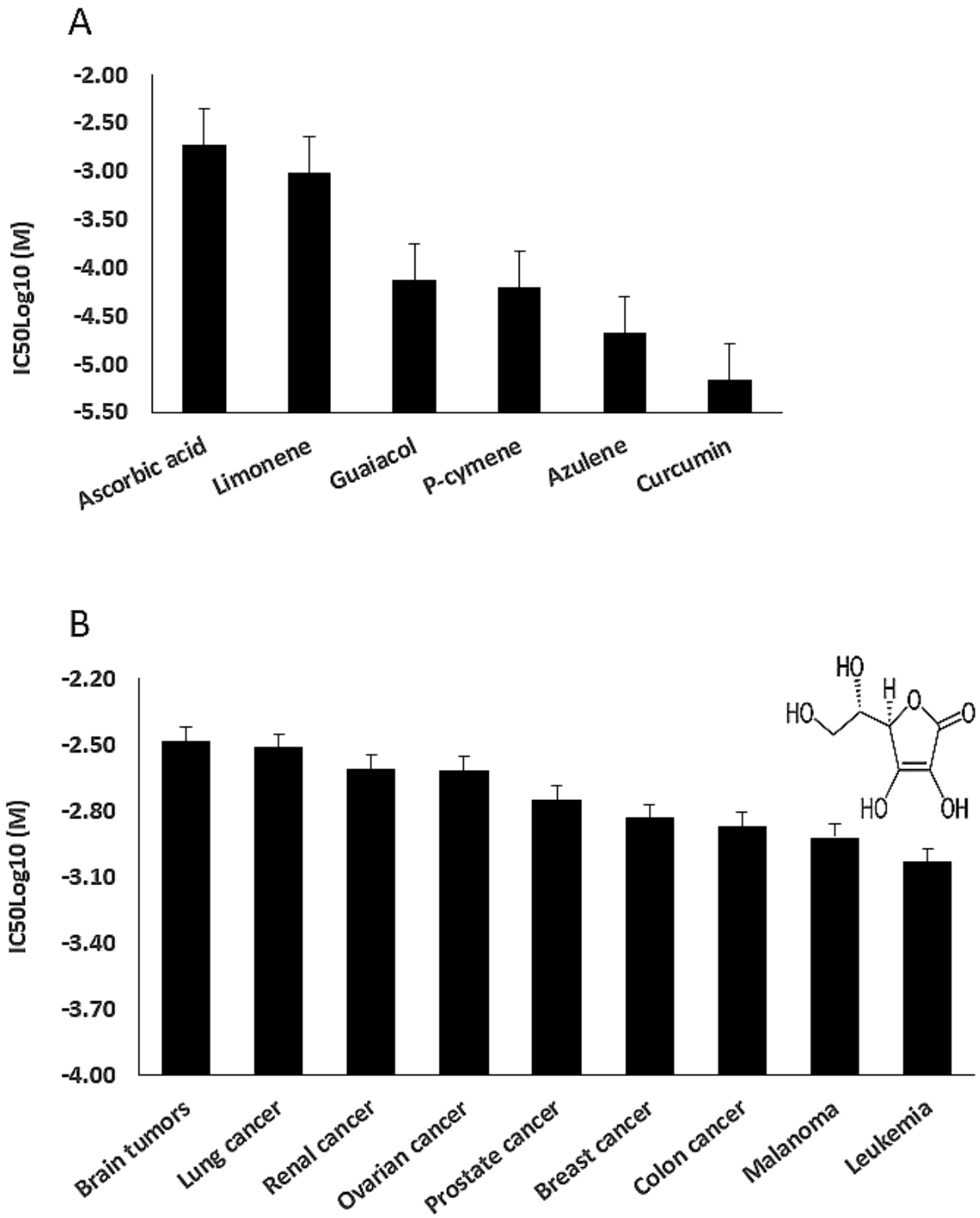

Figure 17: (A) Mean $IC_{50}log_{10}$ values of selected cytotoxic phytochemicals from *Curcuma longa* for the NCl tumor cell line panel as assayed by the sulforhodamine B test. (B) Tumor-type-dependent cytotoxicity of ascorbic acid. Insert: chemical structure of ascorbic acid.

3.2.3 Cytotoxicity of curcumin and AA towards drug resistant cancer cell lines.

Drug-resistant cell lines with different resistance mechanisms (P-glycoprotein, EGFR, mutant p53) towards curcumin and AA were determined. All the cell lines were treated with varying concentrations of curcumin and AA for 72 h, their growth was inhibited in a dose-dependent manner, albeit at different efficacy. The IC_{50} values were calculated from the dose response curves and summarized in **Table 7**. Curcumin inhibited cell growth at lower concentrations than AA. The range of IC_{50} values was 5.22-58.3 µM for curcumin, while that of AA was 389.1-561.2 µM. The CCRF-CEM and CEM/ADR5000 leukemia cell lines were inhibited at concentrations of 5.22 µM and 6.33 µM for respectively. The ΔEGFR-transfectant glioblastoma cells exhibited sensitivity towards curcumin with an IC_{50} value of 46.1 µM, which was slightly lower than the IC_{50} value of wild-type U87MG cells 49.6 µM. Interestingly, the HCT166p53$^{-/-}$ colon cancer cell line was preferentially inhibited by AA with an IC_{50} value of 506.9 µM compared to HCT116p53$^{+/+}$ wild-type cells 561.2µM. The degrees of resistance were calculated by dividing the IC_{50} of the resistant cell line by the IC_{50} of the sensitive cell line. Compared to the high degrees of resistance of these drug-resistant cell lines to standard drugs such as doxorubicin [121], curcumin and AA inhibited these cell lines with similar efficacies. The degrees of resistance were in a range of 0.9 to 1.41 **Table 7**.

Table 7. IC_{50} values of curcumin and vitamin C towards various cell lines. Shown are mean values ± SD of four independent experiments with each six parallel measurements. Degrees of resistance were calculated by the IC_{50} resistant cell line/IC_{50} sensitive cell line ratio.

Cell lines	Curcumin		Vitamin C	
	IC_{50} (µM)	Degree of resistance	IC_{50} (µM)	Degree of resistance
CCRF-CEM	5.22 ± 0.15		502.61 ± 2.24	
CEM/ADR5000	6.33 ± 0.07	1.21	523.12 ± 2.19	1.04
U87MG	49.60 ± 16.40		389.10 ± 53.50	
U87MG.ΔEGFR	46.10 ± 4.80	0.92	532.10 ± 76.40	1.37
HCT116p$^{+/+}$	41.20 ± 12.06		561.20 ± 58.80	
HCT116p53$^{-/-}$	58.30 ± 4.30	1.41	506.90 ± 20.40	0.90

3.2.4 Cytotoxic effects of combination treatments of curcumin and AA and assessment by Loewe additivity model.

Next, we addressed the question, whether the combination of curcumin and AA exhibits additive or synergistic growth inhibition of cancer cells. We applied a universal reference model for evaluating the effects of drug interaction, *i.e.* the Loewe additivity model (isobologram analysis). The cancer cell lines were treated with varying concentrations of AA at indicated concentrations of curcumin for 72 h. In CCRF-CEM and CEM/ADR5000 cells, the IC_{50} values of curcumin in combination with AA were reduced by less than half of the IC_{50} of curcumin alone. In the glioblastoma and colon cancer cell lines, the IC_{50} value of two of the curcumin concentrations (20% IC_{50} curcumin and 40% IC_{50} curcumin) decreased with increasing AA concentrations less than the IC_{50} of curcumin alone. However, the two other concentrations of curcumin reduced the IC_{50} in combination with AA by less than half of the IC_{50} value of curcumin alone. Dose-normalized IC_{50} isobolograms for all cell lines were generated by plotting the combination treatment IC_{50} values of curcumin against AA. Additive effects were observed in CCRF-CEM and CEM/ADR5000 **Figure 18** as well as in HCT116p53$^{+/+}$ and HCT116p53$^{-/-}$ cell lines **Figure 19**, whereas supra/additive effects were visible in U87MG and U87MG.ΔEGFR cells **Figure 20**.

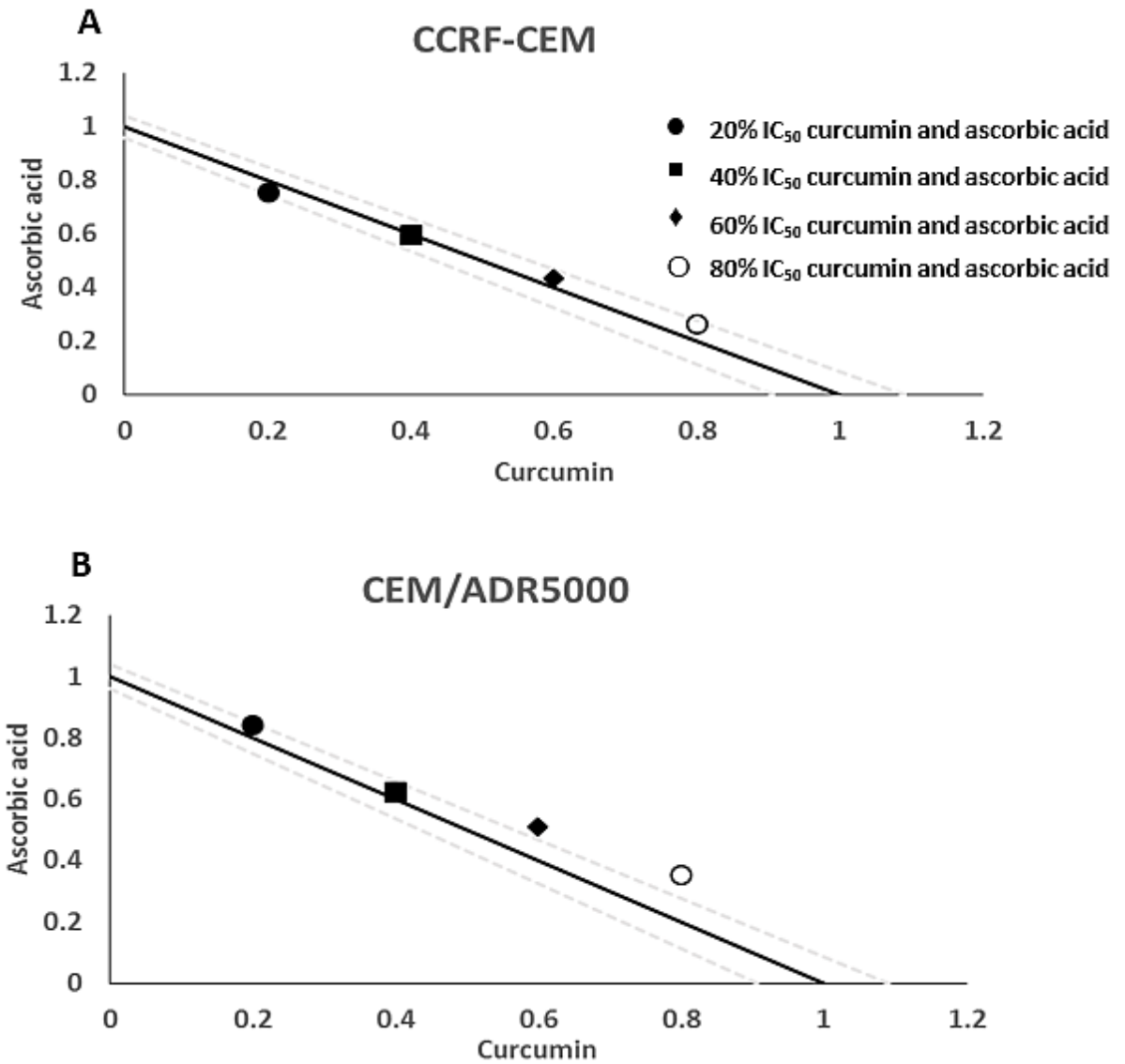

Figure 18. Isobologram analysis for the interaction of various combinations of curcumin and ascorbic acid on (A) CCRF-CEM and (B) CEM/ADR5000 leukemia cell lines.

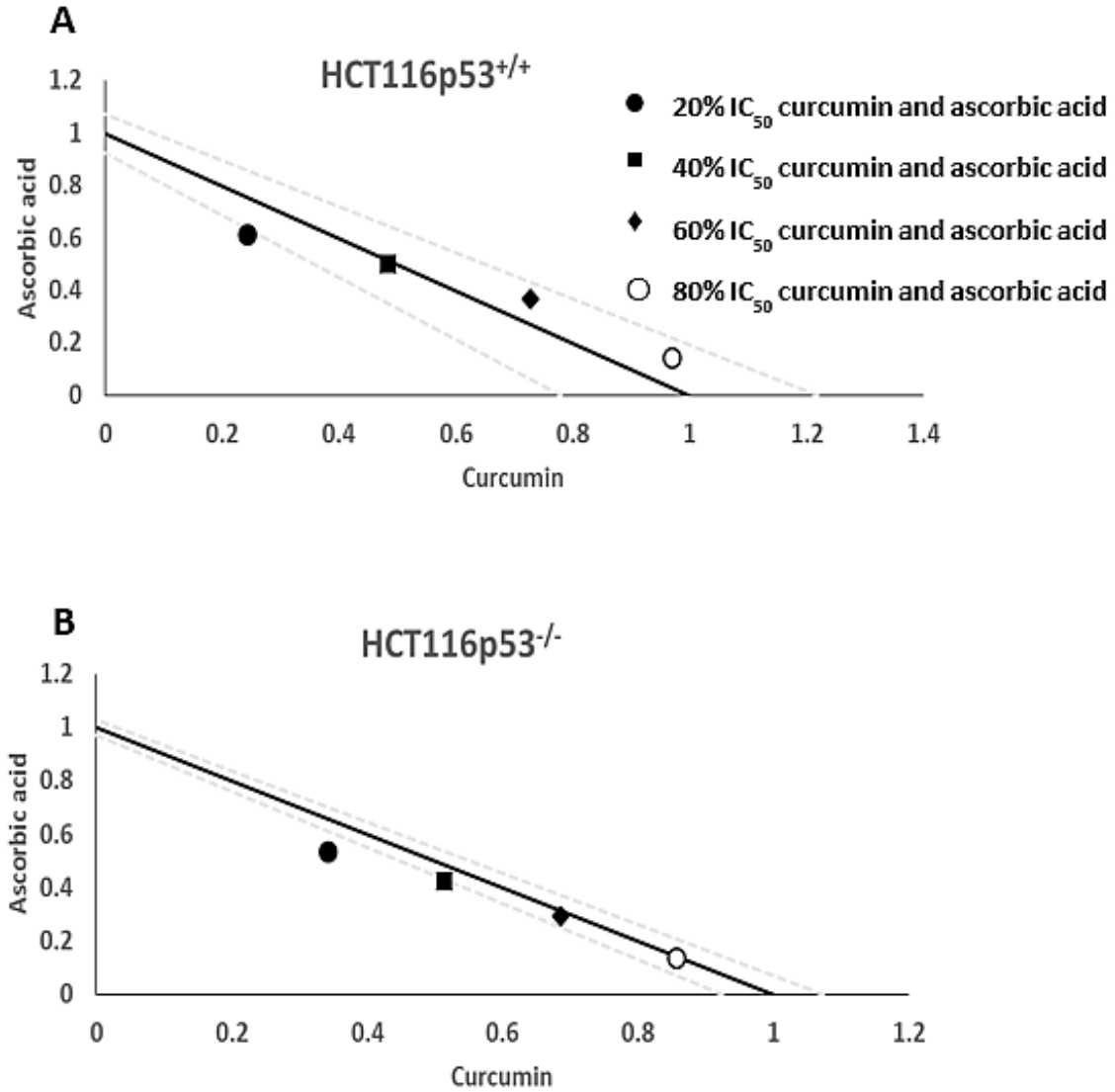

Figure 19. Isobologram analysis for the interaction of various combinations of curcumin and ascorbic acid on (A) HCT116p53$^{+/+}$ and (B) HCT116p53$^{-/-}$ colon cancer cell lines.

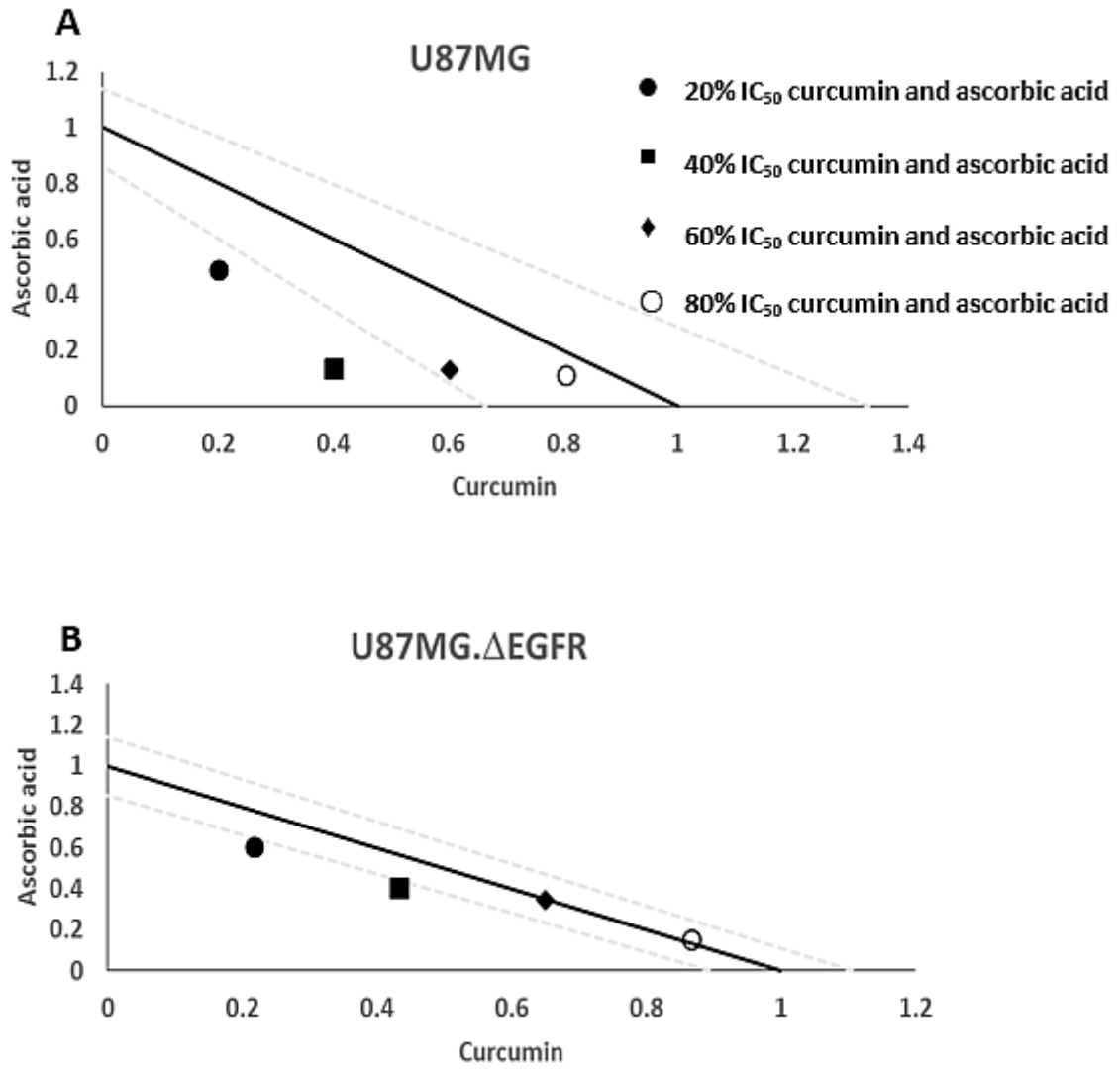

Figure 20. Isobologram analysis for the interaction of various combinations of curcumin and ascorbic acid on (A) U87MG and (B) U87MG.ΔEGFR glioblastoma cell lines.

3.2.5 COMPARE and hierarchical cluster analyses of mRNA expressions.

The transcriptome-wide mRNA expression of the NCI cell lines based on the Novartis microarray platform was investigated by COMPARE analyses and correlated to the $\log_{10}IC_{50}$ values for curcumin and AA. This bioinformatical approach was performed to identify novel putative factors associated with cellular response to curcumin and AA. The top 20 genes with direct and top 20 genes with inverse correlation co-efficient are shown in **Tables 8 and 9**. These genes were subjected to hierarchical cluster analysis to analyze, whether the expression profiles of these genes may predict sensitivity or resistance of the cells to curcumin and AA. The mRNA expression of the identified genes were subjected to hierarchical cluster analysis and cluster image mapping **Figures 21 and 22**. The resulting dendogram with the cell lines analyzed on the left can be divided into five major branches for curcumin and four branches for ascorbic acid. Using the chi-square test, we analyzed whether the distribution of cell lines being sensitive or resistant to curcumin and AA was statistically significant. As shown in **Table 10** the distribution of sensitive or resistant cell lines on the dendogram was significantly different indicating that cellular response to curcumin or AA was predictable by the mRNA expression of these genes. Therefore, it is interesting to know the function of these genes. The specific functions of the proteins encoded by the genes were diverse and included signal transduction, transcription factors, proteasome deregulation, apoptosis regulating genes, proliferation-related genes, pro- as well as anti-oxidative genes **Tables 8 and 9**. For AA the genes belonged to the functional groups of transcription factors (*TFAM, TCERG1, RGS13* and *C11orf31*), apoptosis-regulating genes (*CRADD, CDK7, CDK19, CD81, TOM1*) and signal transduction genes (*NR1D2, HMGN1, ABCA1, DE4ND4B, TRIM27*). For curcumin, we found DNA repair genes (*TOPBP1, RPA2*), mRNA metabolism genes (*RBBP4, HNRNPR, SRSF4, NR2F2, PDK1, and TGM2*), signal transduction genes *(WWC1, DTX2, EGFR, CHRNB4, VPS41, and CRIM1*), proliferation-related genes (*RHOD*), apoptosis-regulating genes *(DFFB*) and transporter genes (*ABCA1*).

Table 8: Meta-data of genes shown in the cluster analysis whose mRNA expression correlated with the $\log_{10}IC_{50}$ values of curcumin in the NCI tumor cell line panel.

Gene Symbol	Gene Acc no.	Gene Name	Gene Function
ABCA1	AI344681	ATP-binding cassette, sub-family A (ABC1), member 1	cAMP-dependent and sulfonylurea-sensitive anion transporter. Key gatekeeper influencing intracellular cholesterol transport.
AK2	U54645	Adenylate kinase 2	Catalyzes the reversible transfer of the terminal phosphate group between ATP and AMP.
ALDH3B1	U10868	Aldehyde dehydrogenase 3 family, member B1	Oxidizes medium and long chain saturated and unsaturated aldehydes. Protective role against the cytotoxicity induced by lipid Peroxidation.
ANXA2P1	M62896	Annexin A2 pseudogene 1	Involved in cell proliferation and membrane physiology and is related to cancer progression.
BAIAP2	AB015020	BAI1-associated protein 2	Adapter protein that links membrane-bound small G-proteins to cytoplasmic effector proteins.
BAIAP2	AB015019	BAI1-associated protein 2	Adapter protein that links membrane-bound small G-proteins to cytoplasmic effector proteins. Participates in actin bundling, if associated with EPS8. Promoting filopodial protrusions.
BTFA1	AF038362	B-TFIID transcription factor-associated, 170kDa	Regulates transcription in association with TATA binding protein (TBP). Removes TBP from the TATA box.
CAPN2	M23254	Calpain 2, (m/II) large subunit	Calcium-regulated non-lysosomal thiol-protease, which catalyzes proteolysis of substrates involved in cytoskeletal remodeling and signal transduction.
CHRNB4	U48861	Cholinergic receptor, nicotinic, beta 4	Leads to opening of an ion-conducting channel across the plasma membrane.
CRIM1	AI651806	Cysteine rich transmembrane BMP regulator 1 (chordin-like)	Role in capillary formation and maintenance during angiogenesis.
DDX39B	AC002400	DEAD (Asp-Glu-Ala-Asp) box polypeptide 39B	Involved in nuclear export of spliced and unspliced mRNA. Assembling component of the TREX complex. Has both RNA-stimulated ATP binding/hydrolysis activity and ATP-dependent RNA unwinding activity.
DFFB	AF064019	DNA fragmentation factor, 40kDa, beta polypeptide	Induces DNA fragmentation and chromatin condensation during apoptosis.
DT-UP-PM	U38980	DTX2P1-UPK3BP1-PMS2P11	Encodes a putative E3-ubiquitin ligase with no known biological function.
DTX2	AI138834	Deltex 2	Regulator of Notch signaling.
EGFR	X00588	Epidermal growth factor receptor	Receptor tyrosine kinase activating several signaling cascades. Activates the NF-kappa-B signaling cascade.
EHD1	AF001434	EH-domain containing 1	Acts in early endocytic membrane fusion and membrane trafficking of recycling endosomes.
HNRNPR	AF000364	Heterogeneous nuclear ribonucleoprotein R	Component of ribonucleosomes, which are complexes of >20 other heterogeneous nuclear ribonucleoproteins (hnRNP). hnRNP play an important role in processing of precursor mRNA in the nucleus.
IQCB1	D25278	IQ motif containing B1	Involved in ciliogenesis.
MTHFD2	X16396	Methylenetetrahydrofolate dehydrogenase (NADP+ dependent) 2	Encodes a nuclear-encoded mitochondrial bifunctional enzyme with methylenetetrahydrofolate dehydrogenase and methenyltetrahydrofolate cyclohydrolase activities.
NFATC2IP	AA152202	Nuclear factor of activated T-cells, cytoplasmic, calcineurin-dependent 2 interacting protein	In T-helper 2 (Th2) cells, regulates NFAT-driven transcription of cytokine genes IL3, IL4, IL5 and IL13. Recruits PRMT1 to the IL4 promoter and facilitates subsequent histone acetylation at the IL4 locus. Promotes robust cytokine expression. Down-regulates formation of poly-SUMO chains by UBE2I/UBC9.
NR2F2	M64497	Nuclear receptor subfamily 2	Ligand-activated transcription factor. Activated by high concentrations of 9-cis-retinoic acid and all-trans-retinoic acid, but not by dexamethasone, cortisol or progesterone (in vitro). Regulation of the apolipoprotein A-I gene transcription.

PDK1	L42450	Pyruvate dehydrogenase kinase, isozyme 1	Role in regulation of glucose and fatty acid metabolism and homeostasis via phosphorylation of the pyruvate dehydrogenase subunits PDHA1 and PDHA2. Role in cellular responses to hypoxia. Important for cell proliferation under hypoxia.
PLEKHM1	AB002354	Pleckstrin homology domain containing, family M (with RUN domain) member 1	Involved in vesicular transport in the osteoclast. Role in sialyl-lex-mediated transduction of apoptotic signals.
POLR2L	N24355	Polymerase (RNA) II (DNA directed) polypeptide L	DNA-dependent RNA polymerase catalyzes the transcription of DNA into RNA using the four ribonucleoside triphosphates as substrates.
PRPF4B	U48736	Pre-mRNA processing factor 4B	Role in pre-mRNA splicing. Phosphorylates SF2/ASF.
PSMG1	AJ006291	Proteasome (prosome, macropain) assembly chaperone 1	Chaperone protein, which promotes assembly of the 20S proteasome as part of a heterodimer with PSMG2.
RBBP4	X74262	Retinoblastoma binding protein 4	Core histone-binding subunit that may target chromatin assembly factors, chromatin remodeling factors and histone deacetylases to their histone substrates.
RBMX2	AL050405	RNA binding motif protein, X-linked 2	Encodes RNA binding motif protein, X-linked 2.
RHOD	U61374	Ras homolog family member D	Involved in endosome dynamics. Coordinates membrane transport with the function of the cytoskeleton.
RPA2	J05249	Replication protein A2	Required for DNA recombination, repair and replication. Required for the recruitment of the DNA double-strand break repair factor RAD51 to chromatin in response to DNA damage.
SLC25A36	AL049246	Solute carrier family 25 (pyrimidine nucleotide carrier), member 36	To catalyze uptake of pyrimidine (deoxy) nucleotide triphosphates into the mitochondrial matrix in exchange for internal pyrimidine (deoxy) nucleotide monophosphates or (deoxy) nucleotide diphosphates.
SNRNP40	AF090988	Small nuclear ribonucleoprotein 40kDa	Component of the U5 small nuclear ribonucleoprotein (snRNP) complex.
SPEN	AL096858	*Spen* family transcriptional repressor	Serve as nuclear matrix platform that organizes transcriptional responses. Essential corepressor protein, which regulates different key pathways such as the Notch pathway. Represses transcription via the recruitment of large complexes containing histone deacetylase proteins.
SRSF4	LI4076	Serine/arginine-rich splicing factor 4	Role in alternative splice site selection during pre-mRNA splicing. Represses the splicing of MAPT/Tau exon 10.
TAF12	X84002	TATA box binding protein (TBP)-associated factor	TAFs are components of the transcription factor IID (TFIID) complex, PCAF histone acetylase complex and TBP-free TAFII complex (TFTC). TAFs components-TIIFD are essential for mediating regulation of RNA polymerase transcription.
TGM2	M55153	Transglutaminase 2	Catalyzes the cross-linking of proteins and conjugation of polyamines to proteins.
TMEM115	U09584	Transmembrane protein 115	Role in retrograde transport of proteins from the Golgi to the endoplasmic reticulum.
TOPBP1	D87448	Topoisomerase (DNA) II binding protein 1	Required for DNA replication. Down-regulates E2F1 activity and inhibits E2F1-dependent apoptosis during G1/S transition and after DNA damage.
VPS41	U87309	Vacuolar protein sorting 41	Required for vacuolar assembly and vacuolar traffic.
WWC1	AB020676	WW and C2 domain containing 1	Regulator of the Hippo/SWH (Sav/Wts/Hpo) signaling pathway, which plays a role in tumor suppression by restricting proliferation and promoting apoptosis. Transcriptional coactivator of ESR1. Regulates collagen-stimulated activation of the ERK/MAPK cascade.

Gene information was taken from the OMIM database, National Cancer Institute, USA (http://www.ncbi.nlm.nih.gov/Omim/) and from the GeneCard database of the Weizman Institute of Science, Rehovot, Israel (http://bioinfo.weizmann.ac.il/cards/index.html).

Table 9: Meta-data of genes shown in the cluster analysis of whose mRNA expression correlated with $log_{10}IC_{50}$ values of vitamin C in the NCI tumor cell line panel.

Gene symbol	GenBank Acc no.	Gene Name	Gene Function
ABCA1	A1344681	ATP-binding cassette, sub-family A (ABC1), member 1	cAMP-dependent and sulfonylurea-sensitive anion transporter. Key gatekeeper influencing intracellular cholesterol transport.
ARHGAP19	U79256	Rho GTPase activating protein 19	GTPase activator for Rho-type GTPases.
CBFB	L20298	Core-binding factor, beta subunit	CBF binds to enhancers and promoters, including murine leukemia virus, polyomavirus enhancer, T-cell receptor enhancers, and LCK, IL3 and GM-CSF promoters.
CD81	M33680	CD81	Regulation of lymphoma cell growth. Involved in signal transduction.
CDK7	X77743	Cyclin-dependent kinase 7	The catalytic subunit of the CDK-activating kinase (CAK) complex.
CRADD	U84388	CASP2 and RIPK1 domain containing adaptor with death domain	Apoptotic adaptor molecule specific for caspase-2 and FASL/TNF receptor-interacting protein RIP.
DBH	X13255	Dopamine beta-hydroxylase (dopamine beta-monooxygenase)	Conversion of dopamine to noradrenaline.
DIMT1	AF091078	DIM1 dimethyladenosine transferase	Dimethylates two adjacent adenosines in the loop of a conserved hairpin near the 3'-end of 18S rRNA in the 40S particle
EED	AF080227	Embryonic ectoderm development	Transcriptional repression of target genes. Constituent of a recruiting platform for DNA methyltransferases, thereby involved in epigenetic repression.
FOXG1	X74143	Forkhead box G1	Transcription repression factor.
GRN	AF055008	Granulin	Cytokine-like activity. Role in inflammation, wound repair, and tissue remodelling.
HDLBP	M64098	High density lipoprotein binding protein	Role in cell sterol metabolism. Protects cells from over-accumulation of cholesterol.
HMGN1	J02621	High mobility group nucleosome binding domain 1	Binds to the inner side of the nucleosomal DNA thus altering the interaction between the DNA and the histone octamer which maintains transcribable genes in a unique chromatin conformation.
HNRNPR	AF000364	Heterogeneous nuclear ribonucleoprotein R	Component of ribonucleosomes, which are complexes of >20 other heterogeneous nuclear ribonucleoproteins (hnRNP). hnRNP play an important role in processing of precursor mRNA in the nucleus.
HPRT1	M31642	Hypoxanthine phosphoribosyltransferase 1	Transfers 5-phosphoribosyl from 5-phosphoribosylpyrophosphate onto purine. Generation of purine nucleotides through the purine salvage pathway.
KLHL35	AA471042	Kelch-like family member 35	A protein coding gene.
KNG1	K02566	Kininogen 1	Role in blood coagulation. Inhibits the thrombin- and plasmin-induced aggregation of thrombocytes.
LRP10	AL080164	Low density lipoprotein receptor-related protein 10	Receptor involved in the internalization of lipophilic molecules and/or signal transduction. May be involved in the uptake of lipoprotein APOE in liver.
MAP2K2	L11285	Mitogen-activated protein kinase kinase 2	Catalyzes the concomitant phosphorylation of threonine and tyrosine residue in a Thr-Glu-Tyr sequence located in MAP kinases. Activates ERK1 and ERK2 MAP kinases.
MEGF8	AB011541	Multiple EGF-like-domains 8	Encodes a single pass membrane protein which participates in developmental regulation and cellular communication
NUP160	D83781	Nucleoporin 160kDa	Involved in poly (A)+ RNA transport.
PCMT1	D25547	Protein-L-isoaspartate (D-aspartate) O-methyltransferase	Catalyzes methyl esterification of L-isoaspartyl and D-aspartyl residues in peptides and proteins repair and/or degradation of damaged proteins.
PLA2R1	U17034	Phospholipase A2 receptor 1	Receptor for secretory phospholipase A2. Activation of the mitogen-activated protein kinase (MAPK) cascade to induce cell proliferation, production of lipid mediators, and selective release of arachidonic acid in bone marrow-derived mast cells. Involved in responses in proinflammatory cytokine productions during endotoxic shock.
PLAUR	X74039	Plasminogen activator, urokinase receptor	Role in localizing and promoting plasmin formation. Mediates the proteolysis-independent signal transduction activation effects of uPA.

PNN	U77718	Pinin, desmosome associated protein	Transcriptional activator of the E-cadherin gene. Regulation of alternative pre-mRNA splicing. Regulates specific excision of introns in specific transcription subsets. Involved in the establishment and maintenance of epithelia cell-cell adhesion. Potential tumor suppressor for renal cell carcinoma.
PNPLA6	AJ004832	Patatin-like phospholipase domain containing 6	Deacylation of intracellular phosphatidylcholine generating glycerophosphocholine.
PPWD1	D38552	Peptidylprolyl isomerase domain and WD repeat containing 1	Accelerates the folding of proteins. Involved in pre-mRNA splicing.
PSAP	J03077	Prosaposin	Stimulates the hydrolysis of glucosylceramide by beta-glucosylceramidase and galactosylceramide by beta-galactosylceramidase. Behaves as a myelinotrophic and neurotrophic factor.
RABAC1	AJ133534	Rab acceptor 1	General Rab protein regulator required for vesicle formation from the Golgi complex. May control vesicle docking and fusion.
RGS13	AF030107	Regulator of G-protein signaling 13	Inhibits signal transduction by increasing the GTPase activity of G protein alpha subunits.
SETD4	AB004848	SET domain containing 4	Role in protein encoding
SI	X63597	Sucrase-isomaltase (alpha-glucosidase)	Role in the final stage of carbohydrate digestion.
SLC7A2	D29990	Solute carrier family 7 (cationic amino acid transporter, y+ system), member 2	Transport of cationic amino acids (arginine, lysine and ornithine). Regulatory role in activation of macrophages.
SMA4	X83300	Glucoridase	Required for signal transduction and it also defines a conserved family of transforming growth factor beta pathway components.
TAF9	U21858	TATA box binding protein (TBP)-associated factor	Gene regulation associated with apoptosis. Regulation of RNA polymerase II-mediated transcription.
TCERG1	AF017789	Transcription elongation regulator 1	Transcription factor that binds RNA polymerase II and inhibits the elongation of transcripts from target promoters in a TATA box-dependent manner.
TFAM	M62810	transcription factor A	Mitochondrial transcription regulation. Maintenance of normal levels of mitochondrial DNA. Organizing and compacting mitochondrial DNA.
TOM1	AJ006973	Target of myb1	Involved in intracellular trafficking. Probable association with membranes.
UBE2N	D83004	Ubiquitin-conjugating enzyme E2N	The UBE2V1-UBE2N and UBE2V2-UBE2N heterodimers catalyze the synthesis of non-canonical 'Lys-63'-linked polyubiquitin chains. This type of polyubiquitination does not lead to protein degradation by the proteasome. Mediates transcriptional activation of target genes. Plays a role in the control of the cell cycle and differentiation. Plays a role in the error-free DNA repair pathway and contributes to the survival of cells after DNA damage. Induction and expression of NF-kappa-B and MAPK-responsive inflammatory genes.
ZNF195	AF003540	Zinc finger protein 195	May be involved in transcriptional regulation.

Gene information was taken from the OMIM database, National Cancer Institute, USA (http://www.ncbi.nlm.nih.gov/Omim/) and from the GeneCard database of the Weizman Institute of Science, Rehovot, Israel (http://bioinfo.weizmann.ac.il/cards/index.html).

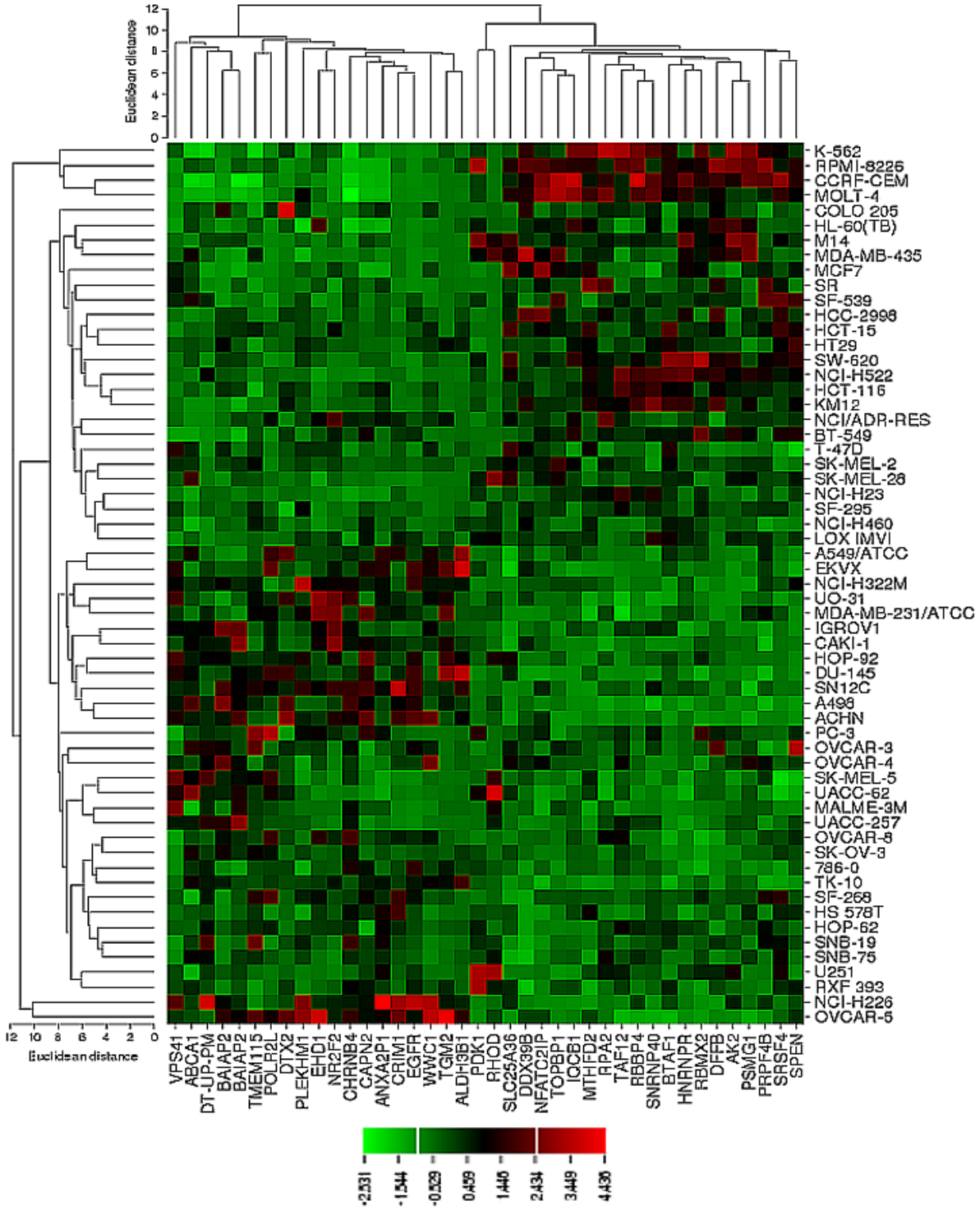

Figure 21: Dendrograms and cluster image map of curcumin obtained by hierarchical cluster analysis of mRNA expression of 40 genes in the NCI cell line panel as analyzed by the Novartis microarray platform. The dendrogram on the left shows the clustering of cell lines and the dendrogram on the top shows the clustering of genes. The cluster image map shows each single mRNA expression value obtained by microarray analysis. The expression values have been normalized and color-coded.

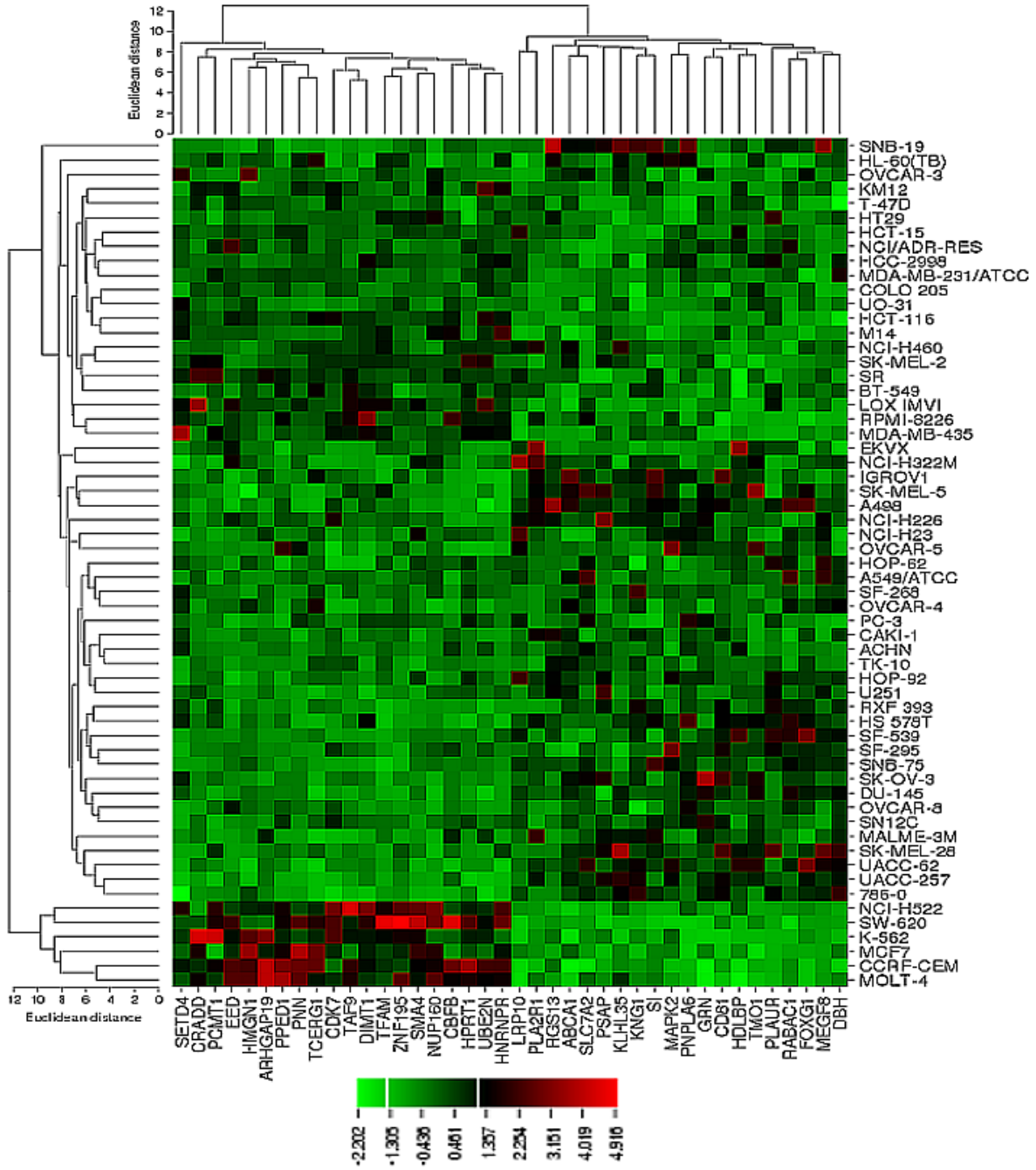

Figure 22: Dendrograms and cluster image map of vitamin C obtained by hierarchical cluster analysis of mRNA expression of 40 genes in the NCI cell line panel as analyzed by the Novartis microarray platform. The dendrogram on the left shows the clustering of cell lines and the dendrogram on the top shows the clustering of genes. The cluster image map shows each single mRNA expression value obtained by microarray analysis. The expression values have been normalized and color-coded.

Table 10. Separation of clusters of NCI cell lines obtained by hierarchical cluster analyses for curcumin (**Figure 6**) or ascorbic acid (**Figure 7**)

	Sensitive	**Resistant**
Curcumin		
Partition	< -5.1M	≥-5.1M
Cluster1	0	4
Cluster2	5	11
Cluster3	16	3
Cluster4	10	8
Cluster5	1	1
Chi-square test	$P = 4.59 * 10^{-3}$	
Ascorbic acid		
Partition	< -2.7M	≥-2.7M
Cluster 1	2	0
Cluster 2	5	14
Cluster 3	12	20
Cluster 4	0	6
Chi-square	P = 0.050	

The median $\log_{10}IC_{50}$ values (-5.1 M for curcumin and -2.7 M for ascorbic acid) were used as cut-off to separate tumor cell lines as being ‘‘sensitive’’ or ‘‘resistant’’.

4. Discussion

4.1 Modulation of P-gp activity by curcumin and its synthetic derivatives

The aim of this section of the study was to evaluate the cytotoxicity of 19 novel synthetic derivatives of curcumin towards CCRF-CEM leukemia cells and its multidrug-resistant subline, CEM/ADR5000. MDR poses a serious challenge to cancer treatment and thus novel cytotoxic drugs with low or no cross resistance and high specificity are urgently needed [127]. Seventeen out of the 19 synthesized curcumin derivatives demonstrated IC_{50} values of below 10 µM in parental CCRF-CEM cells, while similar low values were found for 14 compounds in multidrug-resistant CEM/ADR5000 cells. Three derivatives showed collateral sensitivity. Even the cross-resistance to 10 compounds was only weak, because it did not exceed a value of 3.44-fold. Hence, the new synthetic curcumin derivatives may be useful for further drug development in anticancer therapy. CEM/ADR5000 cells are highly cross-resistant to many standard cancer drugs (doxorubicin, daunorubicin, epirubicin, etoposide, teniposide, vincristine, vinblastine vinorelbine, paclitaxel, docetaxel and others). Compounds that showed collateral sensitivity 1A2, 1A4, 1A6, 1A8, 1A9 and 1B8 may thus be useful to preferentially kill P-gp-expressing tumor cells.

The 19 curcumin derivatives were also evaluated in combination with doxorubicin. Some of them displayed a remarkable ability to increase doxorubicin uptake rates in CEM/ADR5000 cells which was better than that of verapamil. Verapamil was used as control inhibitor of P-gp [128] and revealed a two-fold increase of doxorubicin uptake. Thus, our derivatives can be considered for combination therapy together with standard cancer drugs such as doxorubicin and may lead to lowering of drug doses at comparable anti-tumor efficacy. Curcumin, 1A8 and 1A6 which showed collateral sensitivity when combined with doxorubicin in resazurin assay showed better cytotoxicity than doxorubicin when used alone, this shows that our derivatives in combination with standard drugs can produce remarkable cytotoxicity with much lower doses

of the standard drugs. Synthetic curcumin derivatives binding to P-glycoprotein disturb the outward transport of substrates leading to increased intracellular accumulation of anticancer drug and improved cell killing. The derivatives interact directly with the transporter and possibly bind to the same site as other well-known substrates inhibitors such as verapamil.

P-glycoprotein can be inhibited by blocking of the drug binding site or by interfering with ATP hydrolysis. Inhibition can be achieved by: (1) competitive blocking of the drug binding site; (2) allosteric blocking by interfering with ATP hydrolysis and/or (3) alteration of the cell membrane lipid's integrity by the first method being the most effective[129, 130]. Having this in mind, we performed molecular *in silico* docking experiments with our 19 novel curcumin derivatives as well as with 48 known curcumins taken from the PubChem database. We investigated P-glycoprotein binding sites and, calculated inhibition constants and binding energies, and predicted the amino acids they interact with. Molecular docking was implemented at the two possible interaction sites, the TM-binding domain and the nucleotide-binding domain (NBD). P-gp is composed of two cassettes, each of which contains six TM segments followed by an NBD [131]. The TM-binding domain is made up of three distinct binding sites, which include the H-site, the R-site and the M-site [132]. Our synthetic curcumin derivatives interacted with amino acids prominently found in the M-(modulator) site within the TM-binding domain and this could explain their P-gp inhibiting potential. The M-site is believed to exert a modulatory effect on the P-gp function. Molecular docking was also carried out on the NBD of P-gp and our compounds showed interaction with amino acids in this domain, which may contribute to ATP hydrolysis. This aspect is vital to the understanding of our derivatives, since even though they may bind to NBD1, they might not necessarily be involved in drug-stimulated ATPase activity of P-gp. We further proved that our derivatives were not involved in drug stimulated or basal ATPase activity by the results of the ATPase assay and this strengthens the molecular docking results that our modulators are mainly M-site modulators. The NBD site is close in proximity to the ATP binding site but different from it. Dayan et al reports that domains

between Walker motifs A and B could contribute to the binding of curcumin and its synthetic derivatives to the NBD sites [133].

Looking at the chemical structures of the synthetic curcumin derivatives and their effects on activity and binding, four sites have been exploited for structural modification the aryl side chain, the diketo group, the double bond and the active methylene groups[71]. The A-series of our derivatives has a modification in the active methylene functionality with chlorine. Other modifications are in the aryl side chains and one derivative of this series (1A3) carries a double bond modification. The B-series consists of three derivatives with double bond modifications. These derivatives have modifications of the aryl side chain, but no modification in the active methylene functionality. A-series derivatives showed higher cytotoxicity, which is attributable to the presence of chlorine in the active methylene function. Modification of core scaffold of curcumin confers improved stability and antioxidant activity [134]. In addition, halogen bonding improved the affinity for halogenated ligands and the electrostatic interaction between the hydrogen bond acceptor. A halogen atom acts like a hydrogen bond donor in hydrogen bonding. Other curcumin derivatives reported in the literature support the results we found for derivatives of the A-series [135-137]. Derivative 1A9 carries an aryl side chain modification by the presence of a nitrogen atom, while a substituent on the 4´-position of curcumin invokes an important pharmacophore role for cytotoxicity and caused enhanced potency and selectivity[138]. In addition, nitrogen atoms also serve as hydrogen bond acceptors. Molecular docking studies of the TM binding site led us to conclude that one of the nitrogen atoms of 1A9 formed a hydrogen bond with Asp77 and the other nitrogen interacted with Tyr326. The interaction of the derivatives with the hydrogen bond amino acid contributed to their low binding energy. 1A2 has a modification in the active methylene functionality and lacks OH and OCH_3 groups in its aryl side chains. Modifications in the active methylene, *vide supra,* confers stability and the presence of chlorine makes it a good hydrogen donor. The side chains interacted with Thr333 and Leu214 and the diketo oxygen interacted with the hydrogen bond

to Gly211. In the B-series, 1B8 also exhibited good cytotoxicity. In addition to a modification in the aryl side chain, it reveals a double bond modification. It is known from the literature that modifications of this double bond improve cytotoxicity [139]. This is clearly visible with 1B7 and 1B8, both of which have double bond modifications and their IC_{50} values for both CCRF-CEM and CEM/ADR5000 were lower than those of curcumin. Both 1B7 and 1B8 have an OCH_3 substitution on the 4´-position interacting with hydrogen bond formation to Glu325. The methyl modification of the double bond interacted with the hydrophobic amino acid Thr333, which did not reduce the binding energy. 1A3, which also carried a double bond modification showed however higher cytotoxicity than curcumin. It could be argued that it has a halogen in the active methylene moiety, which increases cytotoxicity compared to curcumin. The lowest binding energies for both TM and NBD domains were -10.37 and -10.11 kcal/mol, respectively. The aromatic amino acid residues Phe303 and Try136 are critical for the poly-specificity of the drug-binding cavity of P-gp [140], as they are located in the center of the drug binding cavity. Indeed, Phe303 was among the amino acids, which was involved in the interaction of P-gp with our curcumins. Other amino acids previously reported to be involved in drug-binding include Phe343, Gly346, Gln347 and Ser222 [140] which is also supported by the results of our molecular docking. Much effort has been spent on substitutions on the aryl side chains as well as the diketo oxygen atoms, which can easily form H-bonds with the NH_2 groups of amino acid groups histamine and glutamate[141]. Our top five curcumin derivatives have substitutions in the D region – the active methylene functionality modification region – and they also exhibit H-bonding to amino acids in this region.

A QSAR model using seven descriptors to predict activity of all 67 derivatives was established. The predicted activities were correlated with the biological activities of the test set (19 derivatives) and the training set (48 derivatives). QSAR models are mathematical regression models, which link a set of predictor variables to the strength of the response variable. Three main components of QSAR model represent the properties to be modeled, the chemical

information, the algorithms used to link the property, and activity of the chemicals [142-144]. In our investigation, the cytotoxicity results did not significantly correlate with the predicted activity from our QSAR model. We therefore focused on the *in silico* molecular docking binding energies and inhibition constants of the 67 curcumin derivatives, which we subjected to QSAR analysis and found high correlations for training and test sets (R=0.791 and 0.794, respectively), indicating that our model had high predictive power[145, 146]. From the descriptors we choose, the number of hydrogen bond donor acceptor atom possibly played an essential role in cytotoxicity but even more the binding energies and inhibition constants exhibited by molecular docking of our inhibitors to P-gp. This feature decreases the *in silico* binding energy obtained from docking however it may also affect the actual binding of the curcumin synthetic derivatives to p-glycoprotein[147]. Closely related to hydrogen bond donor acceptor atom is the orbital molecular descriptors, namely highest occupied molecular orbital (HOMO) energy and lowest unoccupied molecular orbital (LUMO) energy which in other studies have been shown to be good predictors of cytotoxicity. HOMO and LUMO orbital energies describe radical scavenging activities of ligands. HOMO relates to the ionization potential and shows susceptibility of ligands towards attack by electrophiles. LUMO relates to electron affinity and characterizes the likelihood of the ligand being attacked by neutrophils [148, 149]. The descriptor dipole moment characterizes the ligands polarity and we know that polar molecules dissociate better than nonpolar molecules. The solubility of a ligand in water increases with an increase in dipole moment, this also was another descriptor we used. In our analysis the R^2 values were almost similar for both training and test sets, indicating a satisfactory ability to predict activity for the compounds. Our QSAR model correctly predicted binding of the derivatives to P-glycoprotein. With this model, we successfully predicted the power of our 19 novel curcumin derivatives with the help of already known derivatives from PubChem.

4.2 Assessment of the combination of ascorbic acid and curcumin in cancer cells

C. longa contains some 30 different phytochemicals. In this section of the study, we analyzed the cytotoxicity of a combination of two of these phytochemicals of *C. longa*, curcumin and AA. If applied alone, curcumin and AA were cytotoxic towards cell lines of different tumor types with curcumin exhibiting stronger cytotoxicity than AA. Our results are in line with other reports on the inhibitory activity of curcumin [150-155] and AA [156-160]. The anticancer effects of curcumin *in vitro* and *in vivo* are primarily due to the activation of apoptotic pathways in cancer cells as well as the inhibition of mechanisms related to the tumor microenvironments such as inflammation, angiogenesis, invasion and metastasis. In particular, curcumin targets numerous therapeutically important cancer signaling pathways such as p53, Ras, PI3K, AKT, Wnt-β, catenin, mTOR and so on.

AA also reveals anticancer activity *in vitro* and *in vivo,* however at higher concentration than curcumin. A number of suggestions have been put forth on the potential mechanisms, by which AA causes death of cancer cells. The most common is that AA is a precursor for hydrogen peroxide (H_2O_2) generation, which is considered to be preferentially cytotoxic to cancer cells [161]. Exposure to AA concentrations of up to 5 mM for 1 h resulted in decreased survival of cancer cells and cell death was dependent on H_2O_2 production mediated by extracellular AA oxidation [162]. Furthermore, intercellular metals contribute to the production of H_2O_2, with AA losing an electron to form a radical molecule. The free electron is donated to a transition metal. This reduced metal is then available to react with molecular oxygen resulting in the generation of H_2O_2. In the presence of AA, H_2O_2 reacts with another transition metal ion such as ferrous ion to generate a hydroxyl radical [163]. The tumor suppressor p53 may also play a role for this activity. P53-positive cell lines were more sensitive to both AA and H_2O_2 treatment than p53-deficient ones [164].

Thus, having two compounds from one plant with diverse mechanisms of action, we were interested to evaluate, whether their combination would reveal synergistic, antagonistic or

additive interactions. Understanding drug–drug interactions always represents a critical issue in the drug development process, since clinically relevant changes in exposure of co-administered drugs can lead to reduced efficacy or, conversely, adverse drug reactions, depending on the therapeutic window of the drugs. The latter becomes especially important with anti-cancer medications, since they are typically administered at or close to the maximally tolerated dose [165]. In this study, we applied isobologram analyses to evaluate the nature of interaction of curcumin and AA. Isobologram analysis is considered as gold standard to provide evidence for drug interactions. The combination of curcumin and AA exhibited additive effects in leukemia and colon cancer cell lines and supra-additive effects in the glioblastoma cell lines. Our hypothesis is that both natural products may work together by different molecular pathways to achieve their overall cytotoxicity. Unlike chemically synthesized drugs, natural products might be active at lower doses and over longer periods of incubation, which could further support the appearance of additive effects.

We further analyzed molecular determinants of sensitivity and resistance of cancer tumor cell lines towards curcumin and AA. We correlated the IC_{50} values expressed on induction by curcumin and AA of 60 tumor cell lines by COMPARE analysis of microarray-based transcriptome-wide mRNA expression levels of these cell lines [166]. We identified genes from diverse functional groups, which were associated with response of the tumor cells towards curcumin and AA. Under curcumin treatment, these groups of genes included DNA repair, mRNA metabolism, signal transduction, angiogenesis, proliferation, apoptosis etc. While for AA treatment, the COMPARE analysis provided genes that are involved in signal transduction, transcription factors and apoptosis. Although the exact function of these genes for cellular responsiveness to curcumin or AA treatment is still unknown, we have some clues of explanation. On treatment with AA the following genes were downregulated SETD4, TAF9, PNN, CDK7, TFAM and PPWD1. SETD4 is a methyltransferase, which is involved in carcinogenesis. Its down-regulation suppressed cellular proliferation and delayed the G1/S cell

cycle transition without affecting apoptosis. Furthermore, its knockdown decreased cyclin D1 [167]. The TATA-binding protein associated factor 9 (TAF9) interacts with oncogenic GLI family members to form GLI-TAF9 binding, which is important for carcinogenesis activity and malignant growth [168]. PNN is a nuclear and cell adhesion-related protein participating in the regulation of gene expression and thereby, positively promoting cell-cell adhesion, and negatively affecting cell migration and cell proliferation [169]. Cyclin-dependent kinase 7 (CDK7), which promotes transcription during the cell cycle, is critical for the survival of cancer cells. The inhibition of CDK7 suppressed proliferation and induced apoptotic cell death [170]. Mitochondrial transcription factor A (TFAM), a member of the high mobility group (HMG) box protein family, is required for mitochondrial DNA replication and transcription. HMG proteins are often overexpressed in cancer cells and are involved in apoptosis regulation [8, 171]. TFAM may play a significant role in tumorigenesis [172]. PPWD1 has a well-characterized peptide domain (WD40 domain for PPWD1), and this domain has also a critical role in carcinogenesis. The WD40 domain mediates signal transduction and transcriptional regulation during cell cycle and apoptosis. PPWD1 may serve as target for drug development [173, 174]. From the above discussion, AA mechanism revolves around the genes affecting cell proliferation and cell cycle events; it can be assumed that these genes contribute to sensitivity of the tumor cells to AA.

On the other hand, genes potentially responsible for responsiveness on curcumin treatment were identified and curcumin downregulated AK2, PDK1, NR2F2, DFFB, MTHFD2 and ALDH3B1. Adenylate kinases (AKs) represent enzymes that catalyze reversible high-energy phosphoryl transfer reactions between adenine nucleotides in the intermembrane space. During periods of metabolic stress, AK2 increases the amount of available adenosine monophosphate and therefore activates downstream ATP-sensing mechanisms – such as AMP-activated protein kinase (AMPK) – to regulate the cellular metabolism. Inhibition of AK2 expression significantly inhibited the proliferation of cancer cells [175]. PDK1 plays a key role in several

cancer types. Alterations of PDK1 are critical for oncogenic PI3K signaling. PDK1 has an essential role in regulating cell migration, especially in the context of PTEN deficiency. Downregulation of PDK1 levels inhibits migration and metastasis. PDK1 inhibitors may be useful to prevent cancer progression and abnormal tissue dissemination [176]. The nuclear receptor subfamily 2, group F, member 2 (NR2F2) is a master regulator of angiogenesis and acts as oncogene in prostate and other human cancers. NR2F2 is robustly expressed in the stroma of healthy ovary with little or no expression in epithelia lining the ovarian surface, clefts, or crypts. The pattern of NR2F2 expression was severely disrupted in ovarian cancers, in which decreased levels of stromal expression and ectopic epithelial expression were exhibited. Targeting NR2F2 expression in ovarian cancer cell lines enhanced apoptosis and increased proliferation [177]. *DFFB* contributes to both chromosomal condensation and DNA degradation during apoptosis, decreased *DFFB* expression favors DNA damage, which in turn may contribute to both tumorigenesis and better response to DNA damaging chemotherapy [178]. *MTHFD2* mRNA and protein expression is markedly elevated in many cancers and correlated with poor survival in breast cancer. *MTHFD2* is integral to mitochondrial one-carbon metabolism, a metabolic system recently implicated in rapid cancer cell proliferation. Synthesis of one-carbon units carried by the tetrahydrofolate (THF) cofactor is important for proliferating cells, required for nucleotide synthesis and methylation reactions. *MTHFD2* is a bifunctional enzyme, catalyzing the NAD^+ dependent CH2-THF dehydrogenase and CH^+-THF cyclohydrolase reactions within the mitochondria. Within the mitochondrial folate pathway, *MTHFD2* is of special interest, because *MTHFD2* was one of the most consistently overexpressed mRNAs genome-wide across 19 different tumor types. The MTHFD2 protein is specifically expressed in transformed cells, but not the stroma surrounding the tumor tissues. MTHFD2 by RNAi impairs proliferation in a variety of cancer cell lines, independent of the tissue of origin, and decreases invasion and migration in breast cancer cell lines. MTHFD2 is broadly required for cancer cell proliferation and viability [179, 180]. ALDH3B1 is a metabolically active enzyme with distinct specificity for various aldehyde substrates,

particularly medium- and long-chain aliphatic aldehydes. These substrates include many products that are formed during LPO, such as hexanal, 4-hydroxy-2-nonenal (4-HNE), octanal, and trans-2-nonenal. ALDH3B1 plays an important physiological role against cellular oxidative stress by detoxifying aldehydes derived from oxidative processes, such as ethanol metabolism and LPO [181]. Our pharmacogenomics data shows curcumin suppressing cell proliferation by downregulation of anti-apoptotic genes and cell surface adhesion molecules. Curcumin is also seen to regulate cellular metabolism and inhibition of angiogenic cytokines. We can then suggest that the downregulated genes affect the sensitivity of the tumor cells to curcumin.

Previously, we reported the mRNA expression profile induced by curcumin in the NCI cell line panel, which was merged from four different microarray platforms (Novartis, Stanford, Chiron, and Genelogic)[182]. In the present investigation, we focused only on the Novartis microarray platform for the comparison of curcumin and vitamin C and to reduce the degree of complexity. If we compared the top ranked genes in the previous analysis with those of the present investigation, we found some genes in common (*MTHFD2, AK2, NFATC21P, BTAF1, RBBP4*), although the majority of genes were different in both analyses. This result points to an observation that was frequently made by many investigators: different microarray platforms deliver different results. Nevertheless, several biological functional groups were found to be common in our previous and the present paper, *e.g.* cell cycle, DNA damage response, cell migration, inflammation, signaling pathways and apoptosis-regulating genes. To our opinion, microarray data are reliable, if they are used for the generation of testable hypotheses. In this respect, both of our microarray analyses were useful. Microarray data represents the starting point for the elucidation of modes of action of cytotoxic compounds rather than completed end results.

Cluster analyses were applied in the present investigation under the assumption that responsiveness of cancer cells might be predicted by using gene expression patterns and that

appropriate gene expression profiles might be sufficient to predict whether a cancer cell line is sensitive or resistant to a cytotoxic compound [183]. Curcumin revealed two clusters with predominantly sensitive and three with predominantly resistant cell lines. For AA cluster analysis revealed two clusters containing mainly resistant and two clusters containing mainly sensitive cell lines in a comparable fashion to curcumin. The prediction of sensitivity or resistance to cytotoxic drugs by mRNA expression profiles is interesting in the context of individualized or precision medicine, because it may open the possibility to determine prior to treatment, whether or not a tumor will respond to specific drugs. Our data demonstrate that this may not only be feasible to established anticancer drugs, but also to investigative natural products such as curcumin or AA.

The fact that the mRNA expression profiles induced by curcumin and AA related to different gene expression patterns may be related to different modes of actions of both compounds. Medicinal herbs generally contain mixtures of active compounds, which may interact in an additive or synergistic manner. Synergistic interactions may need common mechanisms *e.g.* a common specific pathway that they inhibit. From an evolutionary point of view, synergistic interactions need co-evolutionary selection pressures to evolve. Hence, it can be speculated that synergisms are less likely to occur than additive effects. Therefore, additive drug interactions can be more frequently found in medicinal herbs. Compounds with different modes of action can efficiently and sufficiently fulfill the requirements for plants to survive under specific evolutionary selection pressure. This may explain that we found additive rather than synergistic interactions in isobologram analyses between curcumin and AA in the panel of cell lines tested. This observation is in accordance with previous data with several cytotoxic compounds from *Artemisia annua* L., which also showed additive rather than synergistic interactions [184].

5. Summary and Conclusion

In this study curcumin as a lead agent for anti-cancer was studied. The history of the use of curcumin for treatment in cancer is clean and its shortcomings have been identified. Our study looked into two aspects of curcumin and how this can be better applied in the fight against cancer.

We studied nineteen new synthetic derivatives of curcumin provided to us by our collaborators from the University of Western Cape in South Africa. We evaluated the cytotoxic activity of these novel curcumin synthetic derivatives towards sensitive CCRF-CEM and multidrug resistant CEM/ADR5000 cells. From our assessment they displayed good cytotoxic activity on both cell lines and some of them even exhibited better cytotoxicity that the parent curcumin. We further looked at their ability to inhibit p-gp activity. This we did in two fold; first through the doxorubicin uptake assay where we measured the amount of doxorubicin retained in the cells when the cells were incubated with the synthetic derivatives. The results were remarkable with some ot the derivatives inhibiting doxorubicin extrusion even better than verapamil. Secondly we assessed in silico using molecular docking tools the binding of these synthetic derivatives to P-gp. Molecular docking provided insights into the interactions of the derivatives on binding energies, inhibition constants and amino acids involved in the interaction with P-gp. The QSAR studies further assessed our synthetic derivatives in comparison to other synthetic derivatives of curcumin available in the public domain i.e. the PubChem database. This allowed for further assessment of our synthetic derivatives in a model that confirmed P-gp inhibition while comparing them with already established synthetic derivatives of curcumin.

The other aspect that we looked into was combining curcumin with ascorbic acid and assessing this combinations anticancer activity. We tested this combination on a broad spectrum of cancers and obtained and additive to supra additive effect. We then looked into the

pharmacogenomics of curcumin and AA to evaluate the genes affected by the cytotoxicity of these two compounds. We identified several candidate genes that may regulate the response of cancer cells to curcumin and AA. The genes were involved in a wide array of functions and the two natural compounds work by different mechanisms, this could explain the additive effects obtained from the cytotoxicity assays. The interplay of genes differentially regulated by different natural compounds represents a basis to find explanations for the superior bioactivity of combinations compared to their single compounds. The development of sophisticated methods of network pharmacology will further shed light on the complex regulations of cellular pathways involved in the activities of phototherapies.

6. Materials and Methods

6.1 Chemicals and Equipment

Verapamil, bufalin, and digoxin:

These compounds were purchased from Sigma-Aldrich, Taufkirchen, Germany.

Doxorubicin:

Doxorubicin was kindly supplied from the Hospital Pharmacy, University of Mainz, Germany

Cell culture media, reagents and disposable material

Cell culture media, reagents and disposable material Product	Supplier
96-well, flat bottom cell culture microplate, clear, Nunclon®	Thermo Scientific, Germany
96 well, U-bottom tissue culture plates	Becton-Dickinson Biosciences, Germany
Cell culture flasks (25cm^2), Nunclon®	Thermo Scientific, Germany
Cell culture flasks (75 cm^2), Nunclon®	Thermo Scientific, Germany
Centrifuge tube (15 ml)	Sarstedt, Germany
Centrifuge tube (50 ml)	Sarstedt, Germany
DPBS, no calcium, no magnesium	Life Technologies, Germany

FACS tubes	BD Biosciences, USA; Sarstedt, Germany
FACS tubes with cell strainer cap	BD Biosciences, USA
Fetal Bovine Serum (FBS)	Life Technologies, Germany
L-Glutamine	PAA Laboratories, Germany
Micro tubes (1.5 mL, 2.0 mL)	Sarstedt, Germany
Panserin 413	PAN-Biotech, Germany
Penicillin(10000U/mL)/Streptomycin (10000 µg/mL)	Life Technologies, Germany
Phytohemagglutinin M form	Life Technologies, Germany
Pipette with tip (5 and 10 mL)	Greiner BIO-ONE, Germany
Pipette tip (10, 200 and 1250µL)	Sarstedt, Germany
Roti® PVDF blot membrane (0.45µm)	Roth, Germany
RPMI 1640	Life Technologies, Germany
RPMI 1640 without phenol red	PAA Laboratories, Germany
Trypsin-EDTA 0.25% (1×), phenol red	Life Technologies, Germany

Chemicals, dyes, enzymes and kits

Chemicals, dyes, antibodies, enzymes and kits Product	**Supplier**
30% acrylamide/bis solution 29:1	Bio-Rad, Germany
β-Actin (13E5) rabbit mAb	Cell Signalling, Germany
Ammonium persulfate (APS)	Sigma-Aldrich, Germany
BD Gentest Human P-glycoprotein Membranes	Becton-Dickinson Biosciences, MA, USA
BD Control Memrane Preparation for ABC Transporters	Becton-Dickinson Biosciences, MA, USA
BD Gentest ATPase Assay Kit	Becton-Dickinson Biosciences, MA, USA
Bovine serum albumin (BSA)	Sigma-Aldrich, MO, USA
Bromophenol Blue	Merck, Germany
Bufalin	Sigma-Aldrich, Germany
Complete Mini Protease Inhibitor	Roche, Germany
CD243/P-glycoprotein mouse antibody C219	ThermoFischer Scientific, Germany
Digoxin	Sigma-Aldrich, Germany
Dimethyl sulfoxide (DMSO)	Sigma-Aldrich, Germany
Doxorubicin	JGU Medical Center, Germany

FITC-coupled anti-P-glycoprotein mouse antibody (17F9)	Becton-Dickinson Pharmingen, Germany
Glycine	AppliChem, Germany
Histopaque®	Sigma-Aldrich, Germany
HRP-linked anti-mouse IgG	Cell Signaling, Germany
HRP-linked anti-rabbit IgG	Cell Signaling, Germany
Hydrochloric Acid 37% (HCl)	AppliChem, Germany
LuminataTM Classico Western HRP substrate	Merck Millipore, Germany
MagicMark™ XP Western Standard	Life Technologies, CA, USA
Mayer's hemalum solution	Merk Millipore, Germany
Methanol	J. T. Baker, NJ, USA
Na+/K+-ATPase α1 rabbit antibody	Cell Signaling, Germany
Radioimmunoprecipitation (RIPA) buffer	Sigma-Aldrich, Germany
Resazurin	Sigma-Aldrich, Germany
Sodium bicarbonate	Sigma-Aldrich, MO, USA
Sodium chloride	Grüssing, Germany
Sodium dodecyl sulfate (SDS)	J. T. Baker, NJ, USA
Tetramethylethylenediamine (TEMED)	AppliChem, Germany

Tris(hydroxymethyl) aminomethane (Tris)	AppliChem, Germany
Tween20	Sigma-Aldrich, Germany
β-Mercaptoethanol	AppliChem, Germany
(±)-verapamil hydrochloride	Sigma-Aldrich, Germany
Ultravision Quanto Detection System HRP	Thermo Scientific, Germany

Technical equipment and software

Technical equipment and software Device	**Supplier**
Adobe Photoshop CS5 v 12.0.0.2	Adobe Systems, USA
Alpha Innotech FluorChem Q system	Biozym, Germany
AutoDock 4.2 software	Molecular Graphics Laboratory, CA, USA
AutoDockTools 1.5.6rc3 software	Molecular Graphics Laboratory, CA, USA
AutoGrid 4.2 software	Molecular Graphics Laboratory, CA, USA
BD LSRFortessa cell analyzer	Becton-Dickinson Biosciences, CA, USA
BD High Throughput Sampler (HTS)	Becton-Dickinson Biosciences, CA, USA
BD FACSDiva software	Becton-Dickinson Biosciences, CA, USA
Centrifuge 5424	Eppendorf, Germany
ChemSketch	ACD, Canada
Coulter Counter Z1	Beckman Coulter, Germany

Eppendorf 8-channel electric pipette	Eppendrof, Germany
FlowJo software	FlowJo LLC, OR, USA
Forma Steri-Cult 3310 CO2-Incubator	Thermo Scientific, Germany
Heraeus Cytospin	Thermo Scientific, Germany
Heraeus Fresco 21 microcentrifuge	Thermo Scientific, Germany
Heraeus Labofuge 400 R centrifuge	Thermo Scientific, Germany
ImageJ 1.4.6	NIH, MD, USA
Infinite M2000 Pro™ plate reader	Tecan, Germany
Microsoft Office	Microsoft Corporation, WA, USA
Milli-Q ultrapure water purification system	Millipore, Germany
Mini-PROTEAN® Tetra Cell	Bio-Rad, Germany
MODELLER 9.11	University of California, CA, USA
Molecular Operating Environment (MOE) 2012.10	Chemical Computing Group Inc., Canada
NanoDrop 1000 Spectrophotometer	PEQLAB, Germany
Neubauer counting chamber	Marienfeld, Germany
Optika XDS-2 trinocular inverted microscope	Optika, Italy
PyMOL 1.3	Schroedinger LLC, USA

Precisa BJ2200C balance	Precisa Gravimetrics AG, Switzerland
REAX 2000 vortexer	Heidolph, Germany
Safe 2020 Biological Safety Cabinets	Thermo Scientific, Germany
Sartorius R 160 P balance	Sartorius, Germany
Sonorex RK 102 H Ultrasonic Cleaning Unit	Babdelin, Germany
Spectrafuge™ Mini Centrifuge	Labnet, Germany
SPSS Statistics version 22	IBM, NY, USA
SUB Aqua 26 waterbath	Grant Scientific, Germany
Thermomixer comfort	Eppendorf, Germany

6.2 Cell culture

Cells were grown in in a humidified, 5% CO2-containing incubator at 37°C. Passaging took place twice a week. Cells were counted using either Coulter Counter Z1 (Beckman Coulter) or a Neubauer counting chamber (Marienfeld). Experiments were carried out on cells in the logarithmic phase of growth. Drug sensitive CCRF-CEM and multidrug-resistant P-glycoprotein overexpressing CEM/ADR5000 leukemic cells were generously provided by Prof. Axel Sauerbrey (Department of Pediatrics, University of Jena, Germany). They were cultured in RPMI-1640 medium supplemented with 10% FBS and 1% penicillin/streptomycin (Invitrogen, Darmstadt, Germany). Doxorubicin (5000 ng/mL) was added to maintain overexpression of P-gp (*MDR1*, *ABCB1*) in resistant cells [185]. Human wild-type HCT116

colon cancer cells ($p53^{+/+}$) and knockout clones ($p53^{-/-}$) derived by homologous recombination [186, 187] were generously provided by Dr. B. Vogelstein and H. Hermeking (Howard Hughes Medical Institute, Baltimore, MD, USA). Both colon cancer cells were cultured in DMEM medium supplemented with 10% FBS and 1% penicillin/streptomycin (Invitrogen). Wild-type human U87MG glioblastoma multiform cells and cells transfected with control mock vector or an expression vector harboring *EGFR* cDNA with a deletion in exons 2–7 (U87MG.ΔEGFR), were kindly provided by Dr. W. K. Cavenee (Ludwig Institute for Cancer Research, San Diego, CA, USA) [188].

6.2.1 Leukemia cell lines

The parental CCRF-CEM cells are lymphoblastic leukemia cells, which were isolated from peripheral blood of a child with acute lymphoblastic leukemia. Cells were maintained in RPMI 1640 medium (Life Technologies, Schwerte, Germany) containing phenol red and supplied with 10% fetal bovine serum (Life Technologies) and 1% penicillin [100 U/mL]-streptomycin [100 µg/mL] (Life Technologies). To ensure the multidrug-resistant phenotypes, the MDR1-expressing CEM/ADR5000 cells were treated with 5000 ng/mL doxorubicin on a weekly basis. Selection of multidrug sublines by certain cytostatic has been previously described [185]. The multidrug resistance profile of these cell lines has been reported [189]. For flow cytometry experiments, same conditions were applied, except for the use of culture medium lacking phenol red (PAA, Cölbe, Germany).

6.3 Cytotoxicity assay

We used the resazurin reduction assay to detect cell viability. Only viable cells are able to reduce resazurin to the highly fluorescent resorufin via cellular oxidoreductases. The fluorescence of resorufin can be measured simply by a microplate reader [190-192].

6.3.1 Cytotoxicity of curcumin and its synthetic derivatives in sensitive and MDR leukemia cell lines

Both CCRF-CEM and CEM/ADR5000 cells were seeded in 96-well transparent flat-bottomed plates at a density of 20,000 cells/well with a final volume of 200 μL. Compounds were tested in at least three independent experiments in two ranges each containing 10 concentrations (0.001, 0.003, 0.01, 0.03, 0.1, 0.3, 1, 3, 10, and 100 μM) and (0.00003, 0.0001, 0.0003, 0.001, 0.003, 0.01, 0.03, 0.1, 0.3, and 1 μM), respectively, to cover a wide concentration range. Doxorubicin and verapamil were used as control drugs. Each concentration was tested at least in triplicates within each single experiment. In all samples, the percentage of DMSO was kept at 1%. After an incubation of 72 h at 37°C and 5% CO2, 20 μL of freshly prepared resazurin 0.01% (w/v) solution were added to each well. A further incubation for 4 h was applied and the plates were finally measured with a Tecan Reader Infinite m200 Pro (Crailsheim, Germany) at an excitation wavelength of 544 nm and an emission wavelength of 590 nM. Dose response curves were generated for each curcumin derivative proportional to vehicle (DMSO in the case of the compounds and medium in the case of doxorubicin and verapamil)-treated cells as the 100% viability control.

6.4 Assessment of combination effect

The effect of a combined treatment can be classified as additivity, in which the response of a drug combination is just what is expected from the dose-response relationships of drugs; synergism, in which the response is greater than expected; and antagonism, in which the response is less than expected [193]. Two most commonly used reference models to evaluate drug combination efficacy are the Bliss independence and Loewe additivity models. They handle the same question from two different perspectives: the Bliss independence model focuses on treatment effect enhancement while the Loewe additivity model focuses on dose reduction [194].

6.4.1 Loewe additivity model

The Loewe additivity model was used to confirm the drug interaction between curcumin and AA in inhibiting cell growth [195, 196]. In this model, the combination index (CI) was defined as CI □d1/D1 □d2/D2, where D1 and D2 were the doses of drug 1 and drug 2 that produced an response Y (*e.g.* 50% inhibition) when used alone, d1 and d2 were the doses of drug 1 and drug 2 in combination, which can generate the same response Y. If the CI is equal, less than, or greater than 1, the combination dose (d1, d2) is termed as additive, synergistic or antagonistic, respectively. The drug interaction was illustrated geometrically by isobologram.

6.5 Quantitative structure activity relationship (QSAR)

In addition to the molecular docking of the 19 curcumin derivatives synthesized in the course of the present project, a further 48 curcumin derivatives were mined from the Pub Chem Database (http://www.ncbi.nlm.nih.gov/pccompound/) and canonical SMILES notations for each compound were retrieved and PDM structure files were then created by CORINA Online (https://www.molecular-networks.com/online_demos/corina_demo). These compounds were docked using the molecular docking procedure described above. The 48 derivatives mined from PubChem together with the 19 derivatives synthesized by us were further prepared by Corina Molecular Networks and saved in MOL file format and uploaded in the Molecular Operating Environment (MOE 2012. 10, Chemical Computing group Inc. Montreal, Canada). The compounds were divided into training set (48 compounds minded from PubChem) and test set (19 compounds synthesized by us) and evaluated by a quantitative structural activity relationship (QSAR) model created based on various descriptors. Ionization potential, water accessible surface area, number of H-bond donor acceptor atoms, number of rotatable single bonds, log octane/water partition coefficient, dipole moment and molecular weight were calculated for each compound to obtain predictor variables to calculate predicted activity. The

predicted activity was correlated with doxorubicin uptake values, cytotoxicity values and binding energies obtained from molecular docking. The training set was analyzed by partial least squares regression for the correlation plot. Correlation coefficients were calculated for both training and test sets.

6.6 Doxorubicin uptake assays

The anticancer drug doxorubicin is a P-gp substrate and can be used as fluorescent probe to measure uptake by flow cytometry and consequently allow to measure the inhibition of P-gp function by curcumin derivatives. Doxorubicin (20 μM) was used in all experiments as a substrate for P-glycoprotein and verapamil (20 μM) as positive control for inhibition of P-glycoprotein mediated efflux [143]. Both CCRF-CEM and CEM/ADR5000 cells were seeded in complete RPMI 1640 culture medium lacking the indicator phenol red in 96-well, U-bottomed tissue culture plates (Becton-Dickinson) at a density of 4 × 104 cells per well. Directly before each measurement, treatment medium was removed by centrifugation at 1200 rpm for 5 min and cell pellets were re-suspended with the same medium mentioned above. Exponentially growing CCFR-CEM and CEM/ADR5000 cells were exposed for 24 h to 10 μM doxorubicin in the presence or absence of verapamil, curcumin and its derivatives (10 μM). The cells were harvested and suspended in phenol red free RPMI medium.

Florescence measurements of doxorubicin were performed using a Becton-Dickinson FACS caliber equipped with an ultraviolet argon laser (excitation at 488 nm, emission at 530/30 and 570/30 nm band–pass filters). Forward and side light-scatter plots of 50,000 cells per measurement were gated to exclude dead cells and debris. Log fluorescence was collected and displayed as single parameter histograms.

6.7 P-glycoprotein-ATPase assay

Human P-glycoprotein expressing membranes prepared from baculovirus infected insect cells were purchased from (Corning Life Sciences). P-glycoprotein-ATPase assay was carried out with the aid of Corning Gentest ATPase Assay kit. Briefly, a 60 μL reaction mixture composed of 20 μg membranes, the desired concentration of the drug (in case of verapamil, the concentration was (20 μM), whereas curcumin and its synthetic derivatives were used at (50 μM) in order to obtain an observable effect), and 4 mM MgATP in assay buffer containing 50 mM Tris-MES, 2 mM Oubain, 2 mM EGTA, 50 mM KCl, 2 mM dithiothreitol and 5 mM sodium azide was incubated for 20 min at 37 °C. 30 μL of 10% SDS were added to each well to stop the reaction. Afterwards, a color reagent (35 mM ammonium molybdate in 15 mM zinc acetate: 10% ascorbic acid (1:4)) was added to each well at a volume of 200 μL. A further incubation of 20 min followed and at the end the absorption of liberated inorganic phosphate was measured using Tecan Reader Infinite m200 Pro. Nunc transparent flat bottomed plates were used throughout the measurements.

6.8 Molecular docking

6.8.1 Ligand selection and preparation

The two-dimensional structures of the ligands to be docked were drawn and subsequently energy-minimized into three-dimensional structures using the Corina program (http://www.molecular-networks.com/online_demos/corina_demo). All 3D structures were saved in PDB format.

6.8.2 Homology modelling of human P-gp

The structure of human P-gp was constructed by homology modelling of the X-ray crystallography-based structure of murine P-gp as template [197], which was retrieved from the Protein Data Bank (www.PDB.org PDB code: 3G60). Afterwards, both sequences were aligned using the EMBOSS needle (http://www.ebi.ac.uk/Tools/psa/emboss_needle/), and subsequent homology models were created using the alignment file with MODELLER 9.11 and Swiss MODEL alignment modes. The Swiss-MODEL structure assessment tool was then used to select the best homology model for molecular docking. The Human P-glycoprotein structure was predicted by protein Homology analogy Recognition Engine V 2.0 (PHYRE^2) after submission of the whole protein sequence to the PHYRE^2 serve [198]. Mouse P-glycoprotein was selected as a template known structure. The whole protein and domain sequences of mouse P-glycoprotein and human P-glycoprotein were obtained from UniProt (http://www.uniprot.org). ClustalW2 a multiple sequence alignment program for proteins was used to align the protein sequences and to determine the identity of the predicted protein (human P-glycoprotein) with known structure protein (Mouse P-glycoprotein) (http://www.ebi.ac.uk/Tools/msa/clustalw2)[117, 198]. Human P-glycoprotein has been reported by us to show an overall homology to murine P-glycoprotein of 89% [199]

6.8.3 Molecular docking

The X-ray crystallography-based structures of murine P-gp and homology-modelled human P-gp were set as rigid receptor molecules. The X-ray crystallography–based structure was first processed with AutodockTools-1.5.6rc3 to toggle problems of incomplete structures due to missing atoms or water and may include multimers or interaction partners of the receptor molecule. The prepared output file was in PDBQT format, where information about atomic partial charges, torsion degrees of freedom and different atom types were added, *e.g.* aliphatic and aromatic carbon or polar atoms forming hydrogen bonds.

A grid box was then constructed to define docking spaces. The dimensions of the grid box were set around the entire P-glycoprotein molecule in a manner that the ligand could freely move and rotate in the docking space. The grid box consisted of 126 grid points in all three dimensions (X, Y and Z axes) separated by a distance of 1 between each one.

Energies at each grid point were then evaluated for each atom type present in the ligand, and the values were used to predict the energy of a particular ligand configuration. Docking parameters were set to 250 runs and 2,500,000 energy evaluations for each cycle. Docking was performed by Autodock4 using the Lamarckian Genetic Algorithm. The corresponding binding energies and the number of conformations in each cluster were attained from the docking log files (dlg).

6.9 Pharmacogenomics

6.9.1 Cell lines. The cancer cell lines of the Developmental Therapeutics Program of NCI (U.S.A.) consisted of a series of non-small cell lung cancer, colon cancer, renal cancer, ovarian cancer cells, leukemia, melanoma, prostate carcinoma, breast cancer and tumor cells of the central nervous system. Their origin and processing have been previously reported [200].

6.9.2 Cytotoxicity Assays. The cytotoxicity towards AA and standard anticancer drugs of the NCI cell line panel was measured by the sulforhodamine B assay. The 50% inhibition concentrations calculated from dose−response curves and converted to logarithmic values (log10IC50) have been deposited in the NCI database (http://dtp.nci.nih.gov).

6.9.3 COMPARE and Cluster Analyses of Microarray Data. The mRNA microarray hybridization of the NCI cell lines has been reported and deposited at the NCI website (http://dtp.nci.nih.gov). COMPARE analyses were performed to produce rank ordered lists of genes expressed in the NCI cell lines. The methodology has been previously described in detail

as a tool to identify candidate genes for drug resistance and sensitivity. To derive COMPARE rankings, a scale index of correlation coefficients (R-values) was created from $\log_{10}IC_{50}$ (M) values of test compounds and microarray-based mRNA expression values. Greater mRNA expression correlated with enhanced drug resistance in the standard COMPARE approach, whereas greater mRNA expression in cell lines indicated drug sensitivity in reverse COMPARE analyses. Pearson's correlation test was used to calculate significance values and rank correlation coefficients as a relative measure for the linear dependency of two variables.

For hierarchical cluster analysis, objects were classified by calculation of distances according to the closeness of between individual distances by means of hierarchical cluster analysis. All objects were assembled into cluster trees (dendrograms). Merging of objects with similar features leads to cluster formation, where the length of the branch indicates the degree of relation. Distances of subordinate cluster branches to superior cluster branches serve as criteria for the closeness of clusters. Thus, objects with tightly related features were clustered closely together, while separation of objects in the dendrogram increased with progressive dissimilarity. Hierarchical clustering and heatmap analysis were performed using Euclidean distance and ward method implemented in 'dist', 'hclust' and 'heatmap' functions in R programming [201, 202]. The results were further confirmed using the CIM miner software by use of the one matrix clustered image map (CIM) https://discover.nci.nih.gov/cimminer/oneMatrix.do.

6.10 Statistical analysis.

The Loewe additivity model was used to calculate synergetic drug interactions between curcumin and vitamin C in inhibiting cell growth. In this model, the combination index (CI) was defined as CI = (d1/D1)/ (d2/D2), where D1 and D2 were the doses of drug 1 and drug 2 that produced an response Y (*e.g.*, 50% inhibition of CCRF-CEM growth) when used alone, d1

and d2 were the doses of drug 1 and drug 2 in combination, which can generate the same response Y. If the CI is equal, less than or more than 1, the combination dose (d1, d2) is termed as additive, synergistic or antagonistic, respectively. The drug interaction was illustrated geometrically as isobologram.

Pearson's correlation test was used to calculate significance values and rank correlation coefficients as a relative measure for the linear dependency of two variables. This test was implemented into the WinSTAT Program (Kalmia Co.). Pearson's correlation test determined the correlation of rank positions of values. Ordinal or metric scaling of data is suited for the test and transformed into rank positions. There is no condition regarding normal distribution of the data set for the performance of this test. We used Pearson's correlation test to correlate microarray-based mRNA expression of candidate genes with the IC_{50} values for curcumin and ascorbic acid.

The χ^2-test was applied to bivariate frequency distributions of pairs of nominal scaled variables. It was used to calculate significance values (p-values) and rank correlation coefficients (R-values) as a relative measure for the linear dependency of two variables. This test was implemented into the WinSTAT program (Kalmia Co.). The χ^2-test determines the difference between each observed and theoretical frequency for each possible outcome, squaring them, dividing each by the theoretical frequency, and taking the sum of the results. Performing the χ^2-test necessitated to define cell lines as being sensitive or resistant to curcumin and ascorbic acid. This has been done by taking the median IC_{50} value ($\log_{10} = -5.1$ M) for curcumin and IC_{50} value ($\log_{10} = -2.7$ M) for ascorbic acid as a cut-off threshold

References

1. Ferlay, J., et al., *Cancer incidence and mortality worldwide: sources, methods and major patterns in GLOBOCAN 2012.* Int J Cancer, 2015. **136**(5): p. E359-86.
2. Gregory, T.K., et al., *Molecular prognostic markers for adult acute myeloid leukemia with normal cytogenetics.* J Hematol Oncol, 2009. **2**: p. 23.
3. Raymond W. Ruddon, M.D., *Cancer Biology*. 4th Eddition ed. 2007: Oxford University Press. 568.
4. Debatin, K.M., *Role of apoptosis in congenital hematologic disorders and bone marrow failure.* Rev Clin Exp Hematol, 2003. **7**(1): p. 57-71.
5. Kelkel, M., et al., *Potential of the dietary antioxidants resveratrol and curcumin in prevention and treatment of hematologic malignancies.* Molecules, 2010. **15**(10): p. 7035-74.
6. Hanahan, D. and R.A. Weinberg, *Hallmarks of cancer: the next generation.* Cell, 2011. **144**(5): p. 646-74.
7. Sharma, S., T.K. Kelly, and P.A. Jones, *Epigenetics in cancer.* Carcinogenesis, 2010. **31**(1): p. 27-36.
8. Vander Heiden, M.G., L.C. Cantley, and C.B. Thompson, *Understanding the Warburg effect: the metabolic requirements of cell proliferation.* Science, 2009. **324**(5930): p. 1029-33.
9. Papac, R.J., *Origins of cancer therapy.* Yale J Biol Med, 2001. **74**(6): p. 391-8.
10. Hickey, R., et al., *Cancer concepts and principles: primer for the interventional oncologist-part II.* J Vasc Interv Radiol, 2013. **24**(8): p. 1167-88.
11. Baskar, R., et al., *Cancer and radiation therapy: current advances and future directions.* Int J Med Sci, 2012. **9**(3): p. 193-9.
12. Chabner, B.A. and T.G. Roberts, Jr., *Timeline: Chemotherapy and the war on cancer.* Nat Rev Cancer, 2005. **5**(1): p. 65-72.
13. DeVita, V.T., Jr. and E. Chu, *A history of cancer chemotherapy.* Cancer Res, 2008. **68**(21): p. 8643-53.

14. Gilman, A., *Therapeutic applications of chemical warfare agents.* Fed Proc, 1946. **5**: p. 285-92.

15. Goodman, L.S., et al., *Landmark article Sept. 21, 1946: Nitrogen mustard therapy. Use of methyl-bis(beta-chloroethyl)amine hydrochloride and tris(beta-chloroethyl)amine hydrochloride for Hodgkin's disease, lymphosarcoma, leukemia and certain allied and miscellaneous disorders. By Louis S. Goodman, Maxwell M. Wintrobe, William Dameshek, Morton J. Goodman, Alfred Gilman and Margaret T. McLennan.* JAMA, 1984. **251**(17): p. 2255-61.

16. Gilman, A. and F.S. Philips, *The Biological Actions and Therapeutic Applications of the B-Chloroethyl Amines and Sulfides.* Science, 1946. **103**(2675): p. 409-36.

17. Lotfi-Jam, K., et al., *Nonpharmacologic strategies for managing common chemotherapy adverse effects: a systematic review.* J Clin Oncol, 2008. **26**(34): p. 5618-29.

18. Gerber, D.E., *Targeted therapies: a new generation of cancer treatments.* Am Fam Physician, 2008. **77**(3): p. 311-9.

19. Phillipson, J.D., *Phytochemistry and medicinal plants.* Phytochemistry, 2001. **56**(3): p. 237-43.

20. Kong, J.M., et al., *Recent advances in traditional plant drugs and orchids.* Acta Pharmacol Sin, 2003. **24**(1): p. 7-21.

21. Newman, D.J. and G.M. Cragg, *Natural products as sources of new drugs over the last 25 years.* J Nat Prod, 2007. **70**(3): p. 461-77.

22. Imbert, T.F., *Discovery of podophyllotoxins.* Biochimie, 1998. **80**(3): p. 207-22.

23. Srivastava, V., et al., *Plant-based anticancer molecules: a chemical and biological profile of some important leads.* Bioorg Med Chem, 2005. **13**(21): p. 5892-908.

24. O'Dwyer, P.J., et al., *Etoposide (VP-16-213). Current status of an active anticancer drug.* N Engl J Med, 1985. **312**(11): p. 692-700.

25. Noble, R.L., *The discovery of the vinca alkaloids--chemotherapeutic agents against cancer.* Biochem Cell Biol, 1990. **68**(12): p. 1344-51.

26. Wani, M.C., et al., *Plant antitumor agents. VI. The isolation and structure of taxol, a novel antileukemic and antitumor agent from Taxus brevifolia.* J Am Chem Soc, 1971. **93**(9): p. 2325-7.

27. Wilson, L. and M.A. Jordan, *Microtubule dynamics: taking aim at a moving target.* Chem Biol, 1995. **2**(9): p. 569-73.

28. Schiff, P.B., J. Fant, and S.B. Horwitz, *Promotion of microtubule assembly in vitro by taxol.* Nature, 1979. **277**(5698): p. 665-7.

29. Oberlies, N.H. and D.J. Kroll, *Camptothecin and taxol: historic achievements in natural products research.* J Nat Prod, 2004. **67**(2): p. 129-35.

30. Hsiang, Y.H., et al., *Camptothecin induces protein-linked DNA breaks via mammalian DNA topoisomerase I.* J Biol Chem, 1985. **260**(27): p. 14873-8.

31. Aggarwal, B.B., A. Kumar, and A.C. Bharti, *Anticancer potential of curcumin: preclinical and clinical studies.* Anticancer Res, 2003. **23**(1A): p. 363-98.

32. Priyadarsini, K.I., *The chemistry of curcumin: from extraction to therapeutic agent.* Molecules, 2014. **19**(12): p. 20091-112.

33. Gupta, S.C., et al., *Multitargeting by curcumin as revealed by molecular interaction studies.* Nat Prod Rep, 2011. **28**(12): p. 1937-55.

34. Chaudhri, K.R., *Turmeric, haldi or haridra, in eye disease.* Antiseptic, 1950. **47**(1): p. 67.

35. Li, C., et al., *[Effect of turmeric volatile oil on the respiratory tract].* Zhongguo Zhong Yao Za Zhi, 1998. **23**(10): p. 624-5, inside back cover.

36. Niederau, C. and E. Gopfert, *[The effect of chelidonium- and turmeric root extract on upper abdominal pain due to functional disorders of the biliary system. Results from a placebo-controlled double-blind study].* Med Klin (Munich), 1999. **94**(8): p. 425-30.

37. Tawatsin, A., et al., *Repellency of volatile oils from plants against three mosquito vectors.* J Vector Ecol, 2001. **26**(1): p. 76-82.

38. Gukovsky, I., et al., *Curcumin ameliorates ethanol and nonethanol experimental pancreatitis.* Am J Physiol Gastrointest Liver Physiol, 2003. **284**(1): p. G85-95.

39. Gulcubuk, A., et al., *Pathologic alterations detected in acute pancreatitis induced by sodium taurocholate in rats and therapeutic effects of curcumin, ciprofloxacin and metronidazole combination.* Pancreatology, 2005. **5**(4-5): p. 345-53.

40. Joe, B., U.J. Rao, and B.R. Lokesh, *Presence of an acidic glycoprotein in the serum of arthritic rats: modulation by capsaicin and curcumin.* Mol Cell Biochem, 1997. **169**(1-2): p. 125-34.

41. Liacini, A., et al., *Inhibition of interleukin-1-stimulated MAP kinases, activating protein-1 (AP-1) and nuclear factor kappa B (NF-kappa B) transcription factors down-regulates matrix metalloproteinase gene expression in articular chondrocytes.* Matrix Biol, 2002. **21**(3): p. 251-62.

42. Holt, P.R., S. Katz, and R. Kirshoff, *Curcumin therapy in inflammatory bowel disease: a pilot study.* Dig Dis Sci, 2005. **50**(11): p. 2191-3.

43. Swarnakar, S., et al., *Curcumin regulates expression and activity of matrix metalloproteinases 9 and 2 during prevention and healing of indomethacin-induced gastric ulcer.* J Biol Chem, 2005. **280**(10): p. 9409-15.

44. Baek, O.S., et al., *Curcumin inhibits protease-activated receptor-2 and -4-mediated mast cell activation.* Clin Chim Acta, 2003. **338**(1-2): p. 135-41.

45. Ram, A., M. Das, and B. Ghosh, *Curcumin attenuates allergen-induced airway hyperresponsiveness in sensitized guinea pigs.* Biol Pharm Bull, 2003. **26**(7): p. 1021-4.

46. Lee, J.J., et al., *Blocking NF-kappaB activation may be an effective strategy in the fever therapy.* Jpn J Physiol, 2003. **53**(5): p. 367-75.

47. Shao, D.Z., et al., *Inhibition of nuclear factor-kappa B prevents staphylococcal enterotoxin A-induced fever.* Mol Cell Biochem, 2004. **262**(1-2): p. 177-85.

48. Tourkina, E., et al., *Curcumin-induced apoptosis in scleroderma lung fibroblasts: role of protein kinase cepsilon.* Am J Respir Cell Mol Biol, 2004. **31**(1): p. 28-35.

49. Bosman, B., *Testing of lipoxygenase inhibitors, cyclooxygenase inhibitors, drugs with immunomodulating properties and some reference antipsoriatic drugs in the modified mouse tail test, an animal model of psoriasis.* Skin Pharmacol, 1994. **7**(6): p. 324-34.

50. Verbeek, R., E.A. van Tol, and J.M. van Noort, *Oral flavonoids delay recovery from experimental autoimmune encephalomyelitis in SJL mice.* Biochem Pharmacol, 2005. **70**(2): p. 220-8.

51. Babu, P.S. and K. Srinivasan, *Influence of dietary curcumin and cholesterol on the progression of experimentally induced diabetes in albino rat.* Mol Cell Biochem, 1995. **152**(1): p. 13-21.

52. Babu, P.S. and K. Srinivasan, *Hypolipidemic action of curcumin, the active principle of turmeric (Curcuma longa) in streptozotocin induced diabetic rats.* Mol Cell Biochem, 1997. **166**(1-2): p. 169-75.

53. Sajithlal, G.B., P. Chithra, and G. Chandrakasan, *Effect of curcumin on the advanced glycation and cross-linking of collagen in diabetic rats.* Biochem Pharmacol, 1998. **56**(12): p. 1607-14.

54. Jiang, M.C., et al., *Curcumin induces apoptosis in immortalized NIH 3T3 and malignant cancer cell lines.* Nutr Cancer, 1996. **26**(1): p. 111-20.

55. Bush, J.A., K.J. Cheung, Jr., and G. Li, *Curcumin induces apoptosis in human melanoma cells through a Fas receptor/caspase-8 pathway independent of p53.* Exp Cell Res, 2001. **271**(2): p. 305-14.

56. Chan, W.H. and H.J. Wu, *Anti-apoptotic effects of curcumin on photosensitized human epidermal carcinoma A431 cells.* J Cell Biochem, 2004. **92**(1): p. 200-12.

57. Lee, C.W., et al., *Transcriptional regulation of VCAM-1 expression by tumor necrosis factor-alpha in human tracheal smooth muscle cells: involvement of MAPKs, NF-kappaB, p300, and histone acetylation.* J Cell Physiol, 2006. **207**(1): p. 174-86.

58. Lin, L.I., et al., *Curcumin inhibits SK-Hep-1 hepatocellular carcinoma cell invasion in vitro and suppresses matrix metalloproteinase-9 secretion.* Oncology, 1998. **55**(4): p. 349-53.

59. Fenton, J.I., et al., *Membrane-type matrix metalloproteinases mediate curcumin-induced cell migration in non-tumorigenic colon epithelial cells differing in Apc genotype.* Carcinogenesis, 2002. **23**(6): p. 1065-70.

60. Shin, E.Y., S.Y. Kim, and E.G. Kim, *c-Jun N-terminal kinase is involved in motility of endothelial cell.* Exp Mol Med, 2001. **33**(4): p. 276-83.

61. Leyon, P.V. and G. Kuttan, *Studies on the role of some synthetic curcuminoid derivatives in the inhibition of tumour specific angiogenesis.* J Exp Clin Cancer Res, 2003. **22**(1): p. 77-83.

62. Bobrovnikova-Marjon, E.V., et al., *Expression of angiogenic factors vascular endothelial growth factor and interleukin-8/CXCL8 is highly responsive to ambient glutamine availability: role of nuclear factor-kappaB and activating protein-1.* Cancer Res, 2004. **64**(14): p. 4858-69.

63. Fujiyama-Fujiwara, Y., R. Umeda, and O. Igarashi, *Effects of sesamin and curcumin on delta 5-desaturation and chain elongation of polyunsaturated fatty acid metabolism in primary cultured rat hepatocytes.* J Nutr Sci Vitaminol (Tokyo), 1992. **38**(4): p. 353-63.

64. Srivastava, R., *Inhibition of neutrophil response by curcumin.* Agents Actions, 1989. **28**(3-4): p. 298-303.

65. Ammon, H.P., et al., *Mechanism of antiinflammatory actions of curcumine and boswellic acids.* J Ethnopharmacol, 1993. **38**(2-3): p. 113-9.

66. Dhillon, N., et al., *Phase II trial of curcumin in patients with advanced pancreatic cancer.* Clin Cancer Res, 2008. **14**(14): p. 4491-9.

67. Wang, Y.J., et al., *Stability of curcumin in buffer solutions and characterization of its degradation products.* J Pharm Biomed Anal, 1997. **15**(12): p. 1867-76.

68. Oetari, S., et al., *Effects of curcumin on cytochrome P450 and glutathione S-transferase activities in rat liver.* Biochem Pharmacol, 1996. **51**(1): p. 39-45.

69. Liu, W., et al., *Oral bioavailability of curcumin: problems and advancements.* J Drug Target, 2016. **24**(8): p. 694-702.

70. Prasad, S., A.K. Tyagi, and B.B. Aggarwal, *Recent developments in delivery, bioavailability, absorption and metabolism of curcumin: the golden pigment from golden spice.* Cancer Res Treat, 2014. **46**(1): p. 2-18.

71. Anand, P., et al., *Bioavailability of curcumin: problems and promises.* Mol Pharm, 2007. **4**(6): p. 807-18.

72. Wahlstrom, B. and G. Blennow, *A study on the fate of curcumin in the rat.* Acta Pharmacol Toxicol (Copenh), 1978. **43**(2): p. 86-92.

73. Shoba, G., et al., *Influence of piperine on the pharmacokinetics of curcumin in animals and human volunteers.* Planta Med, 1998. **64**(4): p. 353-6.

74. Safavy, A., et al., *Design and development of water-soluble curcumin conjugates as potential anticancer agents.* J Med Chem, 2007. **50**(24): p. 6284-8.

75. Ireson, C., et al., *Characterization of metabolites of the chemopreventive agent curcumin in human and rat hepatocytes and in the rat in vivo, and evaluation of their ability to inhibit phorbol ester-induced prostaglandin E2 production.* Cancer Res, 2001. **61**(3): p. 1058-64.

76. Asai, A. and T. Miyazawa, *Occurrence of orally administered curcuminoid as glucuronide and glucuronide/sulfate conjugates in rat plasma.* Life Sci, 2000. **67**(23): p. 2785-93.

77. Mamede, A.C., et al., *The role of vitamins in cancer: a review.* Nutr Cancer, 2011. **63**(4): p. 479-94.

78. Carr, A. and B. Frei, *Does vitamin C act as a pro-oxidant under physiological conditions?* FASEB J, 1999. **13**(9): p. 1007-24.

79. Carr, A.C. and B. Frei, *Toward a new recommended dietary allowance for vitamin C based on antioxidant and health effects in humans.* Am J Clin Nutr, 1999. **69**(6): p. 1086-107.

80. Gilliam, L.A. and D.K. St Clair, *Chemotherapy-induced weakness and fatigue in skeletal muscle: the role of oxidative stress.* Antioxid Redox Signal, 2011. **15**(9): p. 2543-63.

81. Mikirova, N., et al., *Effect of high-dose intravenous vitamin C on inflammation in cancer patients.* J Transl Med, 2012. **10**: p. 189.

82. Du, J., J.J. Cullen, and G.R. Buettner, *Ascorbic acid: chemistry, biology and the treatment of cancer.* Biochim Biophys Acta, 2012. **1826**(2): p. 443-57.

83. Rebouche, C.J., *Ascorbic acid and carnitine biosynthesis.* Am J Clin Nutr, 1991. **54**(6 Suppl): p. 1147S-1152S.

84. Harrison, F.E. and J.M. May, *Vitamin C function in the brain: vital role of the ascorbate transporter SVCT2.* Free Radic Biol Med, 2009. **46**(6): p. 719-30.

85. May, J.M., Z.C. Qu, and M.E. Meredith, *Mechanisms of ascorbic acid stimulation of norepinephrine synthesis in neuronal cells.* Biochem Biophys Res Commun, 2012. **426**(1): p. 148-52.

86. Mc, C.W., *Ascorbic acid as a chemotherapeutic agent.* Arch Pediatr, 1952. **69**(4): p. 151-5.

87. Klenner, F.R., *The treatment of poliomyelitis and other virus diseases with vitamin C.* South Med Surg, 1949. **111**(7): p. 209-14.

88. Cameron, E., L. Pauling, and B. Leibovitz, *Ascorbic acid and cancer: a review.* Cancer Res, 1979. **39**(3): p. 663-81.

89. Gonzalez, M.J., et al., *Orthomolecular oncology review: ascorbic acid and cancer 25 years later.* Integr Cancer Ther, 2005. **4**(1): p. 32-44.

90. Chen, Q., et al., *Ascorbate in pharmacologic concentrations selectively generates ascorbate radical and hydrogen peroxide in extracellular fluid in vivo.* Proc Natl Acad Sci U S A, 2007. **104**(21): p. 8749-54.

91. Hoffer, L.J., et al., *Phase I clinical trial of i.v. ascorbic acid in advanced malignancy.* Ann Oncol, 2008. **19**(11): p. 1969-74.

92. Chen, Q., et al., *Pharmacologic doses of ascorbate act as a prooxidant and decrease growth of aggressive tumor xenografts in mice.* Proc Natl Acad Sci U S A, 2008. **105**(32): p. 11105-9.

93. Kuroiwa, Y., et al., *Combined ascorbic acid and sodium nitrite treatment induces oxidative DNA damage-associated mutagenicity in vitro, but lacks initiation activity in rat forestomach epithelium.* Toxicol Sci, 2008. **104**(2): p. 274-82.

94. Rozanova Torshina, N., J.Z. Zhang, and D.E. Heck, *Catalytic therapy of cancer with ascorbate and extracts of medicinal herbs.* Evid Based Complement Alternat Med, 2010. **7**(2): p. 203-12.

95. Verrax, J. and P.B. Calderon, *Pharmacologic concentrations of ascorbate are achieved by parenteral administration and exhibit antitumoral effects.* Free Radic Biol Med, 2009. **47**(1): p. 32-40.

96. Yeom, C.H., et al., *High dose concentration administration of ascorbic acid inhibits tumor growth in BALB/C mice implanted with sarcoma 180 cancer cells via the restriction of angiogenesis.* J Transl Med, 2009. **7**: p. 70.

97. Al-Lazikani, B., U. Banerji, and P. Workman, *Combinatorial drug therapy for cancer in the post-genomic era.* Nat Biotechnol, 2012. **30**(7): p. 679-92.

98. Komarova, N.L. and C.R. Boland, *Cancer: calculated treatment.* Nature, 2013. **499**(7458): p. 291-2.

99. Baguley, B.C., *Multidrug resistance in cancer.* Methods Mol Biol, 2010. **596**: p. 1-14.

100. Lage, H., *An overview of cancer multidrug resistance: a still unsolved problem.* Cell Mol Life Sci, 2008. **65**(20): p. 3145-67.

101. Sevick, E.M. and R.K. Jain, *Geometric resistance to blood flow in solid tumors perfused ex vivo: effects of tumor size and perfusion pressure.* Cancer Res, 1989. **49**(13): p. 3506-12.

102. Park, H., S. Lee, and J. Suh, *Structural and dynamical basis of broad substrate specificity, catalytic mechanism, and inhibition of cytochrome P450 3A4.* J Am Chem Soc, 2005. **127**(39): p. 13634-42.

103. Mast, N., et al., *Broad substrate specificity of human cytochrome P450 46A1 which initiates cholesterol degradation in the brain.* Biochemistry, 2003. **42**(48): p. 14284-92.

104. Gate, L. and K.D. Tew, *Glutathione S-transferases as emerging therapeutic targets.* Expert Opin Ther Targets, 2001. **5**(4): p. 477-489.

105. Krishna, R. and L.D. Mayer, *Multidrug resistance (MDR) in cancer. Mechanisms, reversal using modulators of MDR and the role of MDR modulators in influencing the pharmacokinetics of anticancer drugs.* Eur J Pharm Sci, 2000. **11**(4): p. 265-83.

106. Ling, V. and L.H. Thompson, *Reduced permeability in CHO cells as a mechanism of resistance to colchicine.* J Cell Physiol, 1974. **83**(1): p. 103-16.

107. Juliano, R.L. and V. Ling, *A surface glycoprotein modulating drug permeability in Chinese hamster ovary cell mutants.* Biochim Biophys Acta, 1976. **455**(1): p. 152-62.

108. Croop, J.M., et al., *The three mouse multidrug resistance (mdr) genes are expressed in a tissue-specific manner in normal mouse tissues.* Mol Cell Biol, 1989. **9**(3): p. 1346-50.

109. Fromm, M.F., *Importance of P-glycoprotein at blood-tissue barriers.* Trends Pharmacol Sci, 2004. **25**(8): p. 423-9.

110. Lum, B.L. and M.P. Gosland, *MDR expression in normal tissues. Pharmacologic implications for the clinical use of P-glycoprotein inhibitors.* Hematol Oncol Clin North Am, 1995. **9**(2): p. 319-36.

111. Dean, M., A. Rzhetsky, and R. Allikmets, *The human ATP-binding cassette (ABC) transporter superfamily.* Genome Res, 2001. **11**(7): p. 1156-66.

112. Hyde, S.C., et al., *Structural model of ATP-binding proteins associated with cystic fibrosis, multidrug resistance and bacterial transport.* Nature, 1990. **346**(6282): p. 362-5.

113. Bruggemann, E.P., et al., *Two different regions of P-glycoprotein [corrected] are photoaffinity-labeled by azidopine.* J Biol Chem, 1989. **264**(26): p. 15483-8.

114. Gottesman, M.M. and I.H. Pastan, *The Role of Multidrug Resistance Efflux Pumps in Cancer: Revisiting a JNCI Publication Exploring Expression of the MDR1 (P-glycoprotein) Gene.* J Natl Cancer Inst, 2015. **107**(9).

115. Sharom, F.J., *Shedding light on drug transport: structure and function of the P-glycoprotein multidrug transporter (ABCB1).* Biochem Cell Biol, 2006. **84**(6): p. 979-92.

116. Jones, P.M., M.L. O'Mara, and A.M. George, *ABC transporters: a riddle wrapped in a mystery inside an enigma.* Trends Biochem Sci, 2009. **34**(10): p. 520-31.

117. Aller, S.G., et al., *Structure of P-glycoprotein reveals a molecular basis for poly-specific drug binding.* Science, 2009. **323**(5922): p. 1718-22.

118. Maki, N., P. Hafkemeyer, and S. Dey, *Allosteric modulation of human P-glycoprotein. Inhibition of transport by preventing substrate translocation and dissociation.* J Biol Chem, 2003. **278**(20): p. 18132-9.

119. Regev, R., Y.G. Assaraf, and G.D. Eytan, *Membrane fluidization by ether, other anesthetics, and certain agents abolishes P-glycoprotein ATPase activity and modulates efflux from multidrug-resistant cells.* Eur J Biochem, 1999. **259**(1-2): p. 18-24.

120. Cai, C., H. Zhu, and J. Chen, *Overexpression of caveolin-1 increases plasma membrane fluidity and reduces P-glycoprotein function in Hs578T/Dox.* Biochem Biophys Res Commun, 2004. **320**(3): p. 868-74.

121. Hall, M.D., M.D. Handley, and M.M. Gottesman, *Is resistance useless? Multidrug resistance and collateral sensitivity.* Trends Pharmacol Sci, 2009. **30**(10): p. 546-56.

122. Ferreira, R.J., M.J. Ferreira, and D.J. dos Santos, *Molecular docking characterizes substrate-binding sites and efflux modulation mechanisms within P-glycoprotein.* J Chem Inf Model, 2013. **53**(7): p. 1747-60.

123. Ambudkar, S.V., et al., *The A-loop, a novel conserved aromatic acid subdomain upstream of the Walker A motif in ABC transporters, is critical for ATP binding.* FEBS Lett, 2006. **580**(4): p. 1049-55.

124. Gozalpour, E., et al., *Interaction of digitalis-like compounds with p-glycoprotein.* Toxicol Sci, 2013. **131**(2): p. 502-11.

125. Efferth, T., et al., *Prediction of broad spectrum resistance of tumors towards anticancer drugs.* Clin Cancer Res, 2008. **14**(8): p. 2405-12.

126. Tsuruo, T., et al., *Overcoming of vincristine resistance in P388 leukemia in vivo and in vitro through enhanced cytotoxicity of vincristine and vinblastine by verapamil.* Cancer Res, 1981. **41**(5): p. 1967-72.

127. Brahemi, G., et al., *Exploring the structural requirements for inhibition of the ubiquitin E3 ligase breast cancer associated protein 2 (BCA2) as a treatment for breast cancer.* J Med Chem, 2010. **53**(7): p. 2757-65.

128. McCarthy, M., et al., *In vivo anticancer synergy mechanism of doxorubicin and verapamil combination treatment is impaired in BALB/c mice with metastatic breast cancer.* Exp Mol Pathol, 2014. **97**(1): p. 6-15.

129. Marchetti, S., et al., *Concise review: Clinical relevance of drug drug and herb drug interactions mediated by the ABC transporter ABCB1 (MDR1, P-glycoprotein).* Oncologist, 2007. **12**(8): p. 927-41.

130. Georges, E., T. Tsuruo, and V. Ling, *Topology of P-glycoprotein as determined by epitope mapping of MRK-16 monoclonal antibody.* J Biol Chem, 1993. **268**(3): p. 1792-8.

131. Gottesman, M.M. and I. Pastan, *Biochemistry of multidrug resistance mediated by the multidrug transporter.* Annu Rev Biochem, 1993. **62**: p. 385-427.

132. Safa, A.R., *Identification and characterization of the binding sites of P-glycoprotein for multidrug resistance-related drugs and modulators.* Curr Med Chem Anticancer Agents, 2004. **4**(1): p. 1-17.

133. Dayan, G., et al., *Binding of steroid modulators to recombinant cytosolic domain from mouse P-glycoprotein in close proximity to the ATP site.* Biochemistry, 1997. **36**(49): p. 15208-15.

134. Sardjiman, S.S., et al., *1,5-Diphenyl-1,4-pentadiene-3-ones and cyclic analogues as antioxidative agents. Synthesis and structure-activity relationship.* European Journal of Medicinal Chemistry, 1997. **32**(7–8): p. 625-630.

135. Auffinger, P., et al., *Halogen bonds in biological molecules.* Proc Natl Acad Sci U S A, 2004. **101**(48): p. 16789-94.

136. Hunter, C.A., *Quantifying intermolecular interactions: guidelines for the molecular recognition toolbox.* Angew Chem Int Ed Engl, 2004. **43**(40): p. 5310-24.

137. Lu, Y., et al., *C–X···H Contacts in Biomolecular Systems: How They Contribute to Protein−Ligand Binding Affinity.* The Journal of Physical Chemistry B, 2009. **113**(37): p. 12615-12621.

138. Nurfina, A.N., et al., *Synthesis of some symmetrical curcumin derivatives and their antiinflammatory activity.* European Journal of Medicinal Chemistry, 1997. **32**(4): p. 321-328.

139. Vyas, A., et al., *Perspectives on New Synthetic Curcumin Analogs and their Potential Anticancer Properties.* Current pharmaceutical design, 2013. **19**(11): p. 2047-2069.

140. Zhang, J., et al., *Drug promiscuity of P-glycoprotein and its mechanism of interaction with paclitaxel and doxorubicin.* Soft Matter, 2014. **10**(3): p. 438-45.

141. Xu, G., et al., *The Three Dimensional Quantitative Structure Activity Relationships (3D-QSAR) and Docking Studies of Curcumin Derivatives as Androgen Receptor Antagonists.* Int J Mol Sci, 2012. **13**(5): p. 6138-55.

142. Maurya, A., et al., *QSAR, docking and in vivo studies for immunomodulatory activity of isolated triterpenoids from Eucalyptus tereticornis and Gentiana kurroo.* Eur J Pharm Sci, 2012. **47**(1): p. 152-61.

143. Singh, S., et al., *Identification and characterization of novel small-molecule inhibitors against hepatitis delta virus replication by using docking strategies.* Hepat Mon, 2011. **11**(10): p. 803-9.

144. Yadav, D.K., et al., *Development of QSAR model for immunomodulatory activity of natural coumarinolignoids.* Drug Des Devel Ther, 2010. **4**: p. 173-86.

145. Zeino, M., et al., *Cytotoxicity of cardiotonic steroids in sensitive and multidrug-resistant leukemia cells and the link with Na(+)/K(+)-ATPase.* J Steroid Biochem Mol Biol, 2015. **150**: p. 97-111.

146. Yi, P. and M. Qiu, *3D-QSAR and docking studies of aminopyridine carboxamide inhibitors of c-Jun N-terminal kinase-1.* Eur J Med Chem, 2008. **43**(3): p. 604-13.

147. Ishihara, M., et al., *Estimation of relationship between descriptors and cytotoxicity of newly synthesized 1,2,3,4-tetrahydroisoquinoline derivatives.* Anticancer Res, 2009. **29**(10): p. 4077-82.

148. Tuppurainen, K., et al., *About the mutagenicity of chlorine-substituted furanones and halopropenals. A QSAR study using molecular orbital indices.* Mutat Res, 1991. **247**(1): p. 97-102.

149. Rajesh, G., et al., *Effect of hydroxyl substitution of flavone on angiogenesis and free radical scavenging activities: a structure-activity relationship studies using computational tools.* Eur J Pharm Sci, 2010. **39**(1-3): p. 37-44.

150. Bimonte, S., et al., *Curcumin AntiCancer Studies in Pancreatic Cancer.* Nutrients, 2016. **8**(7).

151. Guzzarlamudi, S., et al., *Synergistic Chemotherapeutic Activity of Curcumin Bearing Methoxypolyethylene Glycol-g-Linoleic Acid Based Micelles on Breast Cancer Cells.* J Nanosci Nanotechnol, 2016. **16**(4): p. 4180-90.

152. Kasi, P.D., et al., *Molecular targets of curcumin for cancer therapy: an updated review.* Tumour Biol, 2016.

153. Ye, H., et al., *A novel double carbonyl analog of curcumin induces the apoptosis of human lung cancer H460 cells via the activation of the endoplasmic reticulum stress signaling pathway.* Oncol Rep, 2016. **36**(3): p. 1640-8.

154. Yu, X., et al., *Curcumin exerts antitumor effects in retinoblastoma cells by regulating the JNK and p38 MAPK pathways.* Int J Mol Med, 2016. **38**(3): p. 861-8.

155. Zeng, Y., et al., *Curcumin reduces the expression of survivin, leading to enhancement of arsenic trioxide-induced apoptosis in myelodysplastic syndrome and leukemia stem-like cells.* Oncol Rep, 2016. **36**(3): p. 1233-42.

156. Chen, N., et al., *Vitamin B(2) Sensitizes Cancer Cells to Vitamin-C-Induced Cell Death via Modulation of Akt and Bad Phosphorylation.* J Agric Food Chem, 2015. **63**(30): p. 6739-48.

157. Fukui, M., et al., *Mechanism of Ascorbate-Induced Cell Death in Human Pancreatic Cancer Cells: Role of Bcl-2, Beclin 1 and Autophagy.* Planta Med, 2015. **81**(10): p. 838-46.

158. Jacobs, C., et al., *Is there a role for oral or intravenous ascorbate (vitamin C) in treating patients with cancer? A systematic review.* Oncologist, 2015. **20**(2): p. 210-23.

159. Sunil Kumar, B.V., S. Singh, and R. Verma, *Anticancer Potential of Dietary Vitamin D and Ascorbic Acid: A Review.* Crit Rev Food Sci Nutr, 2015: p. 0.

160. Venturelli, S., et al., *Molecular mechanisms of pharmacological doses of ascorbate on cancer cells.* Wien Med Wochenschr, 2015. **165**(11-12): p. 251-7.

161. Parrow, N.L., J.A. Leshin, and M. Levine, *Parenteral ascorbate as a cancer therapeutic: a reassessment based on pharmacokinetics.* Antioxid Redox Signal, 2013. **19**(17): p. 2141-56.

162. Chen, Q., et al., *Pharmacologic ascorbic acid concentrations selectively kill cancer cells: action as a pro-drug to deliver hydrogen peroxide to tissues.* Proc Natl Acad Sci U S A, 2005. **102**(38): p. 13604-9.

163. Kehrer, J.P., *The Haber-Weiss reaction and mechanisms of toxicity.* Toxicology, 2000. **149**(1): p. 43-50.

164. Kim, J., et al., *Enhanced antitumor activity of vitamin C via p53 in cancer cells.* Free Radic Biol Med, 2012. **53**(8): p. 1607-15.

165. Waters, N.J., *Evaluation of drug-drug interactions for oncology therapies: in vitro-in vivo extrapolation model-based risk assessment.* Br J Clin Pharmacol, 2015. **79**(6): p. 946-58.

166. Scherf, U., et al., *A gene expression database for the molecular pharmacology of cancer.* Nat Genet, 2000. **24**(3): p. 236-44.

167. Faria, J.A., et al., *SET domain-containing Protein 4 (SETD4) is a Newly Identified Cytosolic and Nuclear Lysine Methyltransferase involved in Breast Cancer Cell Proliferation.* J Cancer Sci Ther, 2013. **5**(2): p. 58-65.

168. Yoon, J.W., et al., *p53 modulates the activity of the GLI1 oncogene through interactions with the shared coactivator TAF9.* DNA Repair (Amst), 2015. **34**: p. 9-17.

169. Shi, Y., et al., *Change in gene expression subsequent to induction of Pnn/DRS/memA: increase in p21(cip1/waf1).* Oncogene, 2001. **20**(30): p. 4007-18.

170. Wang, Y., et al., *CDK7-dependent transcriptional addiction in triple-negative breast cancer.* Cell, 2015. **163**(1): p. 174-86.

171. Krynetskaia, N.F., et al., *Chromatin-associated proteins HMGB1/2 and PDIA3 trigger cellular response to chemotherapy-induced DNA damage.* Mol Cancer Ther, 2009. **8**(4): p. 864-72.

172. Guo, J., et al., *Frequent truncating mutation of TFAM induces mitochondrial DNA depletion and apoptotic resistance in microsatellite-unstable colorectal cancer.* Cancer Res, 2011. **71**(8): p. 2978-87.

173. Davis, T.L., et al., *The crystal structure of human WD40 repeat-containing peptidylprolyl isomerase (PPWD1).* FEBS J, 2008. **275**(9): p. 2283-95.

174. Jeon, J., et al., *A systematic approach to identify novel cancer drug targets using machine learning, inhibitor design and high-throughput screening.* Genome Med, 2014. **6**(7): p. 57.

175. Dzeja, P. and A. Terzic, *Adenylate kinase and AMP signaling networks: metabolic monitoring, signal communication and body energy sensing.* Int J Mol Sci, 2009. **10**(4): p. 1729-72.

176. Raimondi, C. and M. Falasca, *Targeting PDK1 in cancer.* Curr Med Chem, 2011. **18**(18): p. 2763-9.

177. Hawkins, S.M., et al., *Expression and functional pathway analysis of nuclear receptor NR2F2 in ovarian cancer.* J Clin Endocrinol Metab, 2013. **98**(7): p. E1152-62.

178. McDonald, J.M., et al., *Attenuated expression of DFFB is a hallmark of oligodendrogliomas with 1p-allelic loss.* Mol Cancer, 2005. **4**: p. 35.

179. Nilsson, R., et al., *Metabolic enzyme expression highlights a key role for MTHFD2 and the mitochondrial folate pathway in cancer.* Nat Commun, 2014. **5**: p. 3128.

180. Lehtinen, L., et al., *High-throughput RNAi screening for novel modulators of vimentin expression identifies MTHFD2 as a regulator of breast cancer cell migration and invasion.* Oncotarget, 2013. **4**(1): p. 48-63.

181. Marchitti, S.A., et al., *Aldehyde dehydrogenase 3B1 (ALDH3B1): immunohistochemical tissue distribution and cellular-specific localization in normal and cancerous human tissues.* J Histochem Cytochem, 2010. **58**(9): p. 765-83.

182. Sertel, S., et al., *Pharmacogenomic determination of genes associated with sensitivity or resistance of tumor cells to curcumin and curcumin derivatives.* J Nutr Biochem, 2012. **23**(8): p. 875-84.

183. Sertel, S., et al., *Factors determining sensitivity or resistance of tumor cell lines towards artesunate.* Chem Biol Interact, 2010. **185**(1): p. 42-52.

184. Efferth, T., et al., *Cytotoxic activity of secondary metabolites derived from Artemisia annua L. towards cancer cells in comparison to its designated active constituent artemisinin.* Phytomedicine, 2011. **18**(11): p. 959-69.

185. Kimmig, A., et al., *Susceptibility of multidrug-resistant human leukemia cell lines to human interleukin 2-activated killer cells.* Cancer Res, 1990. **50**(21): p. 6793-9.

186. Waldman, T., K.W. Kinzler, and B. Vogelstein, *p21 is necessary for the p53-mediated G1 arrest in human cancer cells.* Cancer Res, 1995. **55**(22): p. 5187-90.

187. Bunz, F., et al., *Requirement for p53 and p21 to sustain G2 arrest after DNA damage.* Science, 1998. **282**(5393): p. 1497-501.

188. Huang, H.S., et al., *The enhanced tumorigenic activity of a mutant epidermal growth factor receptor common in human cancers is mediated by threshold levels of constitutive tyrosine phosphorylation and unattenuated signaling.* J Biol Chem, 1997. **272**(5): p. 2927-35.

189. Gillet, J.P., et al., *Microarray-based detection of multidrug resistance in human tumor cells by expression profiling of ATP-binding cassette transporter genes.* Cancer Res, 2004. **64**(24): p. 8987-93.

190. Trump, D.L., *Commentary on "Abiraterone in metastatic prostate cancer without previous chemotherapy." Ryan CJ, Smith MR, de Bono JS, Molina A, Logothetis CJ, de Souza P, Fizazi K, Mainwaring P, Piulats JM, Ng S, Carles J, Mulders PF, Basch E, Small EJ, Saad F, Schrijvers D,*

Van Poppel H, Mukherjee SD, Suttmann H, Gerritsen WR, Flaig TW, George DJ, Yu EY, Efstathiou E, Pantuck A, Winquist E, Higano CS, Taplin ME, Park Y, Kheoh T, Griffin T, Scher HI, Rathkopf DE; COU-AA-302 Investigators, Genitourinary Medical Oncology Program, Helen Diller Family Comprehensive Cancer Center, University of California, San Francisco, CA. N Engl J Med 2013;368(2):138-48 [Epub 2012 Dec 10]; N Engl J Med 2013;368(6):584. Urol Oncol, 2013. **31**(8): p. 1846.

191. Batchelor, R.H. and M. Zhou, *Use of cellular glucose-6-phosphate dehydrogenase for cell quantitation: applications in cytotoxicity and apoptosis assays.* Anal Biochem, 2004. **329**(1): p. 35-42.

192. Wiench, B., et al., *Shikonin directly targets mitochondria and causes mitochondrial dysfunction in cancer cells.* Evid Based Complement Alternat Med, 2012. **2012**: p. 726025.

193. Lee, S.I., *Drug interaction: focusing on response surface models.* Korean J Anesthesiol, 2010. **58**(5): p. 421-34.

194. Zhao, W., et al., *A New Bliss Independence Model to Analyze Drug Combination Data.* J Biomol Screen, 2014. **19**(5): p. 817-21.

195. Lee, J.J., et al., *Interaction index and different methods for determining drug interaction in combination therapy.* J Biopharm Stat, 2007. **17**(3): p. 461-80.

196. Zhang, W., et al., *Histone deacetylase inhibitor romidepsin enhances anti-tumor effect of erlotinib in non-small cell lung cancer (NSCLC) cell lines.* J Thorac Oncol, 2009. **4**(2): p. 161-6.

197. Tajima, Y., et al., *Nitensidine A, a guanidine alkaloid from Pterogyne nitens, is a novel substrate for human ABC transporter ABCB1.* Phytomedicine, 2014. **21**(3): p. 323-32.

198. Kelley, L.A. and M.J. Sternberg, *Protein structure prediction on the Web: a case study using the Phyre server.* Nat Protoc, 2009. **4**(3): p. 363-71.

199. Saeed, M., et al., *Activity of the dietary flavonoid, apigenin, against multidrug-resistant tumor cells as determined by pharmacogenomics and molecular docking.* J Nutr Biochem, 2015. **26**(1): p. 44-56.

200. Alley, M.C., et al., *Feasibility of drug screening with panels of human tumor cell lines using a microculture tetrazolium assay.* Cancer Res, 1988. **48**(3): p. 589-601.

201. Eisen, M.B., et al., *Cluster analysis and display of genome-wide expression patterns.* Proc Natl Acad Sci U S A, 1998. **95**(25): p. 14863-8.

202. Gu, Z., R. Eils, and M. Schlesner, *Complex heatmaps reveal patterns and correlations in multidimensional genomic data.* Bioinformatics, 2016.

Permission to publish

Text figures and tables from own publication:

Reprinted from: Toxicol Appl Pharmacol, vol. 305 (1), Ooko E, Alsalim T, Saeed B, Saeed ME, Kadioglu O, Abbo HS, Titinchi SJ, Efferth T. "Modulation of P-glycoprotein activity by novel synthetic curcumin derivatives in sensitive and multidrug-resistant T-cell acute lymphoblastic leukemia cell lines." pp. 216-233, 2016. Copyright 2016, with permission from Elsevier.

doi: 10.1016/j.taap.2016.06.002;

http://www.sciencedirect.com/science/article/pii/S0041008X16301363